

**AN ULTRAVIOLET BASED METHYL  
MERCAPTAN SYSTEM FOR HALITOSIS  
USING AN OPTICAL FIBRE SENSOR**



**SUZALINA BINTI KAMARUDDIN**

**UMP**

**MASTER OF SCIENCE**

**UNIVERSITI MALAYSIA PAHANG**

**UNIVERSITI MALAYSIA PAHANG**

**DECLARATION OF THESIS AND COPYRIGHT**

Author's Full Name : SUZALINA BINTI KAMARUDDIN

Date of Birth : 20/07/1974

Title : AN ULTRAVIOLET BASED METHYL MERCAPTAN  
SYSTEM FOR HALITOSIS USING AN OPTICAL  
FIBRE SENSOR

Academic Session : SEM 2 2019/2020

I declare that this thesis is classified as:

- CONFIDENTIAL (Contains confidential information under the Official Secret Act 1997)\*
- RESTRICTED (Contains restricted information as specified by the organization where research was done)\*
- OPEN ACCESS I agree that my thesis to be published as online open access (Full Text)

I acknowledge that Universiti Malaysia Pahang reserves the following rights:

1. The Thesis is the Property of Universiti Malaysia Pahang
2. The Library of Universiti Malaysia Pahang has the right to make copies of the thesis for the purpose of research only.
3. The Library has the right to make copies of the thesis for academic exchange.

Certified by:

\_\_\_\_\_  
(Student's Signature)

740720065130

\_\_\_\_\_  
(Supervisor's Signature)

PROFESOR MADYA  
TS. DR. HADI BIN MANAP

\_\_\_\_\_  
New IC/Passport Number  
Date: 20 FEBRUARY 2020

\_\_\_\_\_  
Name of Supervisor  
Date: 20 FEBRUARY 2020

NOTE : \* If the thesis is CONFIDENTIAL or RESTRICTED, please attach a thesis declaration letter.

### **SUPERVISOR'S DECLARATION**

I hereby declare that I have checked this thesis and in my opinion, this thesis is adequate in terms of scope and quality for the award of the degree of Master of Science.

---

(Supervisor's Signature)

Full Name : PROFESOR MADYA TS. DR. HADI BIN MANAP  
Position : SENIOR LECTURER  
Date : 20 FEBRUARY 2020



UMP

### STUDENT'S DECLARATION

I hereby declare that the work in this thesis is based on my original work except for quotations and citations which have been duly acknowledged. I also declare that it has not been previously or concurrently submitted for any other degree at Universiti Malaysia Pahang or any other institutions.

---

(Student's Signature)

Full Name : SUZALINA BINTI KAMARUDDIN

ID Number : MKE 13001

Date : 20 FEBRUARY 2020



UMP

AN ULTRAVIOLET BASED METHYL MERCAPTAN SYSTEM FOR HALITOSIS  
USING AN OPTICAL FIBRE SENSOR



SUZALINA BINTI KAMARUDDIN

Thesis submitted in fulfillment of the requirements  
for the award of the degree of  
Master of Science

UMP

Faculty of Electrical and Electronic Engineering Technology

UNIVERSITI MALAYSIA PAHANG

FEBRUARY 2020

## ACKNOWLEDGEMENTS

Alhamdulillah, I thank Allah for the years of ups and downs of this Masters study. This beautiful journey will always be the foundation of the great destination. I would like to express sincere gratitude to those who have provided all the supports and encouragement for me to finally finish my study. First and foremost, I would like to thank my supervisor, Prof. Madya TS. Dr. Hadi Manap, for his guidance and assistance throughout my study. His great enthusiasm, insightful perspective and work ethics have helped me grow professionally and extensively. His continuous understanding and kind words are the inspiration that keep me going on the right path.

My sincere gratitude goes to the Faculty of Engineering Technology (FTEK) at Universiti Malaysia Pahang for supporting my work with the allocated education grant and usage of facilities. The generous deal allowed me to carry out my experiment smoothly and getting the best out of it.

I would also like to express my sincere gratitude to the management of Malaysian Meteorological Department (MMD) for giving me the chance to further my study while I am working as the Meteorological Officer.

My biggest thank and never ending loves to my late father who initiated the strong will to further my study and to my mother who always believe in whatever I do.

Last but not least, I thank my husband, Muhammad Ridzudin, for his unconditional support, love, understanding, encouragement, assistance and patience while I was completing my study. His continuing willingness to care for our children to lessen my burden and help me go through the milestones of the thesis writing is deeply appreciated. To all my six children, you are my strength and my reason to live.



UMP

## ABSTRAK

Halitosis adalah bau busuk dari mulut, yang berasal terutamanya dari pereputan bakteria yang menghasilkan sebatian sulfur tidak seimbang (VSC) terutamanya methyl mercaptan ( $\text{CH}_3\text{SH}$ ). Ia adalah masalah kritikal yang telah menjadi kebimbangan masyarakat dan memerlukan prosedur yang teratur untuk pengesanan. Kebanyakan sistem atau kaedah pengesanan semasa gagal mengenal pasti dan membezakan VSC, sensitif terhadap persekitaran dan memberikan hasil yang tidak dapat diukur. Didapati bahawa sistem pengesanan optik adalah lebih sesuai digunakan berbanding *gas chromatograph*, *portable sulphide monitors*, *electronic noses* dan ujian kimia atau enzim. Tujuan utama tesis ini adalah untuk membina alat pengesanan halitosis berasaskan sinar lampau ungu (UV) dan sensor kabel optik (OFS). Alat ini diguna untuk mendapatkan spektra keratan rentas penyerapan bagi  $\text{CH}_3\text{SH}$ , komponen utama VSC untuk analisis dan mencari rantau panjang gelombang sistem. Untuk tujuan validasi sistem, penilaian terhadap kemungkinan gangguan daripada gas-gas pernafasan dan pengiraan kepekatan  $\text{CH}_3\text{SH}$  dilakukan. Metodologi penyelidikan berasaskan kaedah spektroskopi penyerapan. Prinsip kerja sistem ini melibatkan pergerakan cahaya UV dari sumbernya melalui kabel fiber dan kemudian dimodulasi oleh bahan di dalam zon modulasi sebelum dikesan oleh spektrometer yang juga dihubungkan dengan kabel fiber. Teknik laluan terbuka berlaku di dalam zon modulasi. Dengan menggunakan sistem pengesanan ini, jenis gas boleh dikenalpasti melalui ciri unik yang ada pada setiap gas. Menggunakan persamaan daripada Hukum *Beer Lambert* yang diubahsuai, keratan rentas penyerapan,  $\sigma$  bagi  $\text{CH}_3\text{SH}$  diperolehi daripada eksperimen yang dibuat menggunakan gas  $\text{CH}_3\text{SH}$  sebagai bahan ujikaji, dan graf berkaitan diplot. Keputusan yang didapati mempunyai korelasi yang tinggi (*coefficient* = 0.99) dengan data teori yang didapati daripada pangkalan data *UV-VIS MPI Mainz*.  $\sigma$  bagi oksigen ( $\text{O}_2$ ) dan karbon dioksida ( $\text{CO}_2$ ) diperolehi untuk tujuan validisasi. Penilaian gas  $\text{CH}_3\text{SH}$  dengan gas pernafasan, air ( $\text{H}_2\text{O}$ ),  $\text{O}_2$  dan  $\text{CO}_2$  mendapati bahawa tiada isu gangguan oleh gas pernafasan bagi rantau panjang gelombang 200 hingga 270 nm. Dan, kepekatan gas  $\text{CH}_3\text{SH}$  memberi nilai 97.46 ppm iaitu menghampiri 100 ppm seperti yang dinyatakan oleh pengeluar. Akhirnya, sistem pengesanan yang dicadangkan ini berupaya mengesan gas  $\text{CH}_3\text{SH}$  dalam rantau UV-C, dengan rantau panjang gelombang 200 hingga 210 nm adalah pilihan terbaik untuk sistem pengesanan berasaskan UV, dimana puncak penyerapan berada di sini. Sistem ini adalah sesuai dan boleh diharapkan sebagai pengesanan halitosis. Sistem pengesanan berasaskan UV dengan gabungan OFS dibina daripada komponen yang sedia ada di pasaran dapat digunakan untuk mengesan halitosis, kenalpasti gas yang berbeza, tidak sensitif terhadap gangguan gas lain dan boleh diukur untuk penggunaan rutin klinik dalam bidang pergigian.

## ABSTRACT

Halitosis is a foul smell from the mouth, mainly originates from the putrefactive bacteria that produce volatile sulphur compounds (VSCs), predominantly methyl mercaptan ( $\text{CH}_3\text{SH}$ ). It has become a public concern which needs a well-structured procedure for detection purposes. However, current systems or methods failed to identify and distinguish the main components of VSCs, sensitive to the environment and provide measurable results. Optical detection systems are found to be more reliable than gas chromatography, portable sulphide monitors, electronic noses and chemical or enzymatic tests. The main purpose of this study is to develop an ultraviolet (UV) based methyl mercaptan system using an optical fibre sensor (OFS) to detect halitosis. The proposed system is utilised to obtain the absorption cross-section spectra of  $\text{CH}_3\text{SH}$ , the main component of VSCs for analysis and wavelength spectral determination. To validate the proposed system, cross-sensitivity evaluation with breathing gases and calculation of  $\text{CH}_3\text{SH}$  gas concentration is performed. The methodology of the study is based on the absorption spectroscopy method. The working principle of the proposed system involves propagation of UV light signal from its source through the input fibre and then modulated by the measurand in the modulation zone before it is sensed by the spectrometer as the detector through the output fibre. The modulation zone is where the open-path technique will take place. Each gas has its unique characteristic which corresponds to its identification and can be determined using this detection system as the measurand. By manipulating the Beer-Lambert Law equation, the datasets of absorption cross-section,  $\sigma$  for  $\text{CH}_3\text{SH}$  were obtained and plotted against wavelength. The result was found to be highly correlated (coefficient = 0.99) with theoretical datasets from the MPI Mainz UV-VIS database.  $\sigma$  for  $\text{O}_2$  and  $\text{CO}_2$  were obtained for system validation purposes. Cross-sensitivity evaluation of  $\text{CH}_3\text{SH}$  which was carried out with breathing gases  $\text{O}_2$ ,  $\text{CO}_2$  and water ( $\text{H}_2\text{O}$ ) proved that interference was not an issue for UV wavelength regions of 200 to 270 nm. And, the calculated  $\text{CH}_3\text{SH}$  gas concentration is 97.46 ppm, almost reaching the 100 ppm that was stated by the manufacturer. Finally, the proposed system is capable of detecting  $\text{CH}_3\text{SH}$  in the UV-C region, with the best potential band of 200 to 210 nm where the excellent peak is located. The UV-based detection system with OFS, which was constructed with available manufactured components, is able to detect halitosis, distinguish different gases, is not sensitive to interference and can produce measurable results for routine clinical usage in the dental field.



## TABLE OF CONTENTS

<b>DECLARATION</b>	
<b>TITLE PAGE</b>	
<b>ACKNOWLEDGEMENTS</b>	<b>ii</b>
<b>ABSTRAK</b>	<b>iii</b>
<b>ABSTRACT</b>	<b>iv</b>
<b>TABLE OF CONTENTS</b>	<b>v</b>
<b>LIST OF TABLES</b>	<b>viii</b>
<b>LIST OF FIGURES</b>	<b>ix</b>
<b>LIST OF SYMBOLS</b>	<b>xi</b>
<b>LIST OF ABBREVIATIONS</b>	<b>xii</b>
<b>CHAPTER 1 INTRODUCTION</b>	<b>1</b>
1.1 Background of Research	1
1.2 Problem Statement	3
1.3 Research Objectives	5
1.4 Scope and Limitation	5
1.5 Contributions of Research	5
1.6 Outline of the Thesis	6
<b>CHAPTER 2 LITERATURE REVIEW</b>	<b>7</b>
2.1 Introduction	7
2.2 Classic Technique for Halitosis Detection	7
2.3 Quantitative Analysis of Halitosis	9

2.3.1	Gas Chromatography	10
2.3.2	Compact and Simple Gas Chromatography	12
2.3.3	Portable Sulphide Monitors	14
2.3.4	Electronic Noses	18
2.3.5	Chemical or Enzymatic Tests	19
2.4	Optical Based Gas Detection System	27
2.4.1	Light Source	27
2.4.2	Optical Fibres	30
2.4.3	Optical Fibre Sensor	32
2.4.4	Photo Detector	33
2.4.5	Various Applications of Optical Detection System	35
2.4.6	UV Based System with OFS	38
2.5	Summary	40
<b>CHAPTER 3 METHODOLOGY</b>		<b>41</b>
3.1	Introduction	41
3.2	Research Methodology	41
3.3	Theoretical Background	42
3.4	Proposed System	46
3.5	Analyse the Absorption Cross Section Spectra of Methyl Mercaptan	54
3.6	Validation of the Proposed System	55
3.6.1	Cross Sensitivity Evaluation with Breathing Gases	55
3.6.2	Calculation of Concentration	55
3.7	Summary	56

<b>CHAPTER 4 RESULTS AND DISCUSSIONS</b>	<b>57</b>
4.1 Introduction	57
4.2 Absorption Cross Section Spectra of Methyl Mercaptan	57
4.3 Absorption Cross Section Spectra of Oxygen and Carbon Dioxide	60
4.4 Cross Sensitivity with Breathing Gases	61
4.5 Calculation of CH <sub>3</sub> SH Concentration	63
4.6 Summary	64
<b>CHAPTER 5 CONCLUSIONS</b>	<b>65</b>
5.1 Introduction	65
5.2 Conclusions	65
5.3 Suggestions and Future Works	66
<b>REFERENCES</b>	<b>68</b>
APPENDIX A MANUAL FOR CALIBRATING THE WAVELENGTH OF THE MAYA2000PRO SERIES SPECTROMETERS	80
APPENDIX B EXPERIMENTAL DATA OF CH <sub>3</sub> SH ABSORPTION CROSS SECTION SPECTRA	84
APPENDIX C CH <sub>3</sub> SH ABSORPTION CROSS SECTION SPECTRA FROM MPI-MAINZ DATABASE	85
APPENDIX D ABSORPTION CROSS SECTION OF WATER VAPOUR, H <sub>2</sub> O FROM VARIOUS STUDIES	86
<b>LIST OF PUBLICATIONS</b>	<b>87</b>

## LIST OF TABLES

Table 1.1	Summary of the Methyl Mercaptan Gas Properties	2
Table 2.1	Rosenberg Organoleptic Scoring Scale	8
Table 2.2	Halitosis Detection Methods, Advantages and Disadvantages	23
Table 2.3	Summary of Commercially Available Broadband Sources	28
Table 3.1	Values of Regression Statistics	51
Table 3.2	Calibration Coefficients Data for Spectrometer	51
Table 3.3	Experimental Conditions for Intensity Measurement	54
Table 4.1	Summary of Correlation Coefficient for CH <sub>3</sub> SH Absorption Cross Section Spectra	59
Table 4.2	Values of Peaks and Wavelength of CH <sub>3</sub> SH Absorption Spectral	59
Table 4.3	Measured Intensity and Calculated CH <sub>3</sub> SH Gas Concentration	64

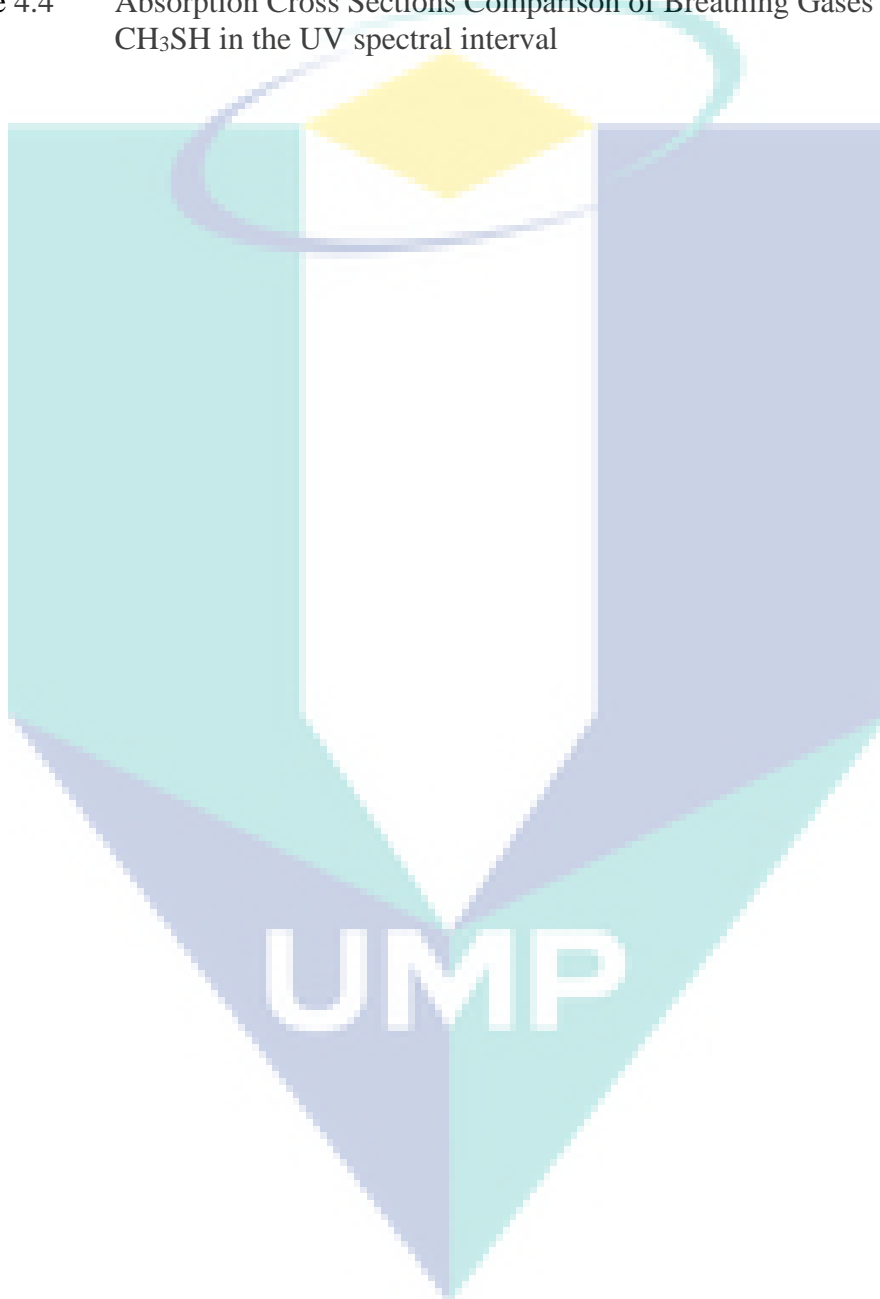
The logo for UMP (Universitas Muhammadiyah Purwokerto) is a large, downward-pointing arrow shape. It is composed of four triangular sections meeting at a central point. The top-left and bottom-right sections are light blue, while the top-right and bottom-left sections are a slightly darker shade of blue. The letters 'UMIP' are printed in a bold, white, sans-serif font across the center of the arrow.

UMIP

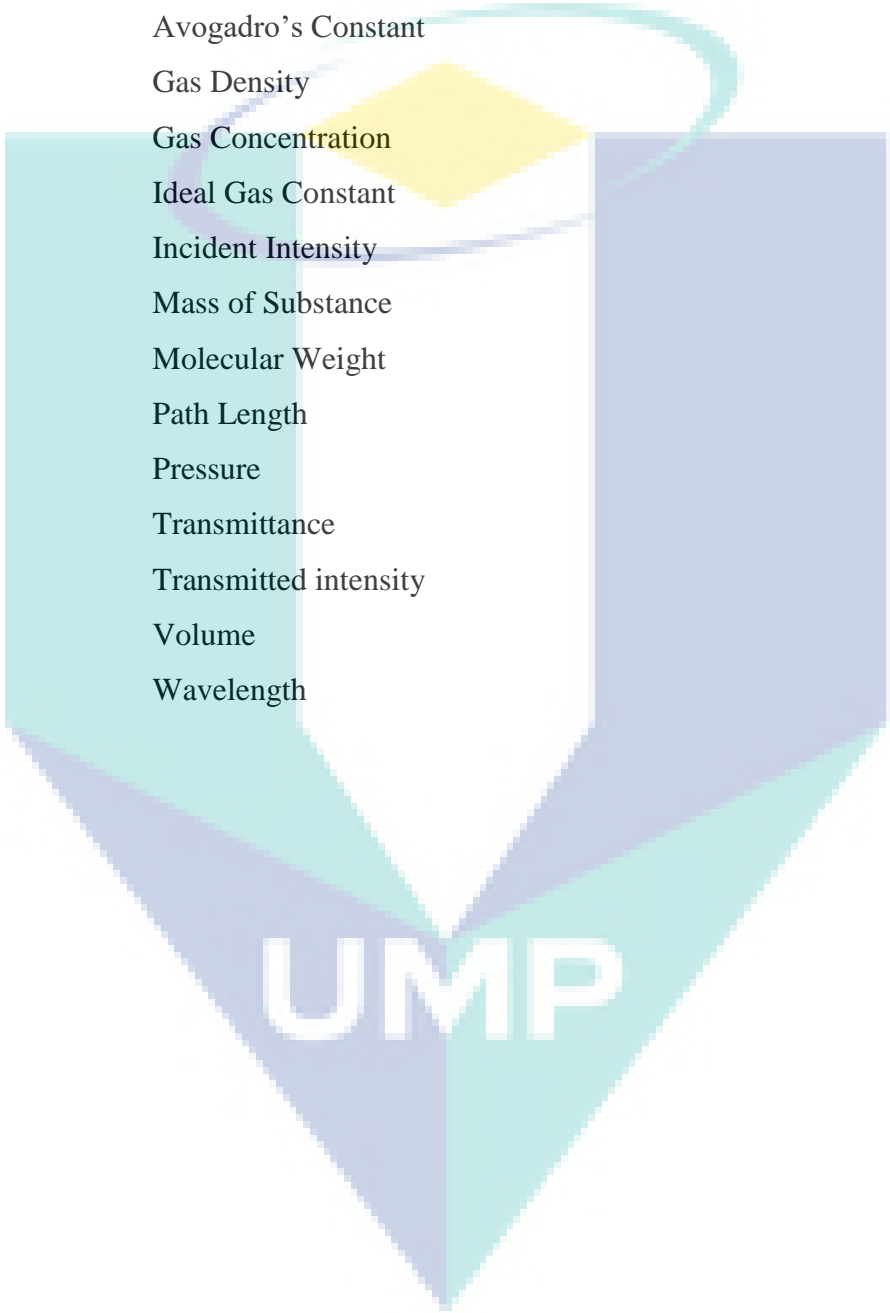
## LIST OF FIGURES

Figure 2.1	Schematic Diagram of GC-FPD system	10
Figure 2.2	Schematic Diagram of the GC-MS	11
Figure 2.3	The OralChroma using GC-SGS Analyzer Method	12
Figure 2.4	A Patient using Twin Breasor for Halitosis Assessment	14
Figure 2.5	Halimeter as the Device for Measurement of VSCs	15
Figure 2.6	The Breathtron as the Sulphur Compounds Measurement Device	16
Figure 2.7	A Portable Sulphide Monitor, BB Checker with the Adapter.	17
Figure 2.8	Diamond Probe/Perio 2000 System	18
Figure 2.9	Cyranose 320, A Portable Handheld Electronic Nose	19
Figure 2.10	BANA-Enzymatic Test Kit	20
Figure 2.11	Indole Test Reaction Process	22
Figure 2.12	Components of the Electromagnetic Spectrum and UV Subdivision	28
Figure 2.13	The Output Intensity of Different UV Sources	29
Figure 2.14	Image of an Optical Fibre and Copper Cable	31
Figure 2.15	Cross Section of a Spectrometer and its Components	34
Figure 2.16	Illustration of a Simple Setup for Breathing Condition Monitoring	35
Figure 2.17	Breath Analysis System by the Optical Bio-sniffer with MAO-A	36
Figure 2.18	Illustration of The Coupled Fibre Optic-IRRAS Instrument	37
Figure 2.19	QCL Array Compared with a Quarter Dollar of the USA.	38
Figure 2.20	Schematic Diagram of the PITSA Prototype Setup	39
Figure 2.21	Experimental Setup for Toulene Detection.	40
Figure 3.1	Flow Chart of the Research Methodology	42
Figure 3.2	Transmission of Light through Absorbing Medium	43
Figure 3.3	Derivation of Beer Lambert Law.	44
Figure 3.4	Ocean Optics UV Broadband Source	47
Figure 3.5	A Basic Diagram of the Extrinsic Sensor	48
Figure 3.6	The Stainless Steel Hollow Cylinder Gas Cell	48
Figure 3.7	UVNS Optical Fibre Cable with SMA Connector	49
Figure 3.8	Maya2000 Pro, the Ocean Optics CCD Spectrometer	50
Figure 3.9	Mercury-Argon Lamp used for the Maya2000 Spectrometer Calibration	50
Figure 3.10	Screen of the SpectraSuite Software upon installation	52

Figure 4.1	Graph of Absorption Cross Section against Wavelength for $\text{CH}_3\text{SH}$	58
Figure 4.2	Graph of Absorption Cross Section against Wavelength for Oxygen	60
Figure 4.3	Graph of Absorption Cross Section against Wavelength for Carbon Dioxide	61
Figure 4.4	Absorption Cross Sections Comparison of Breathing Gases with $\text{CH}_3\text{SH}$ in the UV spectral interval	62



## LIST OF SYMBOLS



$T$	Absolute Temperature
$A$	Absorbance
$\sigma$	Absorption Cross Section
$N_A$	Avogadro's Constant
$\rho$	Gas Density
$N$	Gas Concentration
$R$	Ideal Gas Constant
$I_0$	Incident Intensity
$n$	Mass of Substance
$\omega$	Molecular Weight
$l$	Path Length
$P$	Pressure
$t$	Transmittance
$I$	Transmitted intensity
$V$	Volume
$\lambda$	Wavelength

## LIST OF ABBREVIATIONS

BANA	Benzoyl-DL-arginine-naphthylamide
BC	Before Century
CCD	Charge Couple Device
CH <sub>3</sub> SH	Methyl Mercaptan
CH <sub>3</sub> CH <sub>3</sub> SH	Dimethyl Sulphide
CO <sub>2</sub>	Carbon Dioxide
FPD	Flame Photometric Detector
GC	Gas Chromatography
H <sub>2</sub> S	Hydrogen Sulphide
H <sub>2</sub> O	Water Vapour
MAO-A	Monoamine Oxidase Type-A
MEMs	Micro-Electromechanical Systems
MS	Mass Spectrometer
N <sub>2</sub>	Nitrogen
O <sub>2</sub>	Oxygen
OFS	Optical Fibre Sensor
OT	Organoleptic testing
POF	Plastic Optical Fibre
UV	Ultraviolet
VSC	Volatile Sulphur Compound

UMP



## CHAPTER 1

### INTRODUCTION

#### 1.1 Background of Research

Halitosis or bad breath, which is one type of oral malodour indicate foul smells emanating from the mouth (U. Kapoor et al., 2016). Halitosis comes from the Latin word halitus, meaning breath or exhalation, combined with the Greek suffix, -osis, referring to the state of disease. Originally, the word “halitosis” itself was created as the scientific name of malodour in 1874 by Joseph William Howe (Panicker et al., 2015). Halitosis is an age-old universal problem and was mentioned as early as 1500 BC, it becomes a common complaint only in the early 1990s. Having halitosis frequently causes embarrassment and affects interpersonal social communication. The continuous concern of halitosis for both genders and for all age groups acquires them to seek for consultation from dental professionals. Approximately more than 50% of the general populations have halitosis with varying degrees of severity (Greenman et al., 2014).

However, 5 to 72 % of them may not suffer from genuine halitosis (Aydin et al., 2014; Kayombo et al., 2017). This self-proclaimed halitosis patients believed that they have halitosis and extremely conscious if their breath will be offensive to others. These so-called psychosomatic halitosis patients mostly suffered from self-criticism, inferiority complex, social phobia and poor self-esteem (A. S. Rao et al., 2013). Therefore, it is crucial that the general practitioners can distinguish various cases of halitosis with well-defined protocols. In order to avoid this kind of serious predicament, certain manner of diagnostic and assessment should be carried out. Halitosis is commonly caused by oral disease or nasopharyngeal disease or a combination of both (Lopes et al., 2014).

Halitosis can be identified according to the character of the odour (Yamunadevi et al., 2015). Smells like sulphurous or fecal is caused by VSCs such as hydrogen sulphide ( $H_2S$ ),  $CH_3SH$ , and dimethyl sulphide ( $CH_3CH_3S$ ). Anaerobic bacteria can degrade sulphur-containing amino acids and producing VSCs.  $H_2S$  and  $CH_3SH$  are two main VSCs which contributed to halitosis (Choi et al., 2018).  $CH_3SH$  recognition threshold of the contribution is about 1/30 of  $H_2S$  with a much higher odour potential, indicating that  $CH_3SH$  causes halitosis at much lower concentrations than  $H_2S$  (Oliveira-Neto et al., 2018). Properties of  $CH_3SH$  are represented in Table 1.1 below.

Table 1.1 Summary of the Methyl Mercaptan Gas Properties

<b>Properties of Methyl Mercaptan</b>	
Synonym (s):	Mercaptomethane, methylmercaptan, methyl sulfhydrate
Molecular Formula:	$CH_3SH$
Molecular Weight:	48.11 g/mol
CAS Number:	74-93-1
Appearance:	Colourless gas, water-white liquid when below boiling point, cabbage taste
Odour:	Unpleasant rotten cabbage or garlic
Boiling Point and Melting Point:	279.1 K at 101.3 kPa & 150 K
Heat of Vaporization:	24.59 kJ g/mol @ 298 K
Vapour Pressure:	202.6 kPa @ 299.2 K
Critical Temperature and Pressure:	469.9 K & 7.23 MPa
Octanol/Water Partition Coefficient:	Log Kow = 0.78
Solubility in Water at 293 K:	23.3 g/dm <sup>3</sup>
Specific Gravity as Gas (air = 1)	1.66
Dissociation Constant:	pKa = 10.33 at 298 K
Concentration Conversion Factor:	1 ppm = 2.05 mg/m <sup>3</sup>

Source: U.S. National Library of Medicine (2018)

$CH_3SH$  is considered the key identifiable gas in halitosis and the back of the tongue is found to be the major source of  $CH_3SH$  (Lin, 2018, Ramdurg & Mendigeri, 2014). The microscopic uneven and papillary structure of the surface allows it to become an excellent putrefactive habitat for gram-negative anaerobic bacteria that

metabolise proteins as an energy source and produce  $\text{CH}_3\text{SH}$ .  $\text{CH}_3\text{SH}$  is a colourless gas at room temperature (above 43 °F) with an unpleasant odour described as rotten cabbage. Detecting the main VSC such as  $\text{CH}_3\text{SH}$ , one may detect halitosis. The existence of  $\text{CH}_3\text{SH}$  in the air can be detected based on their unique properties using light. Light can be absorbed or emitted by atoms and molecules. Hence, the structures of atoms and molecules are able to be determined (Blair, 2018). This technique of observing the absorbed or emitted light is referred as spectroscopy. The identification of  $\text{CH}_3\text{SH}$  gas is possible by analysing the unique characteristic of the gas from the absorption spectrum using spectroscopic principles. In general, as the structures of atoms and molecules are able to determine using light we can find out more about the entity involved.

Light which is also known as electromagnetic radiation consists of energy in little packets called photons that have properties of both particles and waves. All waves have a wavelength, and as for light, the wavelength range is quite vast. UV is the electromagnetic radiation with a wavelength range specified between 100 to 400 nm which is shorter than visible light. UV based detection system comprises of a powerful and stable UV light source, a fast data acquisition systems of UV detector and improved fibres for the transportation of UV light (Zou *et al.*, 2018). UV detector is the most useful and extensively-used detector to monitor gas components (Tirpitz *et al.*, 2019).

$\text{CH}_3\text{SH}$  gas absorption spectrum is best identified in the UV region of the electromagnetic spectrum (Dai *et al.*, 2018). In order to do that, the interaction of a significant proportion of the UV light with  $\text{CH}_3\text{SH}$  gas will takes place in a modulation zone outside the UV transportation fibre. This open path technique allows spectroscopic principles to occur for the measurement of  $\text{CH}_3\text{SH}$  gas optical properties by the UV detector (Khan *et al.*, 2019). Thus, the absorption spectrum of  $\text{CH}_3\text{SH}$  gas can be obtained. This so called open path OFS is categorized as an extrinsic optical sensor because it uses the fibre cable to guide the UV light to a sensing zone where the optical signal leaves the cable and enter another medium for modulation to take place.

## 1.2 Problem Statement

The right method for detection and evaluation of the key identifiable compound which characterized halitosis is greatly in need. Eventually, many types of detection

systems or sensors for halitosis were developed with various methods applied. Sulphur monitors such as Twin Breasor, Halimeter, Breathron and Diamond probe (Bollen, 2015) were the devices that used sulphide sensors. The sensors responded to sulphide ions, generated measurable voltage which is proportional to the sulphide concentration. However, such method able to detect the existence of sulphuric compound(s) but failed to identify VSC(s). Since it was found that halitosis detected when  $\text{CH}_3\text{SH}$ , the major component of VSCs is spotted, GC based devices were developed which can distinguish one detected compound from another. Nevertheless, the devices methods were complicated, bulky in size and the results easily affected by the environment (Laleman *et al.*, 2014, Nakhleh *et al.*, 2018). Alternatively, optical sensing of  $\text{CH}_3\text{SH}$  for halitosis was found to be more desired for the merits of non-contact, fast response, high sensitivity and selectivity (Du *et al.*, 2017).

Chemical sensor based electronic noses used the same working principle as sulphide monitors but more sensitive for them to be able to detect and identify complex chemical mixtures which produced halitosis (Hu *et al.*, 2018). This devices use sulphide sensing probe that generate an electrochemical voltage to measure sulphur compounds. For instance, the fully-integrated handheld sensing instrument device Cyranose 320 is able to measure  $\text{CH}_3\text{SH}$  compounds from breath air by placing the probe on the surface of the tongue. Despite from being receptive to sulphur compounds, electronic noses were also sensitive to temperature, humidity and interference with other gases (Chen *et al.*, 2013, Nayak & Das, 2018) due to cross sensitivity issues.

The detection systems which used chemical or enzymatic approach such as BANA and  $\beta$ -galactosidase test were both indirect methods to prove the presence of halitosis. BANA test is a rapid enzymatic test that detects odoriferous periodontal microorganisms, the active VSCs producers (Nani *et al.*, 2017) using test strip. This method was considered as semi-quantitative assessment because the test result depends on the intensity of the blue coloration (Schmidt *et al.*, 2015).  $\beta$ -galactosidase test is based on the principle that amounts of bacteria producing VSCs in saliva are positively correlated with  $\beta$ -galactosidase activity (Aylikci & Çolak, 2013) and measured with paper disc which give result in scale. More objective result and quantitatively measurable rather than just plain detection of halitosis existence is in need (Bicak, 2018).

### 1.3 Research Objectives

The research objectives are as follows:

- i. To develop UV based  $\text{CH}_3\text{SH}$  system for halitosis using an open path OFS.
- ii. To analyse the absorption cross section spectra of  $\text{CH}_3\text{SH}$  and determine the wavelength for absorption within UV range.
- iii. To validate the cross sensitivity of  $\text{CH}_3\text{SH}$  gas with the breathing gases and  $\text{CH}_3\text{SH}$  gas concentration.

### 1.4 Scope and Limitation

This research was designed within a specific scope as follows:

- i.  $\text{CH}_3\text{SH}$  was chosen as the only gas to represent the VSCs particularly and used with the specific methodology for detection of halitosis;
- ii. UV was selected as the light source because  $\text{CH}_3\text{SH}$  gas absorption spectrum is best identified in the UV region of the electromagnetic spectrum; and
- iii. Research engaged in the usage of a laboratory for the experiment to take place in a controlled environment with the same background temperature throughout the procedures.

### 1.5 Contributions of Research

The main contribution of this research is introducing the UV absorption spectroscopy for detection of  $\text{CH}_3\text{SH}$  gas. The characteristic absorption property of  $\text{CH}_3\text{SH}$  gas which is the absorption spectral can be acquired because the overlap of spectral absorption patterns of other gases in the UV wavelength region of 200 to 270 nm did not occur. This is important to distinguish  $\text{CH}_3\text{SH}$  gas in the air due to toxic waste or gas leakage which is hazardous so that prevention measures can be prepared.

The other contribution is this research offered a quantitative method for halitosis detection whereby the concentration of  $\text{CH}_3\text{SH}$  gas can be measured. It is based on the Beer Lambert Law that is applied in the calculation, with the known parameters input and the measurements of the unknown parameters such as the incident intensity and the transmitted intensity. Principle of the open path OFS method is important for obtaining the concentration of any gas.

## 1.6 Outline of the Thesis

This thesis is inclusive of 5 chapters which concentrate on the development of an optical based system for halitosis detection within UV wavelength region and the measurement of  $\text{CH}_3\text{SH}$  gas as the halitosis indicator.

Chapter 2 reviews previously reported halitosis detection methods that have been stated as in the literatures. The methods include quantitative, semi-quantitative and non-quantitative approach. Details explanation of the methods as well as the systems and sensors that have been developed earlier is presented. The advantages and disadvantages of the various halitosis detection methods are discussed. Then, optical methods and sensors are also identified based on the literature. The working principles of the optical gas based detection system and some of the applications were discussed. Recent studies that used UV based detection system with the OFS method were conveyed as the general understanding for the development of the proposed system.

Chapter 3 contains the details of proposed system components, related methods, techniques, instrument calibration, setup and how the detection system used in the investigations based on the objectives of the thesis. The investigations which were carried out include the works to determine the ability of the system to detect  $\text{CH}_3\text{SH}$  as halitosis indicator. Then, the act follows with checking the possibility of interference from the breathing gases and carry out the calculation of  $\text{CH}_3\text{SH}$  gas concentration for validation purpose of the detection system.

Chapter 4 conveys all results and findings of the analyses, evaluations and calculations related with the development of the halitosis detection system. Further discussions on each of the related works are also shared.

Chapter 5 is the final chapter concludes the thesis and suggests some improvement that may need to be carried out in future work.

## CHAPTER 2

### LITERATURE REVIEW

#### 2.1 Introduction

In this chapter, series of halitosis detection methods are explained. The methods as well as the systems and sensors developed earlier include non-quantitative, semi-quantitative and quantitative approached are describe. The details of methodology, advantages and disadvantages are conveyed for each detection system and summarized. Following that, some applications of the optical methods and sensors are also identified based on the literature. The optical based gas detection system working principles, the possible combination of the main components and alternative methods are introduced and discussed. Recent studies of UV based system with OFS are explained briefly for the basic understanding in the development of the proposed system.

#### 2.2 Classic Technique for Halitosis Detection

Halitosis has become continues concern, affect social communications, indicate more serious illnesses and cause unbearable self-crisis that lead to dangerous psychological act (Tungare et al., 2019). Dental professionals consultations have been seek out instead of the local and traditional remedies (Bedos et al., 2018). Since different diagnostic may have different treatment, a new device that can be used as routine clinical application for halitosis detection is proposed in this study. In constructing such halitosis detection system, it is vital to look into written facts on related methods, systems and sensors that initiated earlier by others. In dealing with halitosis, public perception is important and the expectation of the patients towards doctors' action is highly required (Tsuruta et al., 2017).



Organoleptic testing (OT) was among the fundamental halitosis evaluation. The assessment is actually a “sniff test” scoring method used by calibrated judges in an attempt to quantify the odour intensity (Anbardan et al., 2015). It does not require any special devices during the assessment but performed by examiner via smelling the patient's breath and giving a score to the halitosis level (Falcão et al., 2017). OT is also based on smelling the exhaled air of the mouth and nose and comparing the two. OT and scoring have been quite common for ages because of the simplicity even though the method is very subjective (Dudzik et al., 2015).

The human nose can pick up the scents of a large variety of different odourants at very low concentrations that are sometimes below instrumental detection thresholds (Pelosi et al., 2018). It was believed that no tool or equipment can discern or discriminate with more precision than the human nose which led ADA malodour guidelines to assign OT as the gold standard in 2009 (A. Kapoor et al., 2011; Slot et al., 2015). The intensity of halitosis is based on the Rosenberg scale (Thoppay et al., 2019) which rates odour intensity as shown in Table 2.1.

Table 2.1 Rosenberg Organoleptic Scoring Scale

Category	Description
0: Absence of odour	Odour cannot be detected
1: Questionable odour	Odour is detectable, although the examiner could not recognize it as malodour
2: Slight malodour	Odour is deemed to exceed the threshold of malodour recognition
3: Moderate malodour	Malodour is definitely detected
4: Strong malodour	Strong malodour is detected, but can be tolerated by examiner
5: Severe malodour	Overwhelming malodour is detected and cannot be tolerated by examiner (examiner instinctively averts the nose)

However, OT is limited because the results have low objectivity, reproducibility and difficulty in calibrating among examiners (Yoneda et al., 2015). It is not easy to quantify the level of halitosis based on the intensity of an odour itself. Normally, a descriptive scale from no odour, weak, middle and strong is used. However, middle odour is almost impossible to quantify. The base measurement of no odour is tangible,



but the highest range of strong or severe malodour is infinite. OT is not a favourable assessment to patients participating in the test (Alasqah et al., 2016). They normally feel uncomfortable to exhale their breath for the judges to sniff. There are also restrictions to patients such as to avoid taking food which is spicy, contain garlic and onion for at least 48 hours before the test. Usage of scented cosmetics is also prohibited 24 hours prior to the assessment. Patients are refrained from any food and drink for 12 hours before the test.

This method may not be consistent and acceptable for some cases. It is due to evaluation of the examiners which can be different from one another because there are certain aspects which can affect the organoleptic senses of a person (Cavazzana et al., 2018). Factors like hunger, menstrual cycle, head position, degree of attentiveness and expectation are most likely contribute the disparity among examiners. Furthermore, if the assessment has been carried out for such a long period of time, the olfactory sense become accustomed to odours and the examiner will undergo loss of sensitivity (Weiss et al., 2019). Even if a mean score from a panel of examiners can be used as the result, there are also several other complications that contribute to the failure of the organoleptic assessment. The most common cause was discovered in previous studies that the concentration and composition of the sample delivers to an examiner will be different to the next examiner (Laleman et al., 2014). It has been found that diseases can also transmit to the examiners through the exhaled air (Falcão et al., 2017).

### **2.3 Quantitative Analysis of Halitosis**

Quantitative analysis is extremely beneficial for measuring the intensity of halitosis, afterwards to identify the causes and finding the right treatment. In the dental field history, Fair and Wells have made the first attempt to detect halitosis quantitatively in 1934 (Oeding et al., 2017). They used osmoscope specifically to measure odour density in one's breath. Following that, Fosdick and his associates managed to conduct several studies using the osmoscope to acquire general information on the causes and conditions of halitosis (Chawla et al., 2015). However, the methods that they have been using is still very subjective and questionable thus producing semi-quantitative result of the osmoscope (M. U. S. Rao et al., 2015). Reliable diagnosis which could convince the patients was in need and machine-based measurement started to be developed in 1960s

to evaluate the concentration of VSCs quantitatively as an alternative to organoleptic testing as well as the osmoscope.

VSCs are the most common key contributor to halitosis (Yoneda et al., 2015). Indeed, exhaled VSCs have been proposed as biomarkers for diagnosis and monitoring of halitosis (Laleman et al., 2014). Thus, the main approach of constructing halitosis detection system is actually based on assessment of VSCs that produced orally. Following that, many more halitosis detection methods such as gas chromatography (GC) and sulphide monitors were introduced by researchers and practitioner. GC and sulphide monitors are both used quantifiable method and known as halitometers. Generally, halitometer is widely used because it gives a numerical index result.

### 2.3.1 Gas Chromatography

In general, GC is the process when mixture of gases is separated into individual components. Once isolated, the components can be evaluated individually. Conventionally, GC with flame ionization detection has been constructed to detect halitosis. Quite a number of volatile components successfully identified by GC, but it failed to detect VSCs. Improvement was made to GC with development of a Flame Photometric Detector (FPD) system (Nayak et al., 2018; Yaegaki et al., 2012). The schematic diagram of the latest GC-FPD system that uses water stationary phase for analysing organic sulphur compounds is shown in Figure 2.1.

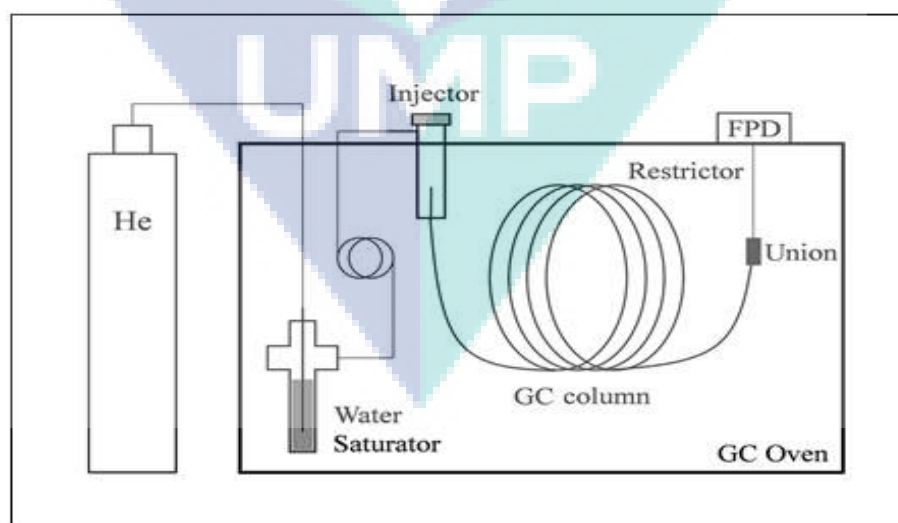


Figure 2.1 Schematic Diagram of GC-FPD system

Source: McKelvie & Thurbide (2017)

GC-FPD was considered one of the most consistent measurements for halitosis detection. The GC method is highly objective and reproducible thus GC-FPD measurement is very reliable. Furthermore, the measurement was specific to sulphur compounds only. Nevertheless, an experienced operator is needed to handle GC-FPD because of its complexity and somewhat a sophisticated piece of equipment. The device is quite expensive and very large which are not practical for routine examinations usage in dental practices.

GC was then coupled to Mass Spectrometer (MS) and become a new device GC-MS which applied techniques such as separation, identification and quantification of chemicals complex mixtures (Reber, 2018). The GC separates the mixture of VSCs into its components and the MS records a spectrum of the individual components as they leave the column. GC-MS can determine very low VSCs concentrations and the analysis is highly accurate (Kim et al., 2016). However, a compound must be sufficiently volatile and thermally stable in order to use GC-MS for the analysis. Highly skilled operators are required for GC-MS handling because it uses sophisticated analytical techniques. The schematics diagram of GC-MS instrument is shown in Figure 2.2.

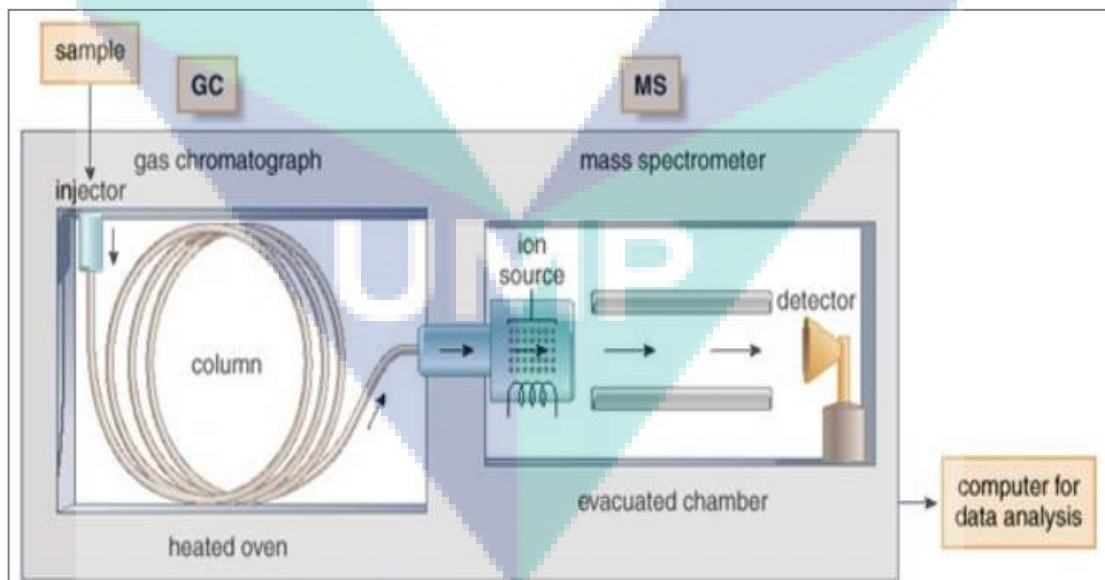


Figure 2.2 Schematic Diagram of the GC-MS

Source: Kim *et al.* (2016)

GC-MS is not really suitable for routine diagnosis at the doctor's clinic or at patient's home (Hakim et al., 2012; Han et al., 2017). As a matter of fact, the procedure

is high in cost and made the device less favourable. In the devices that use GC method, sensitive photometric sensors were installed to get accurate measurements of specific gases. The sensors made possible for VSCs to be discriminated and calculated when needed. There were also evident that GC method could be used to determine the origin of halitosis whether orally or systemic. Moreover, GC based devices have the capability to measure other compounds too (Scully et al., 2012; Thakur, 2019). Thus, they were considered the best and most precise technique used for VSC assessment in human breath for the researchers but their structures were unacceptable for clinical applications.

### 2.3.2 Compact and Simple Gas Chromatography

In order to overcome the disadvantages of the bulky GC units introduced earlier, a compact and simple device such as OralChroma that utilises the GC method was developed. These instruments have similar accuracy to conventional GC-FPD. These simple GCs are compact, and a lot cheaper than the other GCs. Additionally, trained operators are not required for the handling is much easier. OralChroma combines GC method with an indium oxide ( $\text{In}_2\text{O}_3$ ) Semiconductor Gas Sensor (SGS) to detect halitosis (Yoneda et al., 2015). Figure 2.3 shows the schematic diagram of the OralChroma that use GC-SGS analyzer method.

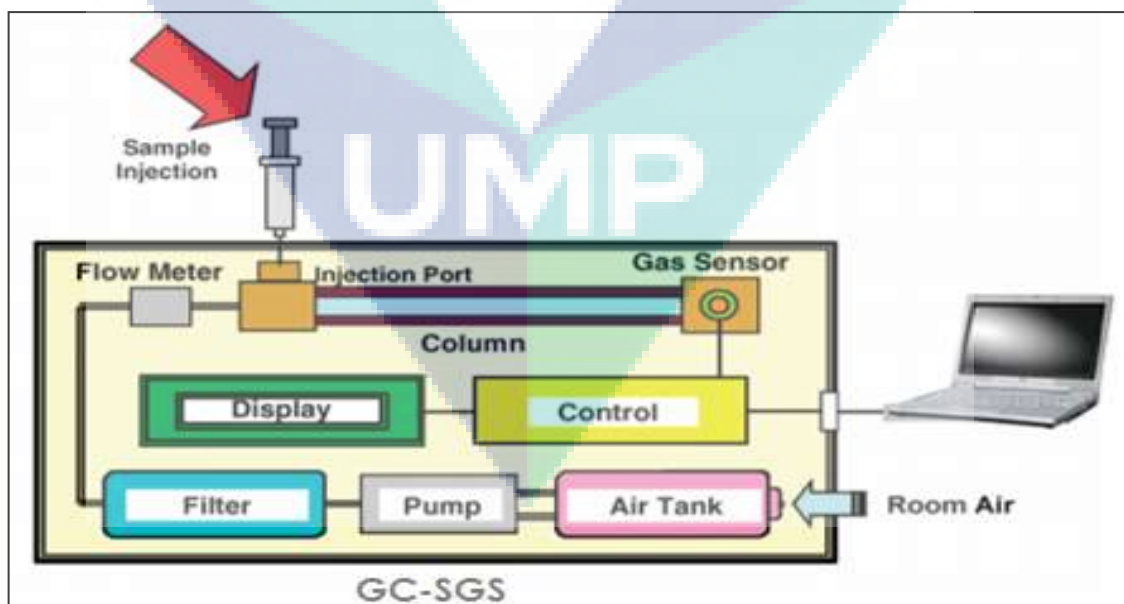


Figure 2.3 The OralChroma using GC-SGS Analyzer Method

Source: Lopes et al. (2014), Murata et al. (2006)

This device can be used anywhere if there is electricity and does not need any specific carrier gas such as Helium or Nitrogen ( $N_2$ ). It can be operated in a normal room and uses the room air as the carrier gas for the chromatographic column. The device is able to measure the amount of each VSC which later will guide the practitioner to determine where the problem lies and to suggest best treatment to eliminate it. The procedure starts with the specific process of the sample acquisition from the patient and putting the sample collected in the syringe into the inlet located at the top of the device (Lopes et al., 2014). The OralChroma will display the result with considerable precision after eight minutes. A computer with a specific software program needs to be connected first to allow the result which consists of a graph corresponding to the peaks and concentrations of VSCs (0 to 2913 ppb) to be displayed and stored in the program.

The device itself has its own storage of the data which can be retrieved at any time and comparisons of the readings before, during and after treatment are possible to do repetitively. Even though the OralChroma takes longer time to measure absolute concentrations for each of  $CH_3SH$ ,  $H_2S$  and  $CH_3CH_3S$  but it is highly accurate even if the measured compound has very low concentrations. The device also has the ability to discriminate the main three VSCs that associated with halitosis. Although the correlation with organoleptic scoring signify moderate accuracy, the device is better because it could contribute both in diagnosis and also in better sub-classification of halitosis. On the other hand, it is expensive and not suitable for routine clinical purpose. Furthermore, the room air act as a carrier gas and this might lead to impurities and contamination of the sample (Laleman et al., 2014).

Another compact, simple and portable GC called the Twin Breasor was also developed. Almost complete correlation was reported when comparing the Twin Breasor with traditional GC (Yoneda et al., 2015). Very accurate measurements were found for the two major VSCs,  $H_2S$  and  $CH_3SH$  with the coefficients of determination were 0.94 and 0.81, respectively. The Twin Breasor can be operated without attaching to a personal computer unlike the OralChroma that need a personal computer for it to be functional. However, it failed to measure concentration of  $CH_3CH_3S$ , a minor component of VSCs and it was also reported that the procedure take long time to finish

because of the prolong measurement time. Figure 2.4 shows a patient is using Twin Breasor in a clinic for halitosis assessment.



Figure 2.4 A Patient using Twin Breasor for Halitosis Assessment  
Source: Tamaki et al. (2011)

### 2.3.3 Portable Sulphide Monitors

Sulphide monitors which was said to be more practical was then established with the used of electrochemical instrument in measuring total VSCs. Sulphide monitors was utilised to identify  $H_2S$  and  $CH_3SH$  which were acknowledged as the major component of halitosis that originated from periodontal disease. The past three decades have seen the creation of quite a few portable and simpler to use devices for VSCs assessment in the breath (Laleman et al., 2014). Many practitioners, investigators and practicing dentists started to use portable sulphide monitors.

Halimeter is a portable monitor that is widely acceptable because it is small, portable and provides a rapid and objective result with a quick turn-around time between measurements (Falcão et al., 2017). It provides a digital display of the total oral VSC concentration and has been in used for quite some time as it was easy to use and with satisfying reproducibility result. The device is based on electrochemical measurements that involved a volumetric non-selective gas sensor method for measuring the total sulphur containing compounds in a given sample. Figure 2.5 shows Halimeter, the portable sulphide monitor that measures VSCs.





Figure 2.5 Halimeter as the Device for Measurement of VSCs  
Source: Agarwal et al. (2013)

The feasibility of the Halimeter was assessed by different studies and it does not meet the requirement to be considered as an ideal device for halitosis detection. Among the issues raised were the diagnostic threshold which ranging from 75 to 150 ppb and the correlation with organoleptic scoring which was inconsistent (Nakhleh et al., 2017). The Halimeter showed different sensitivity to  $\text{CH}_3\text{SH}$  and  $\text{H}_2\text{S}$ . Consequently, if  $\text{CH}_3\text{SH}$  is the predominant VSC detected in patient's breath, a deceptively low reading will be displayed. Furthermore, the Halimeter is highly sensitive to ethanols and essential oils. High readings will be produced if by any chances patients used rinses containing these compounds prior to measurement. The Halimeter shows a loss of sensitivity to the sulphur compounds when the detection take longer time and this modified version of the industrial sulphide monitor also has limited ability to distinguish between various compounds. However, the main drawback of the Halimeter is its difficulty to distinguish between VSCs, and the insensitivity to non-sulphuric volatile compounds (Laleman et al., 2014).

Another halitosis monitor, the Breathtron was then introduced for measurement of sulphur compounds that is based on a zinc oxide membrane semiconductor sensor which is highly sensitive to VSCs (Nakhleh et al., 2017). A more specific measurement than the Halimeter was established for Breathtron where the exhaled non-sulphuric compounds are first trapped and eliminated from the sample and lower down the likelihood of confounding effects (Laleman et al., 2014). The Breathtron retains most of Halimeter's advantages for global measurement of sulphur compounds that is portable, easy to use, reproducible, and providing almost instant results. In addition, the

correlation between the results achieved by the Breathtron and the organoleptic scoring were higher and more consistent (Sakagami et al., 2016). Image of the Breathtron is shown in Figure 2.6.



Figure 2.6 The Breathtron as the Sulphur Compounds Measurement Device  
Source: Sakagami et al. (2016)

Once again, inability to discriminate among different sulphuric compounds and failed to detect the potentially informative non-sulphuric volatile compounds are the major drawbacks (Laleman et al., 2014; Nakhleh et al., 2018) of the Breathtron. Furthermore, various studies debated the diagnostic threshold and shown the possibility of using a wide range of cutoffs within the range between 250 and 400 ppb (Yoneda et al., 2015). Sulphide monitoring using the electrochemical instrument to quantify total VSCs is a reliable method for monitoring malodour and treatment but not suitable for detection purpose. This method primarily identifies  $H_2S$  and to the smallest degree of  $CH_3SH$  but cannot detect other important factors.

Another portable sulphide monitor named B/B Checker has become available. This compact and simple gas monitor developed to measure level of halitosis from exhaled and nasal air. The size of the BB Checker is W 210 mm × D 230 mm × H 80 mm. The result is obtained automatically and output value is printed using a built-in printer. BB Checker was equipped with newly invented direct gas sensor which is capable to detect several kinds of gases in a short time. Figure 2.7 shows the portable sulphide monitor to detect halitosis.



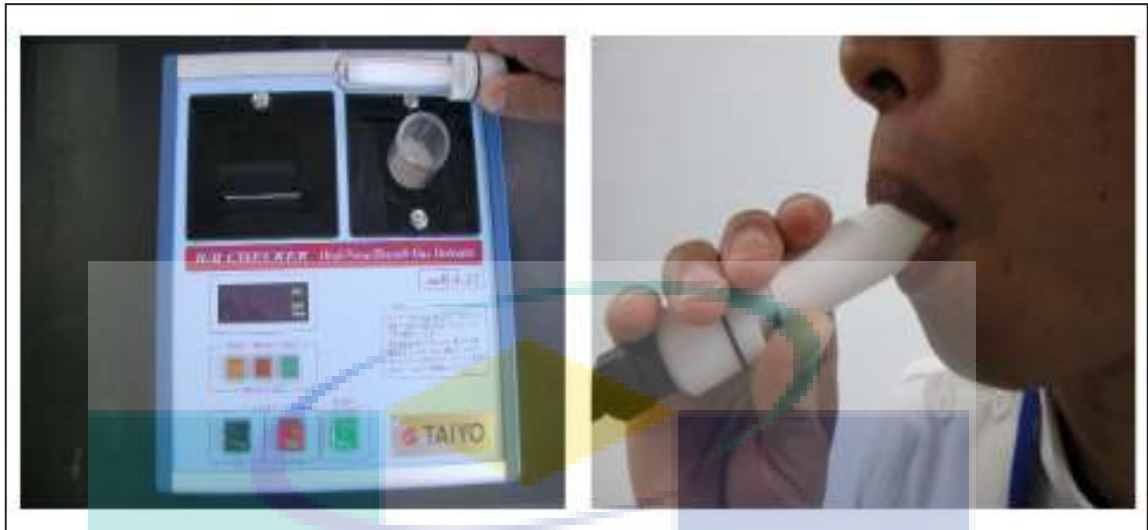


Figure 2.7 A Portable Sulphide Monitor, BB Checker with the Adapter.

Source: Tamaki et al.(2011)

The BB Checker states the bad breath value as the olfactory intensity of human according to the Weber-Fechner law. The measurement method is effortless when applied to halitosis patient as the subject. There are two types of measurement involved, exhaled and nasal air. For exhaled breath, the subject were asked to breathe in deep and held his breath for 15 s, then tried to exhale completely the air from the lungs through the adapter over 15 s. The BB Checker able to measure halitosis levels in the terminal lung gas. Nasal air measurement is carry out using the inserted sensor probe into the right and left nasal, one after the other. The halitosis level in nasal air from both nasal cavities was analyzed separately. However, the drawbacks of this portable device is its overall sensitivity and specificity which do not exceed 50 % (Nayak et al., 2018).

A dental device, Diamond Probe/Perio 2000, designed to detect and measure VSCs produced by periodontal pathogens. This halitosis detection system combines periodontal probe with a micro-sulphide sensor. It is able to measure probing depth, bleeding on probing and sulphide concentrations at the periodontal pockets. Figure 2.8 shows the Diamond Probe/Perio 2000 system.



Figure 2.8 Diamond Probe/Perio 2000 System

Source: Kinane & Lowe (2000)

The unique micro-sulphide sensor which located at the tip of the probe responds to sulphide ions. Thus, generates a voltage that is quantifiable and proportional to the sulphide concentration. High sulphide level will indicates high level of halitosis hence implying high level of anaerobic bacteria activity. Nonetheless, major drawbacks of this portable system are disability in distinguishing one type of sulphide odour from another and difficulty in distinguishing individual compounds from the family of VSCs.

#### 2.3.4 Electronic Noses

Difficulties of GC and less sensitivity of sulphide monitors made possible for electronic noses to be constructed. The imitation of human olfactory abilities made them more sensitive (Dung et al., 2018). This device is easy to use with an integrated probe to measure sulphur compounds. Sulphide compounds from periodontal pockets and on the tongue surface generate an electrochemical voltage through the sulphide sensing probe. Following that, this voltage is measured by an electronic unit and displayed as a digital score on the sensor's screen. This chemical sensor based electronic noses used the same working principle as sulphide monitors (Hu et al., 2018). The sensors are able to measure ammonia and  $\text{CH}_3\text{SH}$  compounds from breath air and some of them can measure each VSC separately. They are called electronic nose because of their sensitivity is similar to GC and measurement results are highly close to OT scores.

The Cyranose 320 as shown in Figure 2.9 is one example of the electronic nose which is able to detect and identify complex chemical mixtures which produced halitosis. The device is constructed to a fully-integrated handheld sensing instrument. It is also utilised to identify simple mixtures and individual chemical compounds. Usage of the Cyranose 320 is not limited to detection of halitosis only but was used in diverse industries such as chemical, food and beverage, petrochemical, packaging materials, other medical research and many more (Gancarz et al., 2017).

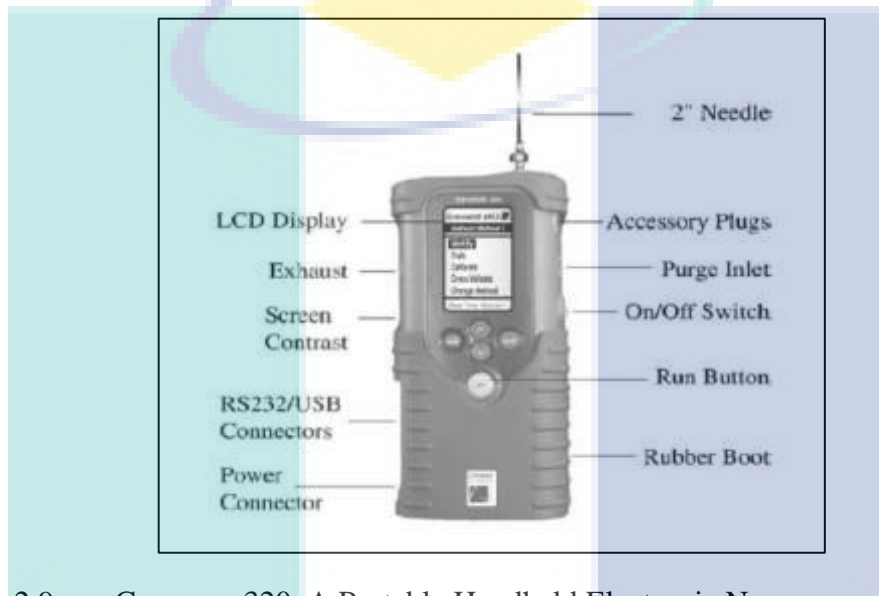


Figure 2.9 Cyranose 320, A Portable Handheld Electronic Nose  
Source: Hidayat et al. (2010)

There are many other electronic noses were established other than Cyranose 320. In order for these electronic noses to be use for clinical diagnosis, versatile sensing techniques were introduced to open up new possibilities. Nevertheless, several studies have shown that electronic noses generally suffer from significant drawbacks that limit their widespread application in clinical diagnosis. The drawbacks include sensitivity to temperature, humidity and interference with other gases (Tian et al., 2016). Moreover, this technique cannot determine volatile chemicals precisely, and it is difficult to distinguish mouth-air compounds from others (Wilson, 2018).

### 2.3.5 Chemical or Enzymatic Tests

Other than electronic noses, chemical or enzymatic approach for halitosis detection system also has been proposed extensively. BANA test is a rapid enzymatic test which can be performed in about 15 minutes (Dhalla et al., 2015). It is a chair side

diagnostic test that detects bacteria such as *Porphyromonas gingivalis*, *Treponema denticola* and *Tannerella forsythia*. These odoriferous periodontal microorganisms are the active VSCs producers indicating the presence of halitosis (Nani et al., 2017). The enzyme capable of hydrolysing BANA present on the test strips which is commercially available. The BANA-Enzymatic test kit is shown in Figure 2.10 below.



Figure 2.10 BANA-Enzymatic Test Kit

Source: Dhalla et al. (2015)

In this procedure, biofilm extracted from the oral cavity is applied to the test strip. If bacteria having hydrolase are present in the biofilm, they will hydrolyse BANA. Positive result of the biochemical reaction obtained when the BANA strips turn to blue colour. BANA strip is able to give such result because these 3 bacteria (or 1 or 2 of them) or another BANA-positive bacterium exist. If the test strip turns bluer, it means that the concentration of organisms is higher and the number also greater. It was found that specificity and sensitivity of the BANA test is above 80 % (Bollen, 2015). However, BANA test is considered unreliable because there are 37 other bacteria that can hydrolyse arginine other than the 3 odoriferous bacteria. It is also an indirect method to prove the presence of halitosis and can be considered as semi-quantitative assessment because the test result depends on the intensity of the blue coloration (Schmidt et al., 2015).

Another enzymatic test,  $\beta$ -galactosidase test identifies an enzyme that may be related with odoriferous bacteria. Amounts of bacteria producing VSCs in saliva are positively correlated with  $\beta$ -galactosidase activity (Aylikci et al., 2013).  $\beta$ -galactosidase activity can be measured using discolouration of paper disc method. Saliva was taken in

the paper disc and discolouring of the paper disc is observed. The scale is based on the colour changes; no colour: 0, faint blue colour: 1 and moderate to dark blue colour: 2. Even though  $\beta$ -galactosidase tests have positive correlation with organoleptic scores but it is still a semi-quantitative assessment. Following that, quantifying  $\beta$ -galactosidase activity was carried out. This quantitative analysis measures an enzyme that is related with odoriferous bacteria. The quantitative analysis of oral bacteria in saliva revealed that the amounts of bacteria producing VSCs were positively correlated with  $\beta$ -galactosidase activity. Thus, salivary levels of the enzyme were found to be correlated with halitosis. Numerous glycoproteins that contained in salivary mucins and epithelial cell components are the active halitosis producer and measurable using  $\beta$ -galactosidase Assay Kit. Although quantifying  $\beta$ -galactosidase activity is able to be done in a clinic, but the procedures is time consuming, meticulous and involved the usage of other devices such as spectrophotometer and Protein Assay Kit (Masuo et al., 2012) .

Ninhydrin method is another enzymatic test that used Ninhydrin colorimetric reaction for detection of amines or polyamines which cannot be measured with sulphide monitors. This halitosis detection method is simple, rapid, and cheap. In a study for detecting low-molecular weight amines in breath air, a sample of saliva and isopropanol is mixed and centrifuged. Then the mixture diluted with isopropanol, a pH 5 buffer solutions and ninhydrin reagent. Following that it is refluxed in a water bath for 30 min, cooled to 21.8°C and diluted with isopropanol until the volume reach 10ml. Spectrometer for determination of light absorbance readings was used. One obvious limitation of the test is the fact that ninhydrin reacts not only with amines but also with ammonia N<sub>2</sub>, resulting in data misleading (Aydin et al., 2016).

Indole test is used to determine the ability of an organism to split amino acid tryptophan to produce indole. Tryptophan is hydrolysed by tryptophanase to form indole and another 2 possible end products, pyruvate and ammonium ion as shown in Figure 2.11. There are two methods for indole test. The first method used a conventional tube for overnight incubation to detect weak indole producing organisms. The second method is a spot indole test which identifies rapid indole producing organisms. Indole which produced from the deamination process has a bad odour. It was assessed in the mouth because the condition which related to halitosis criteria (Schmidt et al., 2015). However, the volatility of indole is low and the correlation of odour concentration with the indole amounts was not clear. Furthermore, it has low perception threshold and remains resolved in saliva as an intercellular signal molecule.



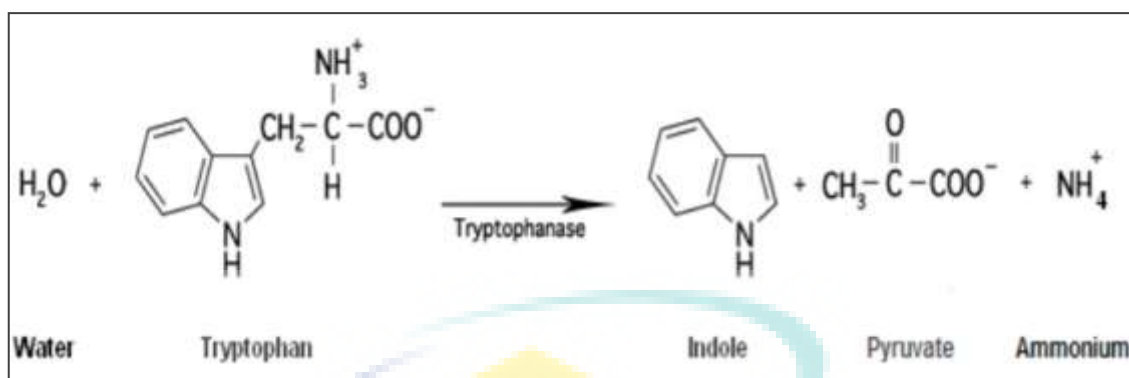


Figure 2.11 Indole Test Reaction Process

Source: Phe (2018)

Salivary incubation test was introduced because its advantage of having much less influenced by external parameters than organoleptic measurements (Aydin et al., 2016). The external parameters include subjectivity, scented cosmetics, drinking coffee, smoking, eating spicy food and odourous food such as garlic and onion. This test uses salivary samples for halitosis examination because it contains sulphur containing substrates that produce VSCs. The saliva which collected in a glass tube was then incubated for several hours at 37°C in an aerobic chamber under an atmosphere of 80% N<sub>2</sub>, 10% CO<sub>2</sub>, and 10% hydrogen. Following that, the odour was measured by an examiner. It was found that the result shown a strong correlation with organoleptic and sulphide monitor measurements. However, this test can only detect halitosis that emanate from the oral cavity but not from extraoral causes (Nani et al., 2017).

Ammonia monitoring is another method that has been developed based on the hypothesis that ammonia produced by oral bacteria point towards halitosis (Agarwal et al., 2013). The concentrations of ammonia produced by the oral bacteria were measured with a portable monitor. This device constructed with a pump, which can draw air through an ammonia gas detector tube connected to a disposable mouthpiece placed inside a patient's mouth. The concentrations of ammonia can be read from a scale. This technique is rarely used because of the procedure is time consuming and high in cost (Anbardan et al., 2015; U. Kapoor et al., 2016).

The related works of developed halitosis detection methods with the advantages and disadvantages are summarized and presented in Table 2.2.

Table 2.2 Halitosis Detection Methods, Advantages and Disadvantages

Detection Methods	Details	Advantages	Disadvantages
OT	A classique technique based on breath sniffing by judges and scoring given using specific scale	Does not require special devices, human nose can pick up various scents at very low concentrations	Uncomfortable to patients, have low objectivity, reproducibility issue and difficulty in calibrating among examiners.
Osmoscope	First attempt for quantitative halitosis detection by measuring odour density.	Managed to acquire general information on the causes and condition of halitosis	Very subjective and questionable method that produced semi-quantitative result.
Conventional GC	Mixture of gases separated into individual components	Volatile components can be identified and evaluated individually	Failed to detect VSCs
GC-FPD	Measurement was specific to VSCs only.	Highly objective and reproducible result	Complex device that need experienced operator to handle, expensive and very large.
GC-MS	Techniques applied inclusive of separation, identification and quantification of chemicals complex mixtures	Able to determine very low concentration of VSCs and highly accurate analysis	Not suitable for routine diagnosis because highly skilled operators needed and high in cost.
OralChroma	Combines GC method with $\text{In}_2\text{O}_3$	Portable GC that does not require trained operators.	Longer measuring time than conventional GC, expensive and usage of room air may lead to contamination of sample.

Table 2.2 Continued

<b>Detection Methods</b>	<b>Details</b>	<b>Advantages</b>	<b>Disadvantages</b>
Twin Breasor	Compact, simple and portable GC	Can be operated independently without attaching to a computer	Failed to measure minor component of VSCs and prolong measurement time.
Halimeter	Device is based on electrochemical measurements	Portable sulphide monitor that provides a rapid and objective result for measurement of VSCs.	Difficulty to distinguish between various compounds especially VSCs and insensitive to non-sulphuric volatile compounds.
BB Checker	Equipped with direct sensor for measurement of halitosis in nasal air.	Compact, simple and used effortless method	Overall sensitivity and specificity do not exceed 50 %.
Diamond Probe/ Perio 2000	Dental device that combines periodontal probe with micro-sulphide sensor	Able to measure probing depth, bleeding on probing and sulphide concentrations at the periodontal pockets	Cannot distinguish one type of sulphide odour from another, and has difficulty distinguishing individual compounds from the family of VSCs.
Cyranose 320	Portable handheld electronic nose.	Able to detect and identify complex chemical mixtures which produced halitosis	Sensitivity to temperature, humidity and interference with other gases. This technique cannot determine volatile chemicals precisely, and difficult to distinguish mouth-air compounds from others.



Table 2.2 Continued

Detection Methods	Details	Advantages	Disadvantages
BANA test	Chair side enzymatic test that detects bacteria producing VSCs.	Rapid test, can be performed in about 15 minutes	Semi-quantitative assessment, unreliable and indirect method to prove halitosis presence.
$\beta$ -galactosidase test	Identifies enzyme that related with amounts of bacteria producing VSCs in saliva.	Positive correlation with organoleptic scores	Time consuming, meticulous and involved usage of other devices to get quantitative result.
Ninhydrin method	Enzymatic test that utilizing Ninhydrin colorimetric reaction for detection of amines or polyamines which cannot be measured with sulphide monitors.	Simple, rapid and cheap	Ninhydrin reacts not only with amines but also with ammonia nitrogen, misleading result.
Indole test	Determine the ability of an organism to split amino acid tryptophan to produce indole which related to halitosis criteria.	Offered 2 choices of tests, overnight incubation to detect weak indole or spot test for rapid indole	Indole is low in volatility, low perception threshold, remains resolved in saliva and shows unclear correlation with odour concentration.
Salivary incubation test	Test involved incubation of collected salivary samples, the odour was then measured by examiner	Test not influenced by external parameters, result shown strong correlation with organoleptic and sulphide monitor measurements	Can only detect halitosis that emanate from the oral cavity but not from extraoral causes.

Table 2.2 Continued

Detection Methods	Details	Advantages	Disadvantages
Ammonia monitoring	Method has been developed based on the hypothesis that ammonia produced by oral bacteria point towards halitosis.	Portable monitor able to display concentrations of ammonia	Time consuming and costly.
The Proposed System	An optical detection system within UV wavelength region applied with an open path technique of the OFS to detect halitosis via existence of CH <sub>3</sub> SH	Able to identify the exact gas components based on their unique properties such as absorption spectra, no cross sensitivity issues with breathing gases and concentration of VSC can be measured	Specifically used CH <sub>3</sub> SH gas only to represent VSC but not the other two components.



## 2.4 Optical Based Gas Detection System

Optical based gas detection systems play an increasingly important role in a variety of scientific, industrial and commercial applications (Jin et al., 2013; Potyrailo, 2016). These systems found to be more reliable not just for halitosis diagnostic but also for breath analysis (Henderson et al., 2018). Detection systems based on the interaction of light with gas molecules can offer high sensitivity and long term operation stability (Tomberg et al., 2018). Most optical based gas detection system rely on absorption spectroscopy (Hodgkinson et al., 2013), where a gas is detected by measuring the light absorbed (due to its interaction with the gas) as a function of wavelength. Light can be absorbed or emitted by atoms and molecules. In general, the structures of atoms and molecules which have been determined using light likely to be able to reveal the properties of the entity involved (Glenn, 2020). The technique of observing the absorbed or emitted light is referred as spectroscopy (X. Zhu et al., 2019). The optical based gas detection system represented by four basic components which are light source, suitable optics for directing light to and from the sensor, sensing materials or sensor and a photo detector for detecting light signals coming from the sensor.

### 2.4.1 Light Source

Light is also known as electromagnetic radiation. It consists of energy in little packets called photons which have properties of both particles and waves. All waves have a wavelength, and as for light, the wavelength range is quite vast (Elliott et al., 2018). Light source with emission in the range of interest is the core component of the optical based gas detection system (Hodgkinson et al., 2013). There are wide selection of light sources which suitable to be used for examples the highly coherent gas and semiconductor diode lasers, broad spectral band incandescent lamps, and narrow-band, solid-state, light emitting diodes (LEDs) (D. Zhu et al., 2016). For various applications purpose, there are many types of technology-based broadband light sources that have been produced commercially (Song et al., 2016) and the wavelength ranges of the light sources may differ from one manufacturer to another (Deng et al., 2017). The summary of commercially available broadband light sources is shown in Table 2.3.

Table 2.3 Summary of Commercially Available Broadband Sources

Broadband Source	Wavelength Range (nm)
Halogen Test	300 – 1700
Deuterium Test	180 – 370
Xenon Arc	220 – 1500
LED	255 – 7000
Laser Diodes	375 – 3800

Corresponding to fundamental vibrational and rotational energy transitions (House, 2018), many important gas molecules have characteristic absorption lines in the UV spectral region which is the wavelength approximately between 180 to 400 nm. Figure 2.12 shows the components of the electromagnetic spectrum and the subdivision of UV light into different classes. The region of UV-A, just next to the visible region in wavelength is called near UV and has the longest wavelength of 320 to 400 nm. UV-B is the middle UV that has the wavelength of 280 to 320 nm and UV-C is the far UV which has the shortest wavelength of 200 to 280 nm. The sun is a natural and strong source of UV radiation, but atmospheric absorption eliminates most of the shorter wavelengths of UV-C.

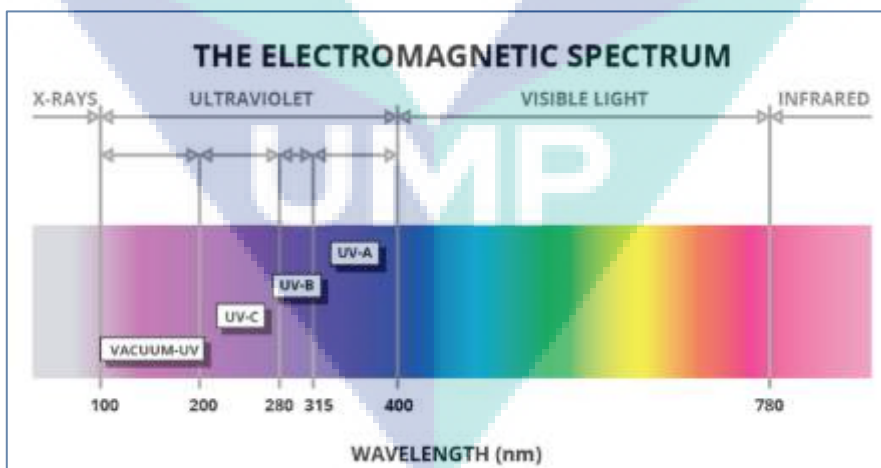


Figure 2.12 Components of the Electromagnetic Spectrum and UV Subdivision  
 Source: Lucas (2017)

UV sources are characterized using wavelength range, optical output stability, lifetime, and input power. In spectroscopy applications, a UV emission source should be stable and have enough power intensity for the desired wavelength. Light stability is commonly characterized by fluctuation (short-term stability) and drift (long-term stability). The stability of emitted light output is usually quantified by the ratio of variation in the intensity of emitted light to the mean intensity of the emitted light. It is an essential factor in defining the accuracy and reliability of a spectrometer. Typically for analytical detection, the concentration is determined with sequential measurements of the sample and reference gases that are alternatively injected into the gas cell. It is therefore important to have a stable light output between the two measurements. Lifetime is usually defined as the time when the light output exceeds a specified range of fluctuations (Li et al., 2018). Lifetime affects the cost of equipment. Shorter lifetime results in frequent replacement impacting the total price of use. Figure 2.13 shows the emission spectra of the common UV sources such as xenon flash lamp, deuterium lamp, mercury lamp, and UV LED for comparison purposes.

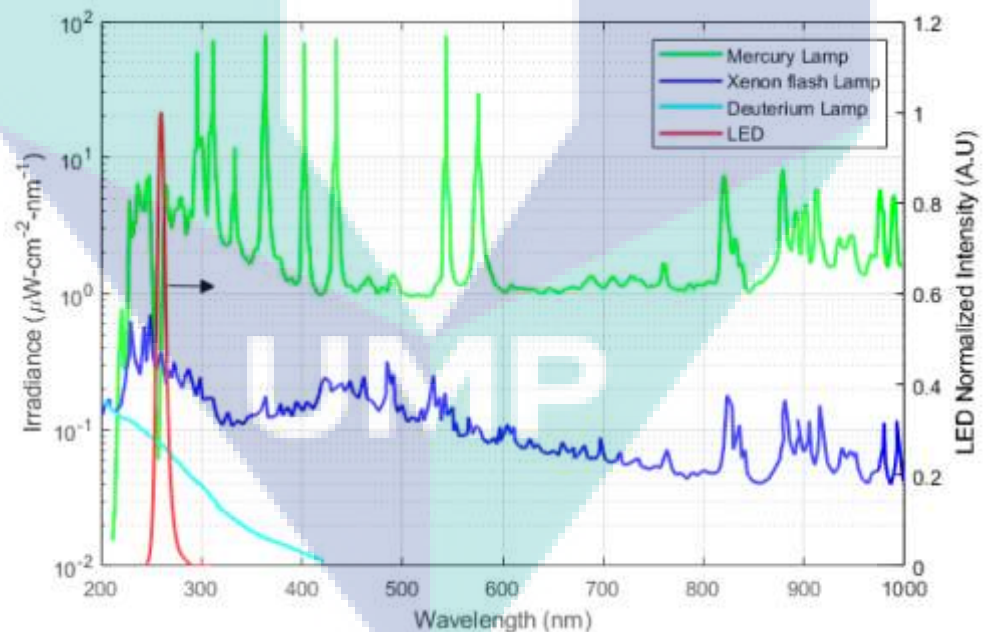


Figure 2.13 The Output Intensity of Different UV Sources  
 Source: Khan et al. (2019)

The mercury and xenon lamp have been used as the UV emitters in spectrometric studies. Their limitations include low output stability and requirement of high power input. In addition, mercury lamps contain hazardous waste. LED-based optical devices normally have been developed for infrared and visible light application because LEDs for lower wavelength which is less than 350 nm need a higher bandgap at the semiconductor junction. At lower wavelength, the photon conversion efficiency is small, which lead to low-power UV emission, high cost of devices, and negative thermal effects. Deuterium lamps are relatively more stable (fluctuation < 0.005%) than other UV lamp alternatives. It has relatively high-intensity light output with longer lifetime. However, in constructing an optical device, in order to cover the whole UV region, a combination of two technology based UV emitters i.e. deuterium lamp and halogen light is needed to provide continuous light (Khan et al., 2019).

#### **2.4.2 Optical Fibres**

In the development of optical detection system, optical fibres normally used as the suitable optics for directing light in the spectral range to and from the sensor (Pospíšilová et al., 2015). Theoretically, light travels in straight lines and reflecting off headed obstacles. But, optical fibres allow light to travel in any direction and bending around corners. Guiding of light by refraction is the principle that originally ignites fibre optics studies (Morris et al., 2016). It was first demonstrated in the early 1840s by Daniel Colladon and Jacques Babinet in Paris (Magoun, 2019). However, optical fibres were seriously studied and used widely only during late 70s throughout the early 80s. It was started with the earliest production of plastic or polymer optical fibre (POF) inspired by the telecommunication industry which later elevated the development of optical fibre sensor (OFS) for detection of humidity change around the nose and mouth area in 1977.

POF is a type of optical fibre that uses polymethyl methacrylate (PMMA) as the core material that allows the transmission of light (Oliveira et al., 2018). The material usually provides good robustness to the sensor design. POF is low in cost and easier to use than glass optical fibre for it can effortlessly cut and bent to fit in hard-to-reach areas. The POF data transfer speed of 2.5GB/s is much faster than traditional copper wire but not as fast as glass optical fibre (Inoue et al., 2018). The low attenuation and large wideband of fibre compared to traditional optical fibre that makes it more suitable

for high bandwidth signal transmission over short distances. Since then, they have been commercially used in communication systems, medical imaging and mechanical engineering inspection (Méndez, 2016; Plümpe et al., 2017).

Optical fibres become widespread and start to replace many transmission lines for communication primarily because of their broad transmission capacities. A basic conventional optical fibre is made of core and cladding (Okamoto, 2006). Core is the thin centre of the fibre where the light travels while cladding is the outer optical material surrounding the core that reflects the light back into the core. In order to protect the fibre from damage and moisture, plastic or polymer coating is use outside the fibre. However, this buffer coating is usually an option. Optical fibres are capable of carrying more information over longer distances. A single mode optical fibre can transmit trillions of bits per second when the signals are wavelength multiplexed (Agrawal, 2016). These are among the reasons why optical fibres are more prevailing than electricity and copper wire when considering any sensor system. Figure 2.14 shows an image of the optical fibre with the illustration of its basic structure and copper cable.

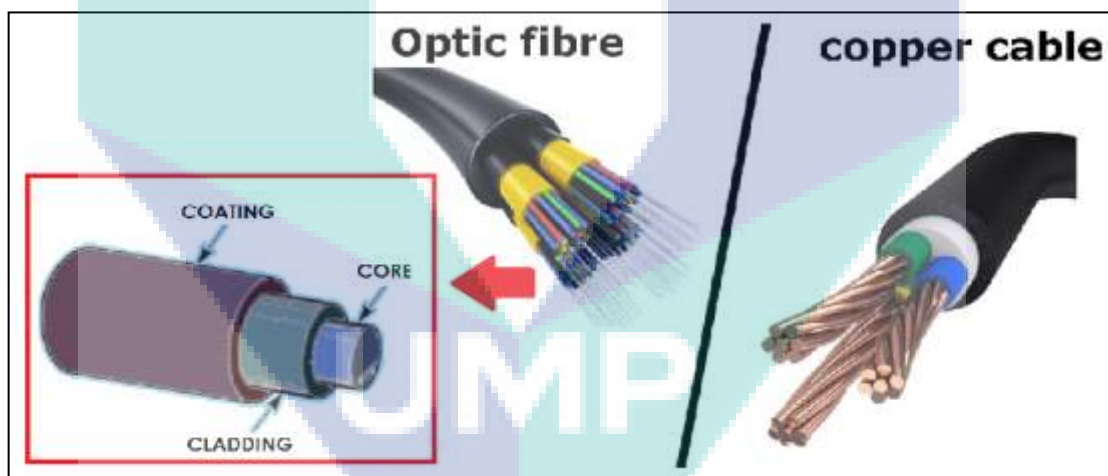


Figure 2.14 Image of an Optical Fibre and Copper Cable

Source: Gong et al. (2019)

Fibre which is lighter and thinner than copper can be less expensive where several miles of optical cable are cheaper than equivalent lengths of copper wire. Even the silica glass as the main production material of the optical fibre is inexpensive and high in supply. Optical fibre promotes less signal degradation compared to copper wire (Ikporo et al., 2016). No electromagnetic interference and highly secure during transmission. Unlike electrical signals in copper wires, light signals from one fibre do



not interfere with those of other fibres in the same cable. Fibre line is not easily ‘tap’ as the copper and the system is recommended to be used in a hazardous environment instead of using electrical system which might instigate sparks. The fibre cable is not easily damage with bending and twisting during handling if adequate precautions are taken (Bilro et al., 2012). Advantages of optical fibre usage are listed below:

- Higher carrying capacity
- Fibre is lighter, smaller in diameter and can be less expensive than copper lines
- There is no electromagnetic interference
- High security, not possible to ‘tap’ an optical line as easy as a copper line
- Fibre system are useful in hazardous environments where electrical signals might cause sparks
- The fibre cable can be bent or twisted without damaging it if adequate precautions are taken
- Less signal loss than copper transmission lines

Optical fibre based measurement techniques have attracted a great deal of attention in a variety of analytical areas such as chemical and biological sensing, environmental and structural health monitoring and medical diagnosis (Korposh et al., 2019).

### **2.4.3 Optical Fibre Sensor**

Sensing material or sensor such as OFS was introduced as early as in 1970s which primarily associated with medical and industrial applications. Among the first was the construction of the fibre optic endoscopes (De Groen, 2017). Ever since, the studies related to OFS technology showed growing pattern till now. New OFS developed for a wide variety of applications to overcome certain difficulties which previous systems could not deliver. They have a number of advantageous characteristics that supported the growing usage in various studies. OFS are classified as intrinsic or extrinsic sensors (Barozzi et al., 2017). Optical fibres offer a convenient method for creating OFS, directing light to, and collecting light from, the measurement region, so called extrinsic sensors or using the fibre itself as the transducer, so called intrinsic sensors (Leal-Junior et al., 2019).



Consequently, the extrinsic OFS let the gaseous compounds to be detected directly by measuring changes in optical properties on the sensing surface such as absorbance, fluorescence and refractive index at their absorption, emission or resonance wavelengths. Extrinsic OFS defined as those in which the light wave is guided by the fibre but the interaction between the light and the measurands take place outside the fibre itself, a modulation zone (Lu et al., 2019). When significant proportion of the light allowed to be interacting with a gas in the modulation zone and sensed by the sensor, it is called an open path technique. This technique is one of the most common methods in gas detection using the spectroscopic principles and widely used because it is also capable to detect different gas substances in mixture simultaneously at real time (Naranjo et al., 2012).

Open path technique for OFS represents by an open path absorption method. The open path absorption method applied to the sensor in order to monitor the absorption spectral lines of gas. Open path technique using gas absorption cell is best suited to measure gases compounds because of the unique characteristic of each compound allows their identification (Kher et al., 2019). In gas absorption spectroscopy, each gas sample gives a unique spectral signature or pattern. This is because each gas species has a unique molecular structure, which will absorb different amounts of light at different wavelengths, resulting in a unique spectral pattern. This feature allows both identification and quantification of the gas species. OFS is compact, lightweight and allow the implementation of multiplexing schemes. The sensors also have shown immunity to electronic interference because the basis of their operation is correlated with the optical signal. However, OFS which is competitive or low in production cost with the usage of POF are still in demand compared to the well-established conventional technologies (Bhowmik et al., 2019).

#### **2.4.4 Photo Detector**

Photo detectors such as optical spectrometer, in particular, show the intensity of light as a function of wavelength or frequency. The deflection is produced either by refraction in a prism or by diffraction in a diffraction grating. These spectrometer utilize the phenomenon of optical dispersion. The light from a source can consist of a continuous spectrum, an emission spectrum (bright lines), or an absorption spectrum (dark lines) (Demtröder, 2014). Because each element leaves its spectral

signature in the pattern of lines observed, a spectral analysis can reveal the composition of the object being analyzed. The light source intensity is not linear, thus the charge-coupled device (CCD) spectrometer which has better UV sensitivity normally used as UV detector (Nehir et al., 2019). CCD spectrometers are compact detectors that provide spectral information about the light that reaches the image sensor component. The working principle involved transmission of light through the optical fibre, coupled into the spectrometer, and collimated by a spherical mirror. The collimated light is diffracted by a plane grating, and the resulting diffracted light is focused by a second spherical mirror. An image of the spectrum is projected onto the linear detector array i.e. CCDs. Figure 2.15 is the illustration of the spectrometer cross section and its components.

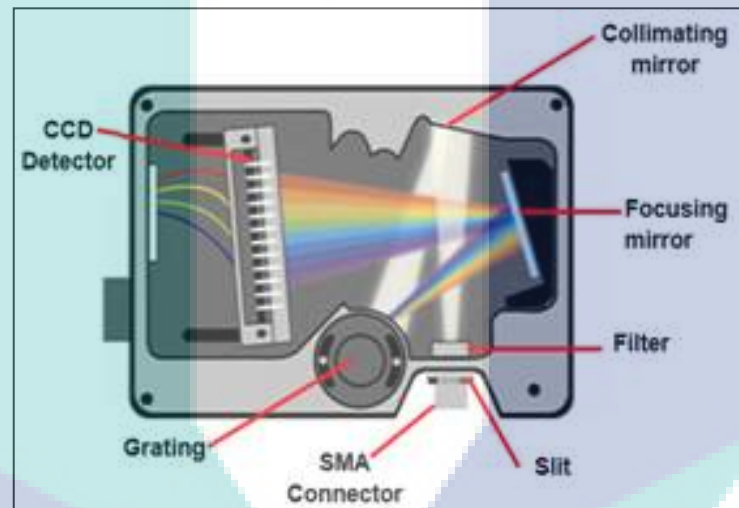


Figure 2.15 Cross Section of a Spectrometer and its Components  
Source: Severn (2018)

Once the light is imaged onto CCDs, the photons are then converted into electrons which are digitized and read out through a USB (or serial port) to a computer. CCD is a detector with a two dimensional array of photodiode that can provide intensity information along two axes. The related spectrometer software then interpolates the signal based on the number of pixels in the detector and the linear dispersion of the diffraction grating to create a calibration that enables the data to be plotted as a function of wavelength over the given spectral range. This data can then be used and manipulated for countless spectroscopic applications (Silva et al., 2017).

### 2.4.5 Various Applications of Optical Detection System

Detection system based on optical methods have been demonstrated for various applications such as breath analysis, indoor air quality and pollution control (Fanchenko et al., 2016). When constructing such optical detection systems, suitable techniques which related to the basic principle were identified and the combination of components proposed accordingly. A simple detection system by Morisawa that used OFS to measure humidity in breathing gases has been introduced much earlier (Correia et al., 2018). This system is also applicable in monitoring other breathing conditions in hospital and in home care. There are many type of sensors developed by Morisawa and Muto that have been investigated and developed via optics method particularly using POF for various kind of usage such as swelling clad-type POF humidity sensor, POF sensing of alcohol concentration in liquors and POF sensing of fuel leakage in soil (Zhang et al., 2019). The principle related to this sensor involved the usage of the optical fibre technology to channel a light signal that is modulated with the ambient humidity and then collected back by a detector, conditioned and processed. Setup of the application is shown in Figure 2.16.

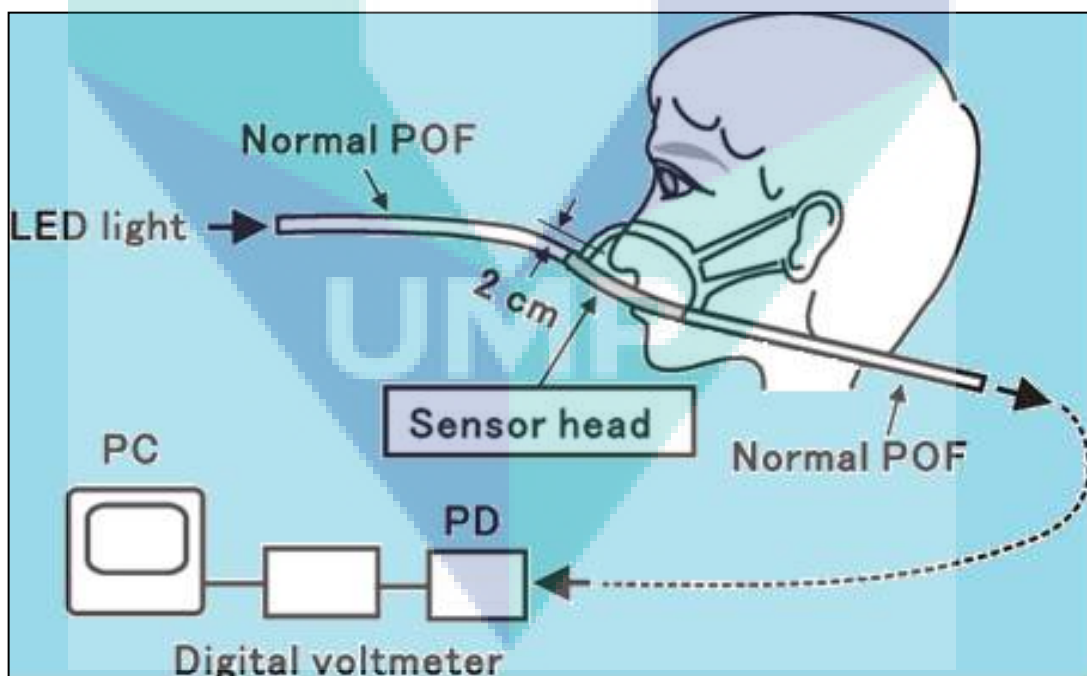


Figure 2.16 Illustration of a Simple Setup for Breathing Condition Monitoring

Source: Morisawa & Muto (2004)

In the previous study of O<sub>2</sub> sensing by Papkovsky, in order for the instrument to detect its luminescent signal, the fibre optic probe of the phase detector can possibly be brought into the vicinity of the sensor (Wei et al., 2019). In fact, O<sub>2</sub> sensitive optical fibre method was applied in the construction of many optical bio-sniffers (Iitani et al., 2018). Among the earliest was the Mitsubayashi system that measures the O<sub>2</sub> consumption induced by MAO-A catalytic reaction with CH<sub>3</sub>SH. The methodology involved MAO-A immobilized membrane that has been applied onto the fibre tip with a tube ring to make the device an O<sub>2</sub> sensitive optical fibre system. In general, the system was utilised for breath analysis but able to detect halitosis also. Experimental setup of the bio-sniffer is shown in Figure 2.17.

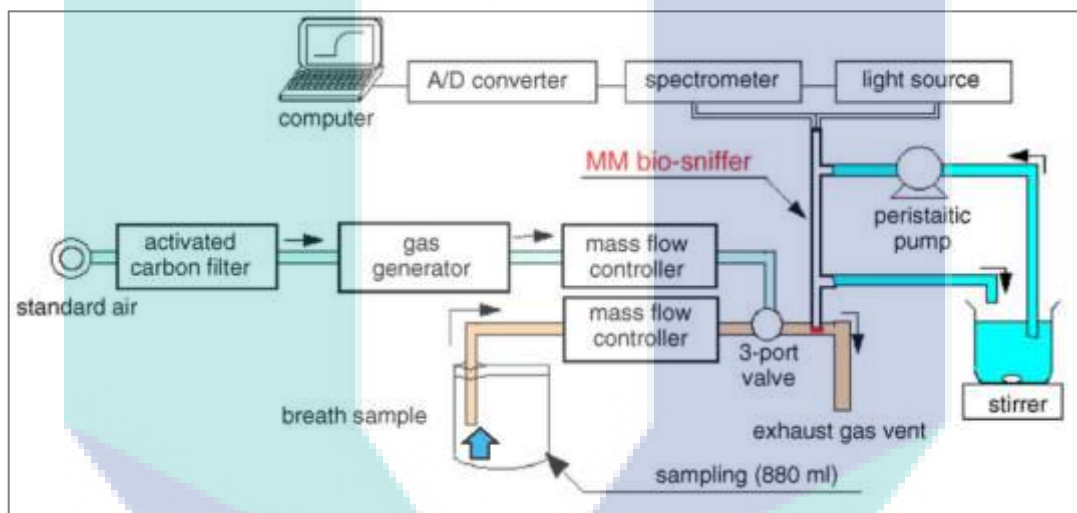


Figure 2.17 Breath Analysis System by the Optical Bio-sniffer with MAO-A  
Source: Saito et al. (2016)

A computer-controlled spectrometer (S2000, Ocean Optics, Inc., FL, USA) with an analog-digital converter (DAQ700, PCMCIA A/D card with 100 kHz sampling frequency, National Instruments Corporation, TX, USA) was optically connected to the bio-sniffer and monitored the optical quenching (fluorescence: 600 nm), thus showing O<sub>2</sub> consumption caused by MAO-A catalytic reaction with CH<sub>3</sub>SH. The device output was monitored graphically and continuously on a computer display and saved on hard disk for later analysis. Performance of the device was reproducible over multiple measurements for at least a few hours. However, the sensitivity of the bio-sniffer would likely to be dropping during long-term measurement due to deactivation of drug metabolizing enzyme.

Optical detection system also developed for the aerospace industry recently. Fibre optic was combined with the infrared reflection-absorption spectroscopy (IRRAS) to identify and measure organic contaminants down to submicrogram levels and produce a direct, near real-time result (Thomson, 2015). The study was done to investigate this in-situ technique has potential in detecting and quantifying the contamination by active pharmaceutical agents on glass and metal surfaces (Pacheco-Londoño et al., 2019). The coupled Fibre Optic-IRRAS instrument is illustrated in Figure 2.18.

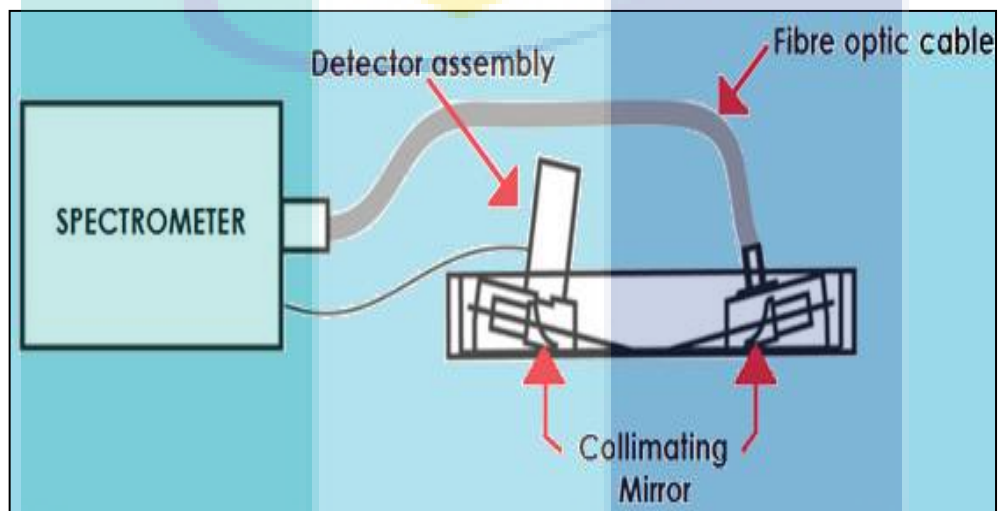


Figure 2.18 Illustration of The Coupled Fibre Optic-IRRAS Instrument  
Source: Zaera (2014)

The development of new light sources such as quantum cascade lasers (QCLs) (Razeghi et al., 2015), LEDs (Fujita et al., 2018), and micro-electro-mechanical systems (MEMS)-based thermal emitters (Lochbaum et al., 2017) combined with optical detectors have emerged in mainstream applications (Vincent et al., 2016) over the past two decades. For instance, the optical breath sensor monitoring system that combined usage of QCL light source and IR spectrometer was constructed to measure CO<sub>2</sub> in respiratory tracts using the optical absorption spectroscopy method (Katagiri et al., 2018). The system which adapt the extrinsic optical sensor working principle used a miniature gas cell attached to the end of the optical fibre as the modulation zone. The gas cell with a diameter that is smaller than 1.2 mm is a stainless steel tube with a gas inlet and a micro-mirror. The experiment used human breaths to monitor CO<sub>2</sub>



absorption spectra and measured the CO<sub>2</sub> concentration with Fourier-transform IR spectrometer.

Additionally, the QCL-based system also used to trace gases present on a patient's breath which indicate medical conditions such as kidney and liver dysfunction, diabetes, asthma and other respiratory problems. The size of the QCL array compared with the United States of America (USA) quarter dollar that has a diameter of 0.955 inches is shown in Figure 2.19.

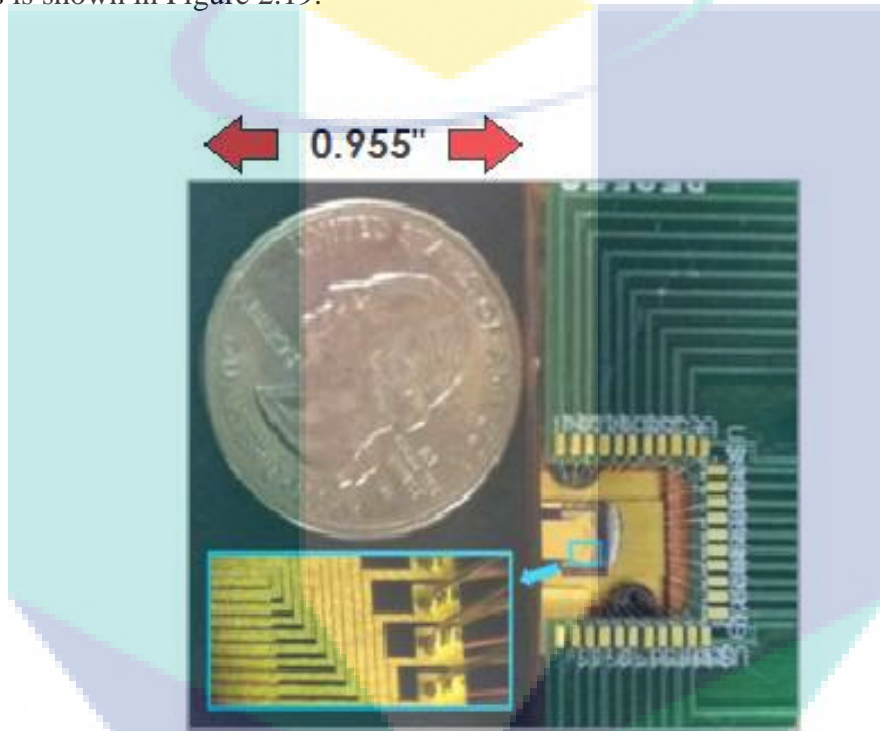


Figure 2.19 QCL Array Compared with a Quarter Dollar of the USA.

Source: Razeghi et al. (2015)

Even though QCL-based systems assures small sized devices, which come with high optical power as well as fast sampling times and accurate results which are important factors in preventing misdiagnosis, QCLs are expensive complex heterostructures (Vitiello et al., 2015).

#### 2.4.6 UV Based System with OFS

UV based detection system with OFS method was a promising new approach. Portable In-situ Sulfur dioxide Analyser (PITSA), new type of instrument for SO<sub>2</sub> detection used as volcanic plume tracer was developed (Tirpitz et al., 2019). The usage

of LED for UV light source was claimed to be cost-effective and compact application but it still suffer from drawback. LEDs have limited emission for wavelength more than  $5 \mu\text{m}$  (Fujita et al., 2018). Figure 2.20 shows the basic setup of the PITSA prototype.

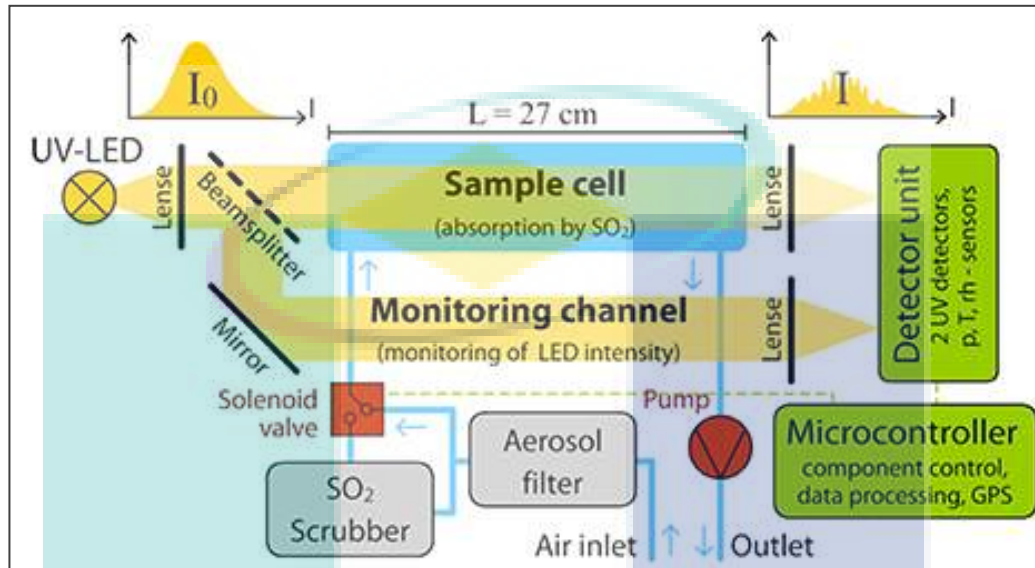


Figure 2.20 Schematic Diagram of the PITSA Prototype Setup

Gas was pumped through an aerosol filter into a 27 cm gas cell, where it was exposed to the parallelized beam of a UV-LED with a well-known emission spectrum in the desired range around 285 nm. The aerosol filter was a 200 nm pore filter which prevented scattering and absorption of light on particles, assuring that  $\text{SO}_2$  absorption was the dominant light attenuating process in the gas. A silicon photodiode as the detector was located behind the cell, measuring the spectrally integrated intensity. Using the absorption spectroscopy principle of the Beer Lambert Law, by comparing the two intensities  $I_0$  and  $I$ , the  $\text{SO}_2$  concentration in the cell was calculated.

Another UV based system was developed for the detection of air-borne toluene (Khan et al., 2019). A deep UV-LED was employed as a light source. A spectrometer was used as a detector with a gas cell in between which connected with fibre cables in which defined as the OFS method. 3D printed opto-fluidics connectors were designed to integrate the gas flow with UV light. The aluminum capillary tube was used as the gas cell. Figure 2.21 shows the experimental setup for toluene detection.

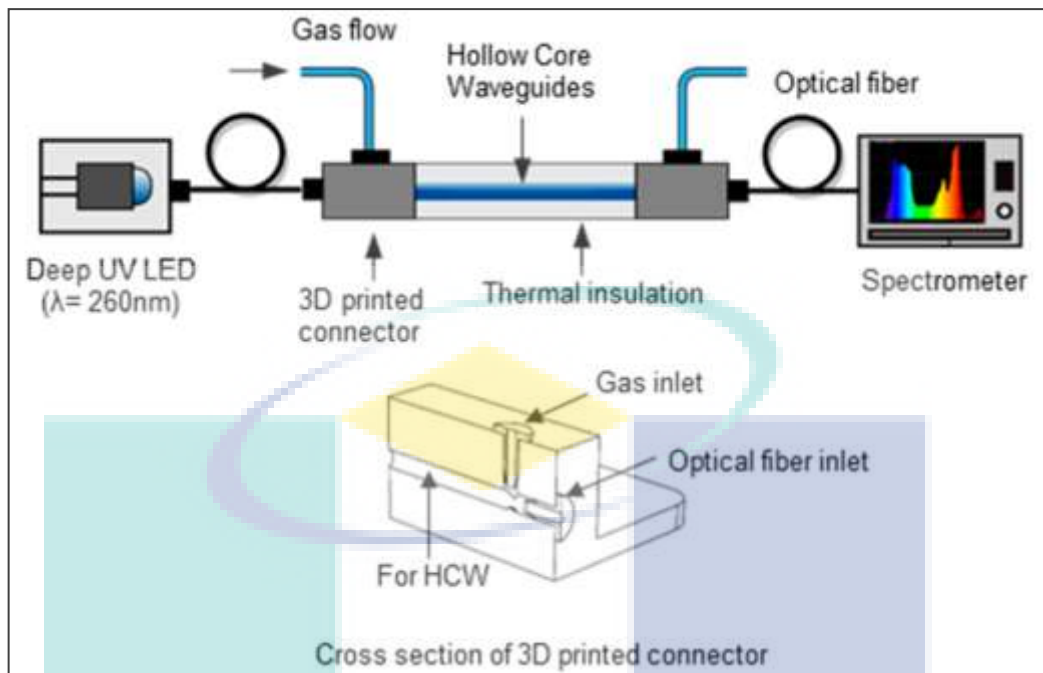


Figure 2.21 Experimental Setup for Toulene Detection.

## 2.5 Summary

Based on previous studies, optical based gas detection system was found to be more reliable than the other methods for halitosis detection. The general principle of the optical based gas detection system involved the transmitting and receiving of light in an optical sensor, then the object to be detected reflects or interrupts a light beam sent out by an emitting light source. In the optical based gas detection system where  $\text{CH}_3\text{SH}$  was concerned, UV light source and detector will be used in the proposed system because absorption spectrum of  $\text{CH}_3\text{SH}$  was reported as to be best suited to the UV region of electromagnetic light spectrum. Absorption spectroscopy principle in the open path OFS is considered to be best paired with the UV based system for gas detection.



## CHAPTER 3

### METHODOLOGY

#### 3.1 Introduction

UV based system that combined the usage of open path OFS to detect halitosis is the proposed system to be developed.  $\text{CH}_3\text{SH}$  gas is used to indicate the existence of VSCs thus, it signify halitosis. The outline of the methodology is represented in the flow chart. Firstly, the derivation of Beer Lambert Law is explain as conjunction with the absorption spectroscopy method. Then the details of proposed system components and related techniques are described. Instrument calibration is carried out and the components are assembled accordingly. The proposed system is used to detect  $\text{CH}_3\text{SH}$  gas. Further investigations were carried out to determine the ability of the system to detect  $\text{CH}_3\text{SH}$  as halitosis indicator. Analyses of  $\text{CH}_3\text{SH}$  absorption spectral are performed to determine the wavelength for absorption. Then, the act follows with validation of the detection system. Checking the possibility of interference from the breathing gases with cross sensitivity testing method is significant in this study in order to decide whether or not the choice of absorption wavelength region is correct and fit for the detection system. Finally, calculation of the  $\text{CH}_3\text{SH}$  gas concentration will be carried out to give an assurance that the detection system is quantitatively reliable to detect halitosis.

#### 3.2 Research Methodology

The general methodology of the thesis is shown as flow chart in Figure 3.1 below.

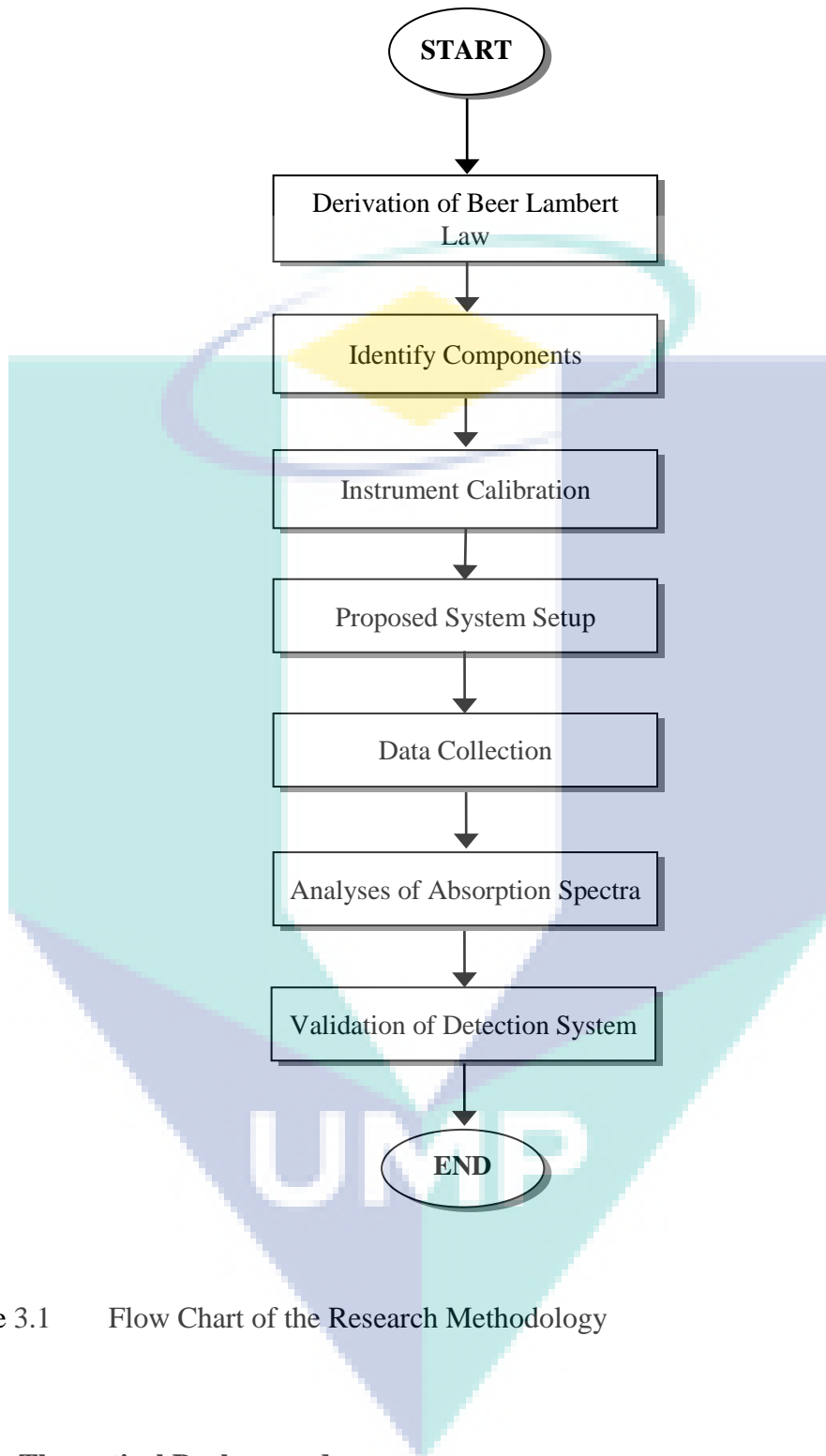


Figure 3.1 Flow Chart of the Research Methodology

### 3.3 Theoretical Background

In order to achieve the first objective of the study, the proposed system should be able to detect the existence of  $\text{CH}_3\text{SH}$  gas with the absorption spectroscopy method. In this optical detection system where spectroscopy was concerned, the OFS operated

by passing the light through the gas cell with the path length,  $l$  which contained the medium and measured the intensity of light reaching the detector. The transmission of light through absorbing medium can be represented as in Figure 3.2.

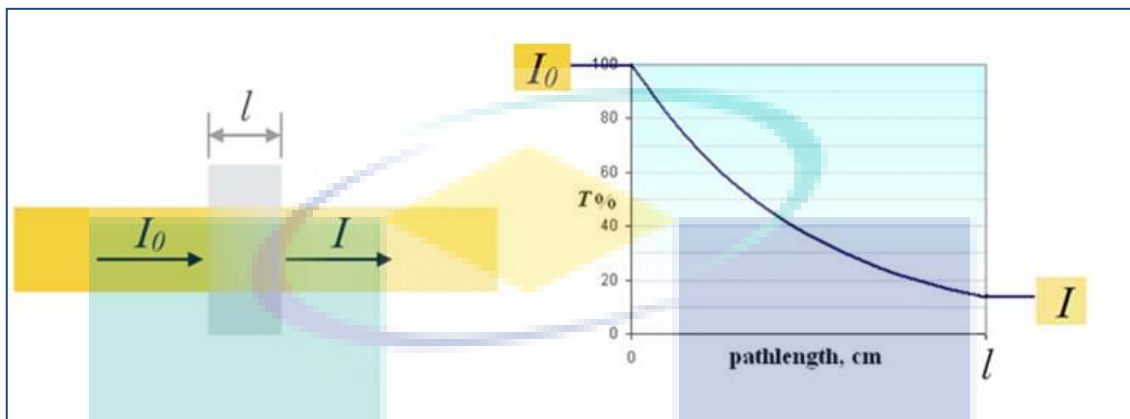


Figure 3.2 Transmission of Light through Absorbing Medium

The transmittance, ( $t$ ) was a measure of the fraction of light that passed through the medium as shown in Equation 3.1.

$$\text{Transmittance, } t = \frac{I}{I_0} \quad 3.1$$

It was the ratio of the transmitted intensity,  $I$  and incident intensity,  $I_0$ . A non linear correlation of the transmittance which observed was in exponential. Even though it was useful to have this information but linear plots of the data was simpler to discuss and easier to compare thus brought in the Beer Lambert Law.

$$\text{Absorbance, } A = -\ln(t) \quad 3.2$$

Absorbance,  $A$ , as shown in Equation 3.2, was the amount of light absorbed by the  $\text{CH}_3\text{SH}$  gas. There was a linear relationship between the absorbance of light and the path length of the gas cell. Thus there was also a linear relationship between the absorbance of light and the concentration of the absorbing medium as stated by the Beer-Lambert Law. The Beer Lambert Law can be derived by assuming the absorbing sample into thin slices that are perpendicular to the beam of light, as shown in Figure 3.3 below.

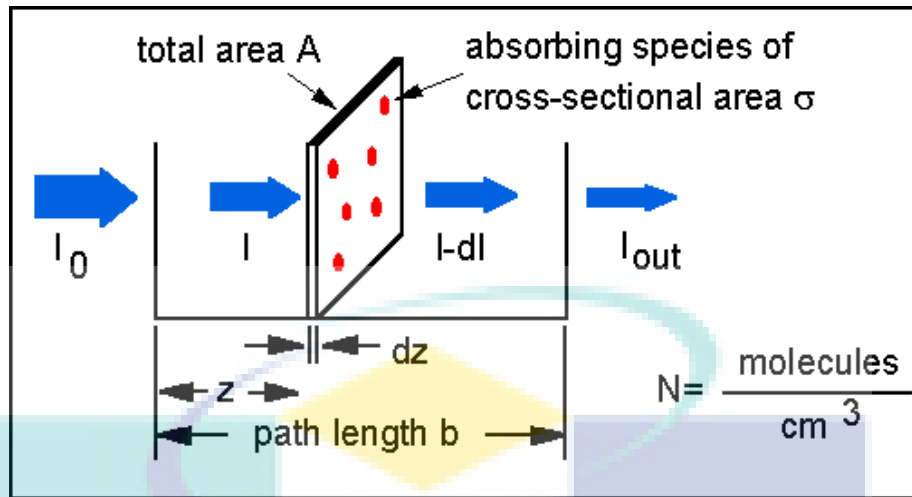


Figure 3.3 Derivation of Beer Lambert Law.

The absorption cross section,  $\sigma$  was represented by an opaque area where the size was the same as the cross-sectional area of a single molecule. The direction that photons of light moved was defined as  $z$  axis,  $A$  was the total area and  $dz$  was the thickness of the slab. It was assumed that  $dz$  sufficiently small that one particle in the slab cannot obscure another particle when viewed along the  $z$  direction. The concentration of particles in the slab was represented by  $N$ . Consider  $I_0$  is the intensity entering the sample at  $z = 0$ ,  $I_z$  is the intensity entering the infinitesimal slab at  $z$ ,  $dI$  is the intensity absorbed in the slab, and  $I$  is the intensity of light leaving the sample. Then, the total opaque area on the slab due to the absorbers is  $\sigma \times N \times A \times dz$ . Thus, the fraction of photons absorbed will be  $(\sigma \times N \times A \times dz) / A$ , hence

$$\frac{dI}{I_z} = -\sigma \cdot N \cdot dz \quad 3.3$$

Integrating this Equation 3.3 from  $z = 0$  to  $z = b$  gives:

$$\ln(I) - \ln(I_0) = -\sigma \cdot N \cdot b \quad 3.4$$

or

$$\ln\left(\frac{I}{I_0}\right) = -\sigma \cdot N \cdot b \quad 3.5$$

The Beer Lambert Law describes the relationship between absorbance and concentration of an absorbing species and its general form was shown in Equation 3.5. It can be rearranged and written as in Equation 3.6 below.

$$\frac{I}{I_o} = e^{(-\sigma.N.l)} \quad 3.6$$

In this study,  $I$ , the transmitted intensity when test gas was released,  $I_o$ , the incident intensity when  $N_2$  was released,  $l$  (cm) was the distance which light travelled through the gas equivalent to the length of the absorption cell,  $\sigma$  ( $\text{cm}^2/\text{Molecules}$ ) was the absorption cross section and  $N$  ( $\text{Molecules}/\text{cm}^3$ ) was the number of molecules in a unit volume or can be defined as concentration. This concentration,  $N$  is given in unit  $\text{Molecules}/\text{cm}^3$ , so the unit was changed to ppm because the gas concentration normally read in this unit.

$$\begin{aligned} \frac{V}{n} &= \frac{RT}{P} = \frac{(0.082 \frac{\text{atm} \cdot \text{L}}{\text{mol} \cdot \text{K}})(273\text{K})}{1 \text{ atm}} \\ &= 22.4 \frac{\text{L}}{\text{mol}} \end{aligned} \quad 3.7$$

The ideal gas law ( $PV = nRT$ ) was also used in this unit conversion, where  $P$  = pressure (atm),  $V$  = volume (L),  $n$  = mass of substance (moles),  $R$  = ideal gas constant ( $0.082 \text{ atm L mol}^{-1}\text{K}^{-1}$ ),  $T$  = absolute temperature ( $^{\circ}\text{C} + 273$ ) in degrees Kelvin. Standard temperature and pressure were defined as 1 atm and  $0^{\circ}\text{C}$  (273 K). Under these conditions, a mole of an ideal gas occupied a volume of 22.4 L. At times, gaseous concentrations were expressed using mixed units of mass per unit volume such as  $\text{mg}/\text{m}^3$ . The relationship between ppm and  $\text{mg}/\text{m}^3$  depends on the density of the gas which depends on its pressure, temperature and molecular weight and represented as Equation 3.8.

$$\rho\left(\frac{\text{mg}}{\text{m}^3}\right) = \frac{\text{ppm} \times \omega}{22.4 \frac{\text{L}}{\text{mol}}} \times \frac{273}{T(\text{K})} \times \frac{P(\text{atm})}{1 \text{ atm}} \quad 3.8$$

Where  $\rho$  ( $\text{mg}/\text{m}^3$ ) is the density of the gas,  $\omega$  is the molecular weight,  $P$  (atm) is the measured pressure and  $T$  (K) is the measured temperature of the test gas. Equation

3.8 has been simplified as in Equation 3.9 with the test gas temperature at room temperature of 300 K and with the pressure at 1 atm.

$$\rho\left(\frac{\text{mg}}{\text{m}^3}\right) = \frac{\text{ppm} \times \omega}{24.4 \frac{\text{L}}{\text{mol}}} \quad 3.9$$

The concentration of the test gas,  $N$  in the Beer Lambert Law in Equation 3.6 was given in unit Molecules/cm<sup>3</sup>. Before converting it to ppm, the relationship between this unit and the density of the gas,  $\rho$  (mg/m<sup>3</sup>) were identified.

Since,

$$N \frac{\text{Molecules}}{\text{cm}^3} \times \frac{1000 \text{ mg}}{1 \text{ g}} \times \frac{1 \text{ cm}^3}{10^{-6} \text{ m}^3} \times \frac{1 \text{ mol}}{6.022 \times 10^{23} \text{ Molecules}} \times \omega \frac{\text{g}}{\text{mol}} = \rho \frac{\text{mg}}{\text{m}^3}$$

Hence the relationship between  $N$  (Molecules/cm<sup>3</sup>) and  $\rho$  (mg/m<sup>3</sup>) was given by,

$$N = \frac{\rho}{\omega} N_A \times 10^{-9} \quad 3.10$$

where  $N_A$  was Avogadro's constant.

In order to get the absorption cross section of the test gas,  $N$  in parts per million, ppm, Equation 3.8 and Equation 3.10 were inserted to the Beer Lambert Law of Equation 3.6 above, thus, gave the Equation 3.11 below.

$$\text{Absorption Cross Section, } \sigma = \frac{-[\ln \frac{I}{I_0}][T \times 22.4]}{\text{ppm} \times N_A \times l \times 273 \times P \times 10^{-9}} \quad 3.11$$

### 3.4 Proposed System

The proposed optical based gas detection system will be developed considering four main components. They are the light source, suitable optics for transmitting light to and from the sensor, sensing materials or sensor and a photo detector for detecting light signals coming from the sensor.

There are many commercially available light sources such as halogen, deuterium, xenon, LED and laser diodes which offer different ranges of wavelength. However, the light source that emits UV in the range of 180 to 400 nm is needed to cover the whole UV region and provide continuous light. In the optical based detection system where CH<sub>3</sub>SH was concerned, UV light source is chosen because absorption spectrum of CH<sub>3</sub>SH gas reported as to be best suited to the UV region of electromagnetic light spectrum (Du et al., 2017; Vaghjiani, 1993). DH-2000 by Ocean Optics is the chosen UV light source because of its' balanced deuterium halogen source. The combination of two technology based UV emitters i.e. deuterium lamp and halogen are able to provide continuous light in the wavelength of 180 nm to 2000 nm. Figure 3.4 shows the UV broadband source by Ocean Optics.



Figure 3.4 Ocean Optics UV Broadband Source

Extensively, OFS are normally classified as extrinsic or intrinsic sensors. The basic principle involves propagation of light signal from the optical source through the input fibre and then modulated by measurand in the modulation zone before it is sensed by the detector through the output fibre. In this case, extrinsic sensor is chosen because the measurand is in gaseous form. Geometrically, extrinsic sensor portray the light wave is guided by the fibre cable but the interaction between the light and the measurands take place in the modulation zone which is outside the fibre. Figure 3.5 shows a basic diagram of the extrinsic sensor where the open path technique will take place in the modulation zone.

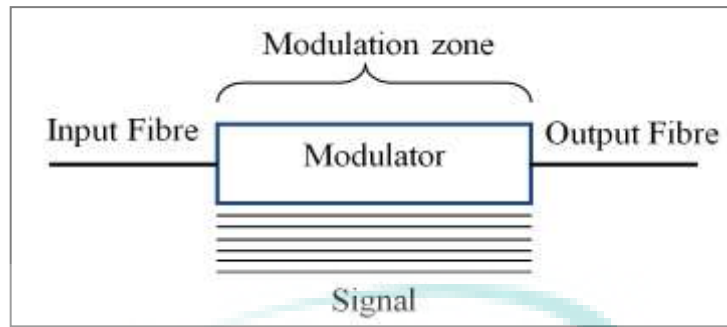


Figure 3.5 A Basic Diagram of the Extrinsic Sensor

The modulation zone is where the significant proportion of UV light interacted with the test gas and sensed by the detector. In order to measure the gas absorption line, a hollow stainless steel cylinder test gas cell was selected. Stainless steel is a reflective metals that let the radiation propagated by metallic reflection inside the hollow core. The length of the chosen gas cell is 10 cm. It has been previously reported that for optimum sensitivity, the longer the path length, the better the sensitivity. Although a longer test gas cell can have a better sensitivity, it is important to choose an optimum length in order to get the best result. This is because the optical radiation detected by the detector is reduced by the increased path length. Therefore the optical path length of the sensor was determined through a compromise between the transmission loss and sensitivity gained for every cm increase in the optical path length. A photograph of the stainless steel hollow cylinder gas cell used as the absorption cell for the modulation zone can be seen in Figure 3.6.

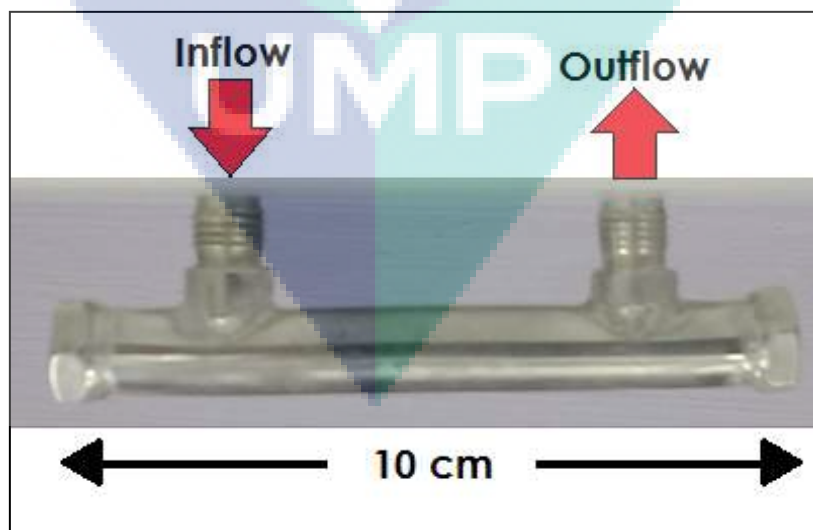


Figure 3.6 The Stainless Steel Hollow Cylinder Gas Cell



To transmit light from the UV emitter, UV Non Solarising (UVNS) optical fibre was used in this detection system. It was developed by CeramOptec with diameter of the core is 644.4  $\mu\text{m}$ . This UVNS optical fibre is able to be used for long duration around 40,000 hours and can be used continuously. The transmission rate is capable to maintain at 95% of the original output at wavelengths between 160 and 1200 nm. Length of the UVNS fibre used as the output fibre and the input fibre is 1 m each. It is not just for the light source input but also used for the data output. Optical fibres which coupled with standard SMA connector linked the UV light source, the spectrometer and the absorption gas cell. SMA is a fibre optic connector that uses threaded connection to keep the plug intact in the socket. It is also compact in size and has mechanical durability. Figure 3.7 shows the photograph of the UVNS optical fibre attached to Sub-Miniature Version A (SMA) connector.

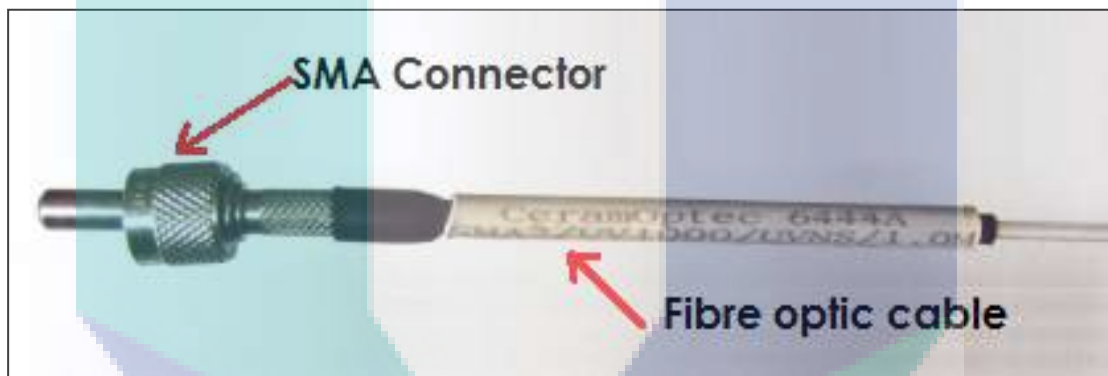


Figure 3.7 UVNS Optical Fibre Cable with SMA Connector

Maya2000 Pro is the CCD spectrometer that was used as the UV detector. The advantage of using CCD spectrometer is that it was arranged in a two-dimensional array thus has the ability to perform side-by-side readings, suited to multiple optical inputs, so that multiple spectra are obtained simultaneously. Hence, a reference signal can be captured on concurrent measurement to trace any various changes such as lamp fluctuations. Therefore the spectrometer with CCD installed is more suitable for use in applications where the light source intensity is not linear. Another reason for the selection of CCD spectrometer was that it has better UV sensitivity. It has been chosen because of its high sensitivity in configurations which cover a range of approximately 165 to 1100 nm. A photograph of the Maya 2000 Pro, the CCD spectrometer by Ocean Optics can be seen in Figure 3.8 below.



Figure 3.8 Maya2000 Pro, the Ocean Optics CCD Spectrometer

Periodically recalibrating of the Maya2000 Pro Series Spectrometer is recommended even though each of the spectrometer is calibrated before it leaves Ocean Optics. After certain period of time and due to environmental effects, the wavelengths for all spectrometers may drift slightly. The spectrometer recalibration was then carried out based on the calibration process which is thoroughly explained in Appendix A which was taken from Maya2000Pro Series Spectrometers Installation and Operation Manual. In order to recalibrate the wavelength of the spectrometer, a light source that is capable in producing spectral lines is a mandatory component other than the spectrometer itself. A Mercury-Argon lamp, HG-1 as shown in Figure 3.9 was used as recommended.



Figure 3.9 Mercury-Argon Lamp used for the Maya2000 Spectrometer Calibration

As referred in the calibration procedures (Appendix A), linear regressions was performed and the output summary of the spectrometer calibration can be seen in Table 3.1 and Table 3.2 below. From the regression statistics values (Table 3.1), the value for R squared is 0.999979466 which is close to 1. Theoretically, the R squared value should

be very close to 1 (0.95-1.00), if not, most likely one of the wavelengths is incorrectly assigned.

Table 3.1 Values of Regression Statistics

Broadband Source	Wavelength Range (nm)
Multiple R	0.999989733
R Square	0.999979466
Adjusted R Square	0.999958932
Standard Error	0.689826013
Observations	8

Calibration coefficients data and the standard error for spectrometer can be seen in Table 3.2. X Variable 1 coefficient, X Variable 2 coefficient and X Variable 3 coefficient in Table 3.2 known as First, Second and Third Coefficient respectively. All these three coefficients values and the intercept coefficient value which were recorded are the important values for the spectrometer recalibration.

Table 3.2 Calibration Coefficients Data for Spectrometer

	Coefficients	Standard Error
Intercept	193.873673	0.267556324
X Variable 1	0.31267445	0.001764863
X Variable 2	-2.137454E-05	6.23117E-06
X Variable 3	-3.789865E-09	1.87966E-10

Ocean Optics programs wavelength calibration coefficients are unique to each spectrometer. Thus, the new calibration coefficients acquired were used to overwrite the old calibration coefficients in the spectrometer memory chip before the spectrometer can be used for any experiments.

As the vendor of the spectrometer, Ocean Optics also provided SpectraSuite, the software package of the spectrometer. It was a spectrometer operating software that can control any Ocean Optics spectrometer and device when they are interfacing to a computer through their USB port. The software package was used to acquire the data from the spectrometer such as the intensity counts for the incident and transmitted light before they were applied to the Beer Lambert Law equation in order to calculate absorption cross section. The intensity counts were also used in the gas concentration calculation. The installation of the software is performed before connecting the spectrometer to the computer. The software installed the drivers required for spectrometer installation in order for the system to properly recognize the spectrometer. The SpectraSuite screen (in Scope mode) with the spectrometer used shown in the Data Sources pane can be seen in Figure 3.10.

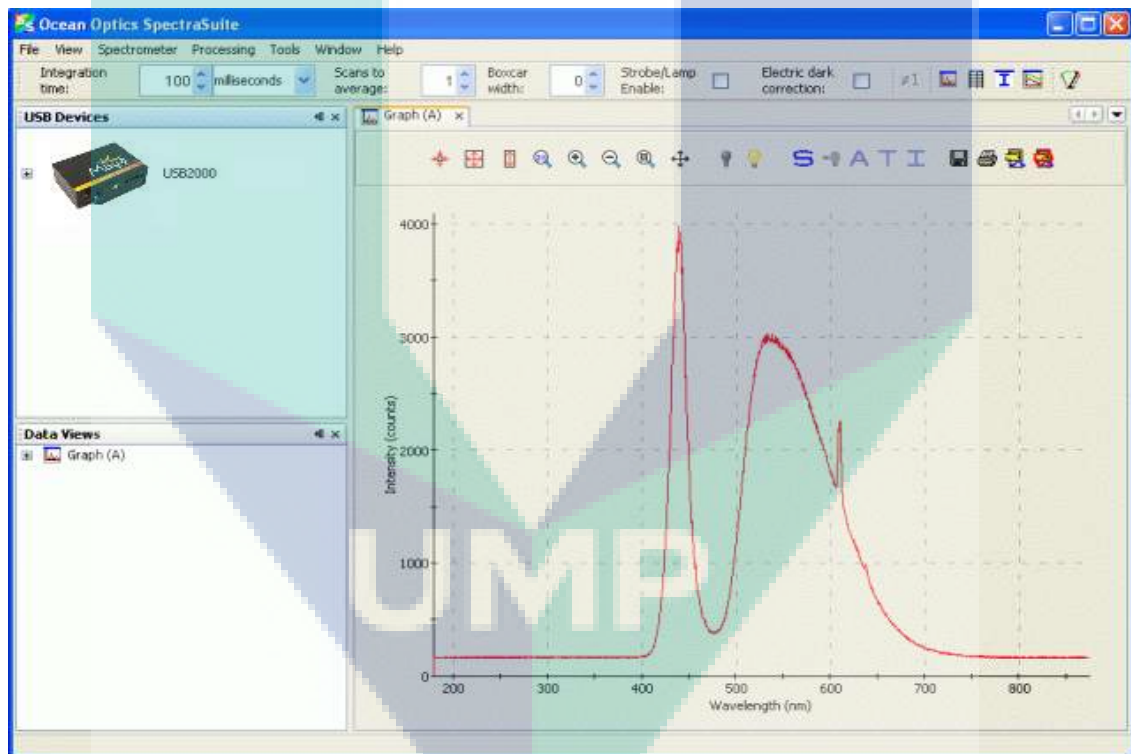


Figure 3.10 Screen of the SpectraSuite Software upon installation

All the main components for the UV based gas detection system were identified and assembled in order to develop the halitosis detection system. The proposed system setup can be seen in Figure 3.11 below.

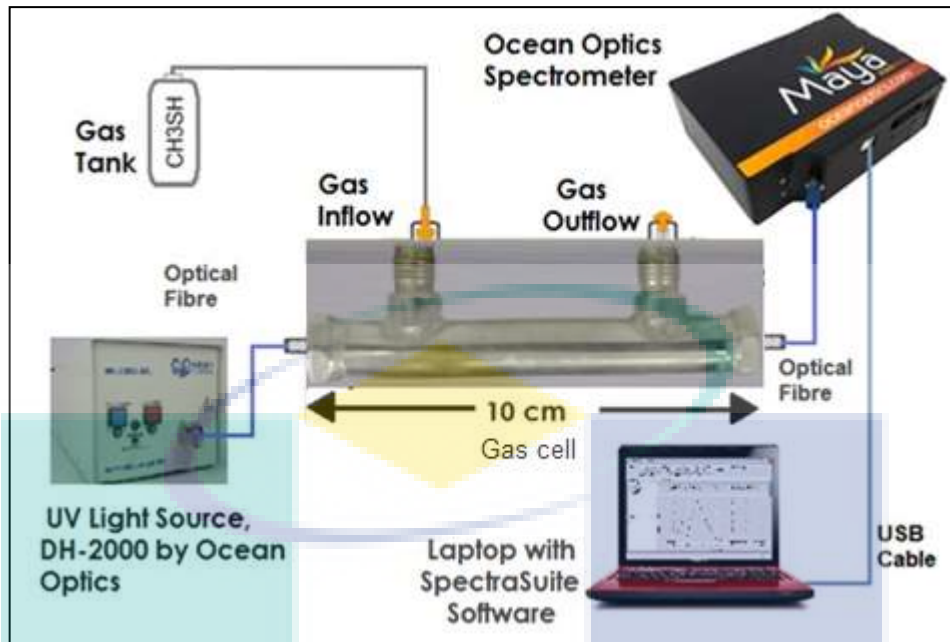


Figure 3.11 Proposed system setup of UV Based Detection System for Halitosis

The main concern in this experiment is to obtain  $\sigma$  for  $\text{CH}_3\text{SH}$  gas. With the gas temperature,  $T$  is  $27^\circ\text{C}$  and the gas pressure,  $P$  is 1 atm and with length of absorption cell,  $l$  is 10 cm, Equation 3.11 for  $\sigma$  can be simplified as,

$$\sigma = \frac{-[\ln \frac{I}{I_0}][24.04]}{\text{ppm} \times N_A \times 10^{-8}} \quad 3.12$$

Thus, there were  $I_0$  and  $I$ , the two parameters which need to be measured.  $I_0$ , the intensity measured when the gas cell was empty from the test gas,  $\text{CH}_3\text{SH}$  or other gas that may affect the experiment. The gas cell have an inlet for receiving  $\text{CH}_3\text{SH}$  or other gas sample from the gas source and an outlet for releasing the gas sample from the gas cell assembly. To begin with,  $\text{N}_2$  was released into the gas cell for flushing purpose. At the left end portion of the gas cell body, the channel provided a path for the incident beam transmitted by the fibre optic cable from the UV light source. The UV light source turned on and the flushing was carried out for 10 s to make sure that the gas cell is neutralize. Modulation process occurred in the gas cell when  $\text{N}_2$  was released.

A detector which is the spectrometer positioned at the other channel on the right end of the gas cell body through the fibre optic cable received the reflected beam. The measured data signal corresponding to the reflected beam was  $I_0$ . The data was

measured and recorded in the SpectraSuite software. The gas source was then changed to CH<sub>3</sub>SH gas tank. Following that, CH<sub>3</sub>SH gas was released into the gas cell for 2 s and the transmitted intensity,  $I$  was measured and recorded with the SpectraSuite software. These two steps of measuring  $I_o$  and  $I$  were repeated for another 2 times to get 3 data sets. Calculation of CH<sub>3</sub>SH gas absorption cross section,  $\sigma$  were carried out and the graph was plotted against wavelength. Table 3.3 shows the experimental conditions for intensity measurements.

Table 3.3 Experimental Conditions for Intensity Measurement

Absorption path length (cm)	10
Gas Cell	Stainless Steel Hollow Cylinder
Light Source	Halogen-Deuterium Balance
UV Wavelength (nm)	180 - 2000
Detector	CCD Spectrometer
Cable	UVNS Optical Fibre with SMA Connector
Temperature (K)	300
Pressure (atm)	1
Avogadro's number, $N_A$	$6.022140857 \times 10^{23}$ molecules

### 3.5 Analyse the Absorption Cross Section Spectra of Methyl Mercaptan

The plotted graph of  $\sigma$  against wavelength represented the absorption spectra of the CH<sub>3</sub>SH gas. Further analyses of the absorption spectra was carried out by finding the correlation with the theoretical spectral data of CH<sub>3</sub>SH gas and determine the wavelength for the absorption occurred. The experimental absorption spectra of CH<sub>3</sub>SH gas was compared with the other two theoretical data from the database which have similar temperature and wavelength range. These data sets are taken from the database of Max Planck Institute, MPI Mainz UV-VIS. The database was the source of CH<sub>3</sub>SH gas absorption spectral data used for comparison purpose. Furthermore, in order to determine the best wavelength region for absorption, peak(s) of the CH<sub>3</sub>SH absorption spectral need to be determined which later to be used for validation purpose.



## 3.6 Validation of the Proposed System

### 3.6.1 Cross Sensitivity Evaluation with Breathing Gases

Cross sensitivity evaluation of CH<sub>3</sub>SH gas with the breathing gases such as O<sub>2</sub>, CO<sub>2</sub> and H<sub>2</sub>O were done to prove that the proposed system was not sensitive to environment within the selected UV range especially the interference from the breathing gases. In addition, it was to decide specifically the region of the absorption wavelength so that the detection system was reliable for usage without any interference. However, experimental evaluations were done for the two main breathing gases O<sub>2</sub> and CO<sub>2</sub> only. For H<sub>2</sub>O, assessment was done theoretically because previous studies (Lampel et al., 2015; Parkinson et al., 2003) shown almost non-existence of significant absorption spectra for H<sub>2</sub>O in the UV wavelength region.

Cross sensitivity testing of the proposed system was done for O<sub>2</sub> and CO<sub>2</sub> used the same method acquiring  $I_o$  and  $I$  of the CH<sub>3</sub>SH gas. The procedure of gas cell flushed with N<sub>2</sub> was repeated each time to neutralize the absorption cell, thus,  $I_o$  measured and recorded. Following that, O<sub>2</sub> gas was released into the cell and  $I$  was measured. The procedures were repeated another 2 times to get 3 sets of data. Then the same procedures were carried out for CO<sub>2</sub> to get 3 sets of  $I_o$  and  $I$ . Calculations of  $\sigma$  were carried out for O<sub>2</sub> and CO<sub>2</sub>. Graphs of  $\sigma$  for O<sub>2</sub> and CO<sub>2</sub> were plotted against wavelength and compared with the theoretical spectral data taken from the database. The experimental data of  $\sigma$  for CH<sub>3</sub>SH gas was plotted on the same graph with O<sub>2</sub>, CO<sub>2</sub> and H<sub>2</sub>O for interference investigation.

### 3.6.2 Calculation of Concentration

Gas concentration, *ppm* of CH<sub>3</sub>SH was calculated for validation purpose with  $\sigma$  already known from previous section. In order to do that, Equation 3.12 which has been derived from Beer Lambert law was manipulated to get the equation for *ppm* as shown in Equation 3.13 below.

$$ppm = \frac{-[\ln \frac{I}{I_o}][24.04]}{\sigma \times N_A \times 10^{-8}} \quad 3.13$$



It can be seen clearly that the difference between Equation 3.13 and Equation 3.12 was the interchanged location of  $ppm$  and  $\sigma$ . For the calculation of  $ppm$ , the values of  $\sigma$  for the wavelengths selected were known. The values of  $\sigma$  vary depending on the wavelengths and were obtained previously using PeakFit. Whereas,  $I_o$  and  $I$  were obtained from the experiment. The proposed system was used and initially,  $N_2$  was released into the cell to neutralize the gas cell.  $I_o$  at selected wavelength was measured and recorded. The value of  $\sigma$  at the peak was used to calculate the  $ppm$ . 100 ppm of  $CH_3SH$  gas was then released into the absorption gas cell for 2 s and  $I$  was recorded at the selected wavelength. The experiment was repeated for 10 times. All the measured data were recorded in a spreadsheet. To obtain the  $ppm$  of  $CH_3SH$  gas in ppm unit, recorded data were inserted into Equation 3.13.

### 3.7 Summary

The research methodology was carried out accordingly. The devices to construct UV based detection system were identified suited the absorption spectroscopy method. The working principle and specifications for each of the components and software related were described. The assembled system used to obtain absorption cross section of  $CH_3SH$ ,  $O_2$  and  $CO_2$  for analyses and validation purposes. All the results and analysis are reported in the next chapter.

The logo for UIMP (Universiti Malaysia Perlis) is a large, stylized 'V' shape. The left side of the 'V' is light blue, the right side is a darker blue, and the bottom point is a teal color. The letters 'UIMP' are written in white, bold, sans-serif font across the center of the 'V'.

## CHAPTER 4

### RESULTS AND DISCUSSIONS

#### 4.1 Introduction

In this chapter, the results of  $\sigma$  for CH<sub>3</sub>SH were plotted against wavelength displayed and compared with the theoretical data taken from the database of Max Planck Institute, MPI Mainz UV-VIS (Keller-Rudek *et al.*, 2013). The database includes most common atmospheric gases molecules spectral data. The plotted graph of  $\sigma$  as a function of wavelength also known as the CH<sub>3</sub>SH absorption cross section spectra. Following that, the descriptive analysis results were discussed and the suitable wavelength region was identified for the detection system. From the determination of the CH<sub>3</sub>SH absorption cross section spectra peak, the value of  $\sigma$  is to be presented and discussed. Results of  $\sigma$  for O<sub>2</sub> and CO<sub>2</sub> against wavelength were plotted, compared with the theoretical values from the database and discussed. Results of cross sensitivity evaluations of the experimental spectral of CH<sub>3</sub>SH gas with O<sub>2</sub>, CO<sub>2</sub> and H<sub>2</sub>O will be presented and discussed. In addition to that, the best possible wavelength region also determined. The output of concentration calculation of CH<sub>3</sub>SH gas will also be conveyed for validation purpose.

#### 4.2 Absorption Cross Section Spectra of Methyl Mercaptan

Proposed system was used to obtain  $I_o$  and  $I$  to get the  $\sigma$  of CH<sub>3</sub>SH. The data acquired in the form of intensity counts based on the spectroscopy method were then applied to the derived Beer Lambert Law to produce datasets of  $\sigma$  for CH<sub>3</sub>SH. Table of the complete datasets are shown in Appendix B. The datasets of  $\sigma$  for CH<sub>3</sub>SH were plotted against wavelength. Figure 4.1 shows the experimental results of  $\sigma$  for CH<sub>3</sub>SH and theoretical data taken from the Max Planck Institute, MPI Mainz UV-VIS database.

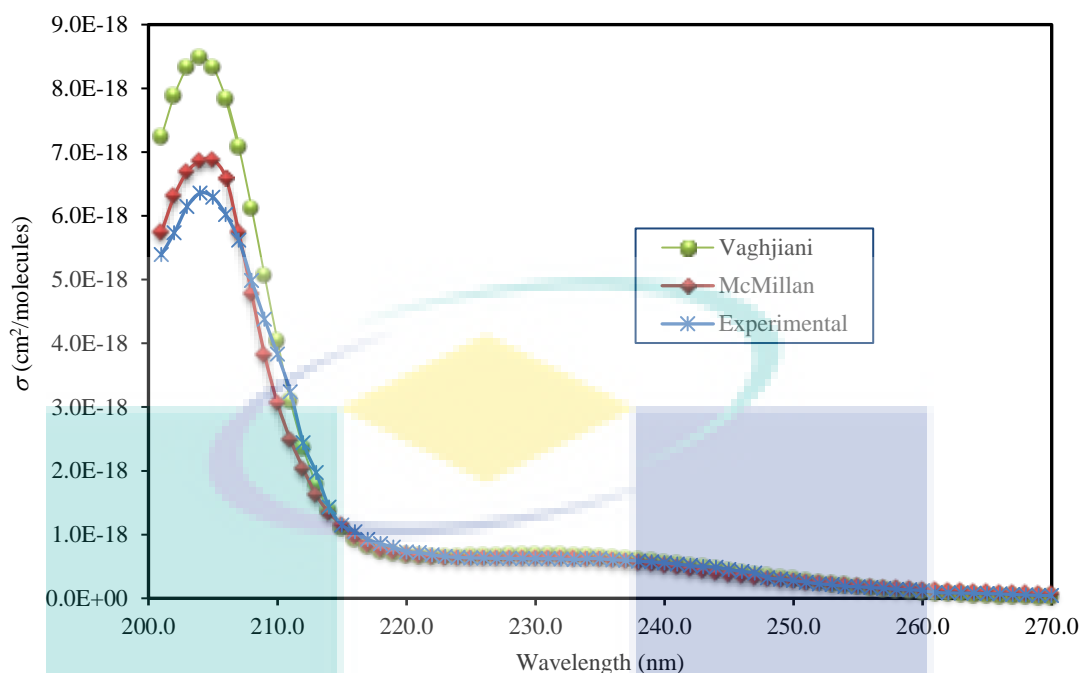


Figure 4.1 Graph of Absorption Cross Section against Wavelength for CH<sub>3</sub>SH

The theoretical datasets of  $\sigma$  are from different studies (McMillan, 1966, Vaghjiani, 1993). These datasets were the only references which appropriate for comparison purpose because they covered almost similar wavelength range of 200 to 270 nm. The table of a complete datasets is shown in Appendix C. Each different gas species absorb light at different characteristic wavelengths thus has its own specific gas absorption cross section spectra. The experimental result showed similar shape of spectral as Vaghjiani and McMillan. All the curves skewed to the left of the graph and each curve has one obviously high peak. So, the obtained data set of  $\sigma$  plotted against wavelength for CH<sub>3</sub>SH is in good agreement with the theoretical data. Thus, it shows that the proposed system is able to spot the existence of CH<sub>3</sub>SH gas.

Further data analysis was carried out to find out the correlation between them. The correlation coefficient of the experimental data for CH<sub>3</sub>SH absorption cross section spectral with McMillan and Vaghjiani are 0.9936 and 0.9946 respectively. Whereby, the correlation coefficient between the two theoretical data is 0.999. These results indicated that the experimental data is highly correlated with both theoretical data. Table 4.1 shows the summary of the correlation coefficients.

Table 4.1 Summary of Correlation Coefficient for CH<sub>3</sub>SH Absorption Cross Section Spectra

	<b>Experimental</b>	<b>McMillan</b>	<b>Vaghjiani</b>
Experimental	1		
McMillan	0.9936	1	
Vaghjiani	0.9946	0.9990	1

The peaks indicate where the maximum absorption of CH<sub>3</sub>SH occurred. Peak value of the experimental curve is 6.357E-18 cm<sup>2</sup>/molecules located at wavelength of 204 nm. Peak value of McMillan's curve is 6.88E-18 cm<sup>2</sup>/molecules located at 205 nm and peak value of Vaghjiani's is 8.49E-18 cm<sup>2</sup>/molecules at 204 nm. The peak of all three datasets have different heights and have different values. Vaghjiani's has the highest peak while the experimental has the lowest. Table 4.2 below shows the results of the values of peaks and the wavelength of CH<sub>3</sub>SH absorption spectral.

Table 4.2 Values of Peaks and Wavelength of CH<sub>3</sub>SH Absorption Spectral

	<b><math>\sigma</math> (cm<sup>2</sup>/molecules)</b>	<b>Wavelength (nm)</b>
Experimental	6.357E-18	204
McMillan	6.88E-18	205
Vaghjiani	8.49E-18	204

There were quite a number of reasons for the difference of the peaks value. Firstly, absorption cross section is temperature dependent (Bingen *et al.*, 2019). Temperature effects affecting the shape or the magnitude of gas absorption cross section spectra (Orphal *et al.*, 2003). The slight difference of the peaks values might resulted from the difference in gas temperature used for each of the study. The gas temperature for the calculation of  $\sigma$  in this experiment used  $T$  value of 27 °C (room temperature) which is equivalent to 300 K. Vaghjiani's work used gas temperature of 296 K and for McMillan the temperature used was 298 K. Another reason would be the usage of different type of UV broadband source during the experiment (Hartl *et al.*, 2012, Wu *et al.*, 2007). However, difference in peaks height is acceptable and considered normal. Nevertheless, the results showed that CH<sub>3</sub>SH is highly absorbed by UV light at wavelength of 204 nm where the peak is located. Since  $\sigma$  is the effective area of the

molecule that photon needs to traverse in order to be absorbed, the higher the  $\sigma$ , the easier it is to photoexcite the molecule.

The experimental CH<sub>3</sub>SH absorption cross section spectra is uniquely in good agreement with the theoretical datasets for the wavelength region of 200 to 270 nm. However the spectral range between 200 to 210 nm is the area where CH<sub>3</sub>SH is well absorbed. Thus, the choice of UV light for the proposed detection system is suitable.

### 4.3 Absorption Cross Section Spectra of Oxygen and Carbon Dioxide

$I_o$  was measured when N<sub>2</sub> was released into the absorption cell and  $I$  was measured when the pure O<sub>2</sub> gas was then released into the cell. Data of intensity counts for incident and transmitted intensity were inserted into the derived Beer Lambert Law to get the data sets of  $\sigma$  for O<sub>2</sub>. Figure 4.2 shows the results of  $\sigma$  is plotted against wavelength and compared to the theoretical datasets (Yoshino et al., 1988) taken from the MPI Mainz UV-VIS database.

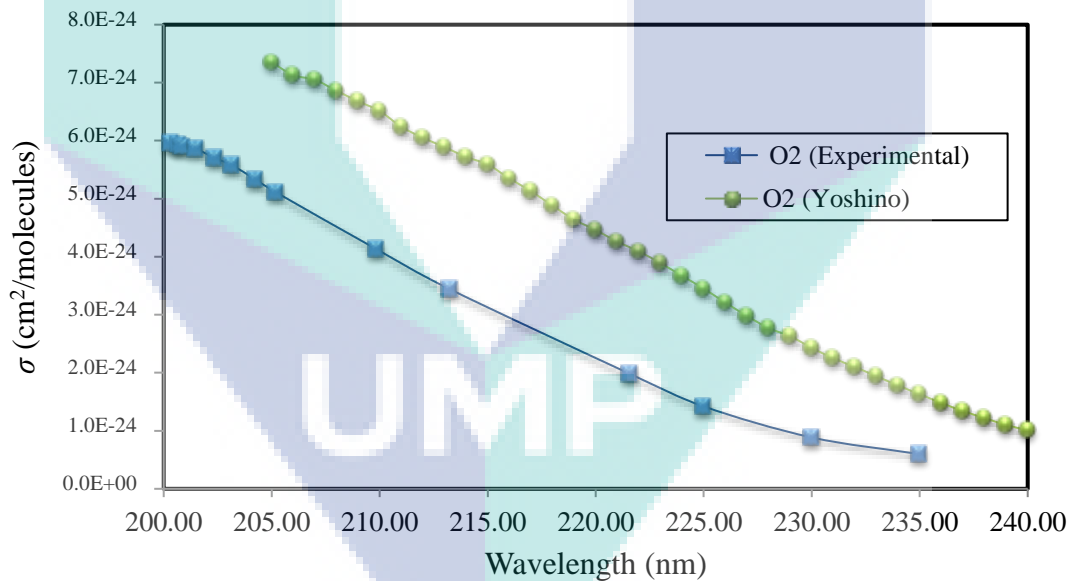


Figure 4.2 Graph of Absorption Cross Section against Wavelength for Oxygen

Comparing the O<sub>2</sub> absorption cross section spectra for experimental and theoretical datasets, based on the shape, they shows similar pattern. Both spectra are almost linear, parallel and statistically significant with P-value equal to 0. Both lines decreasing to the right and experimental results shows significance correlation with the theory, with the correlation coefficient of 0.9291.

The same experimental method of O<sub>2</sub> was carried out for CO<sub>2</sub> to measure  $I_o$  and  $I$  thus, calculated the  $\sigma$ . Figure 4.3 shows the results of absorption cross section spectra for CO<sub>2</sub> compared with the theoretical spectra (Ityaksov et al., 2008) from MPI Mainz UV-VIS database.

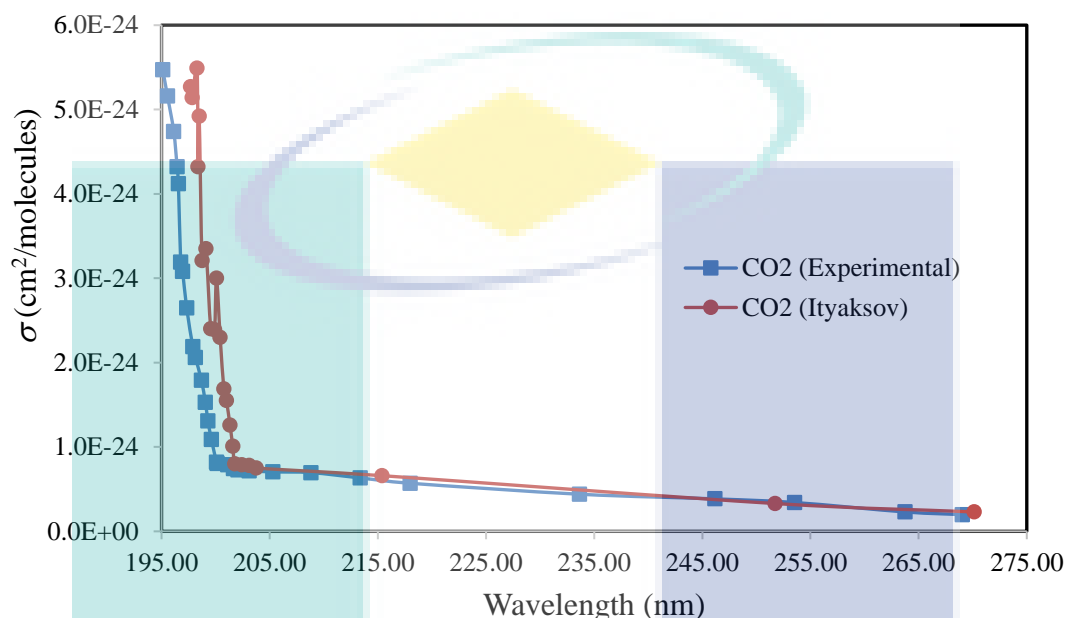


Figure 4.3 Graph of Absorption Cross Section against Wavelength for Carbon Dioxide

When comparing the shape of the experimental CO<sub>2</sub> absorption cross section spectra with theoretical spectra, they shows almost similar pattern. Experimental results of absorption cross section spectra of CO<sub>2</sub> is highly correlated with the theory for wavelength range of 203 to 268 nm, with correlation coefficient of 0.9962. They are statistically significant with P-value equal to 0. But, for the 195 to 202 nm spectral region, correlation coefficient is 0.811.

#### 4.4 Cross Sensitivity with Breathing Gases

In the spectral range of UV, where halitosis is concerned, CH<sub>3</sub>SH is the dominant but not the only absorber in breathing air. Even though negligible in most applications, optical densities of other gases can cause significant false signals (Tirpitz et al., 2019). Thus, cross sensitivity evaluation was carried out. Figure 4.3 shows their absorption cross section in comparison to CH<sub>3</sub>SH.

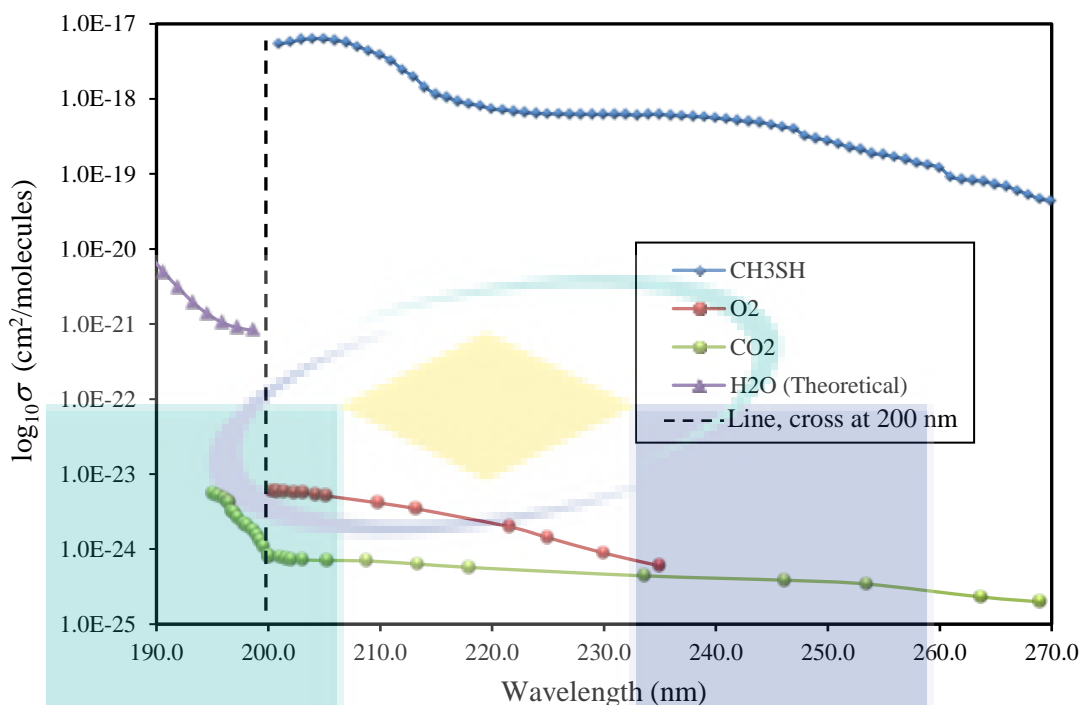


Figure 4.4 Absorption Cross Sections Comparison of Breathing Gases with CH<sub>3</sub>SH in the UV spectral interval

Particularly, for absorption cross section spectra comparison purpose, logarithmic value of  $\sigma$  ( $\log_{10} \sigma$ ) has been introduced to the vertical axis of the graph to clearly distinguished the degree of absorption cross section for O<sub>2</sub>, CO<sub>2</sub> and H<sub>2</sub>O with CH<sub>3</sub>SH. These so called spectra comparison method was regularly used in several previous studies (Austin et al., 2009; Manap et al., 2014). The horizontal axis of wavelength was extended 10 nm to the left to have a complete plot of all the important breathing gases for a comprehensive interference investigation. Theoretical datasets of H<sub>2</sub>O was taken from the database.

When considering the UV spectral range of 200 to 270 nm, there was non-existence of H<sub>2</sub>O spectra. Presence of H<sub>2</sub>O only appreciable below 200 nm and has no significant effect on CH<sub>3</sub>SH absorption. In Appendix D, the absorption cross sections of water vapour from various studies were shown in a graph. The significant absorption cross section spectra of H<sub>2</sub>O featured for wavelength region of 180 to 200 nm. Although there was a study (Zuev et al., 1990) carried out to determine the absorption cross section spectra for H<sub>2</sub>O in the region of 200 to 250 nm but it was only applicable for high temperature of 1000 to 3700 K which is not comparable in this study.



O<sub>2</sub> is the second highest percentage for both inhaled and exhaled gas which is 20.9% and 16% relatively (Walker, 2003). But when comparing the absorption cross section spectra of O<sub>2</sub> with CH<sub>3</sub>SH, the absorption cross section values for O<sub>2</sub> is obviously small to CH<sub>3</sub>SH. It can be considered as zero and negligible. Even the peaks were located at different wavelength. It was observed that absorption cross section spectra H<sub>2</sub>O peak located at 200 nm while for CH<sub>3</sub>SH located at 204 nm. Consequently, this indicates that there is no cross sensitivity issue for CH<sub>3</sub>SH measurement in the presence of O<sub>2</sub> in human breath.

The existence of CO<sub>2</sub> gas in human breath is extremely small compared to O<sub>2</sub>. Every human inhaled 0.04% and exhaled 4% of CO<sub>2</sub>. From the comparison graph, even the absorption cross section clearly shown the values are low. It indicates that CO<sub>2</sub> only absorb extremely small amount of light which can be neglected. This shows that the presence of CO<sub>2</sub> has no significant effect on CH<sub>3</sub>SH in that particular region. Therefore, it was very clear that all absorption cross section spectra of the important breathing gases H<sub>2</sub>O, O<sub>2</sub> and CO<sub>2</sub> did not cross nor overlapped with each other. These breathing gases spectra also obviously shown non-overlapping pattern with the absorption cross section spectra of CH<sub>3</sub>SH within the wavelength region of 200 to 270 nm. The spectra appeared to have different values of  $\sigma$  at the dedicated wavelength region.

While considering the interference study restricted to 200 to 210 nm wavelength region where the excellent peak of experimental CH<sub>3</sub>SH gas was located at 204 nm, cross sensitivity was not an issue at all. These breathing gases seem to absorb very small amount of light within the same wavelength region as CH<sub>3</sub>SH. Therefore, the UV spectral region of 200 to 210 nm is a good potential band which best selected as the absorption point when considering the development of the halitosis detection system.

#### **4.5 Calculation of CH<sub>3</sub>SH Concentration**

Concentration of CH<sub>3</sub>SH gas calculated for the proposed system validation purpose. The known value of  $\sigma$  for CH<sub>3</sub>SH was from the peak determination which is 6.365E-18 cm<sup>2</sup>/molecules at wavelength of 204 nm. Table 4.3 shows the datasets of measured intensity,  $I_0$  and  $I$ , and the calculated CH<sub>3</sub>SH gas concentration.

Table 4.3 Measured Intensity and Calculated CH<sub>3</sub>SH Gas Concentration

Initial Intensity, I <sub>0</sub>	Transmitted Intensity, I	I/I <sub>0</sub>	Concentration, ppm
6654	5688	0.854824166	9.83775E+01
6712	5746	0.856078665	9.74578E+01
6777	5813	0.857754169	9.62315E+01
6501	5570	0.856791263	9.69360E+01
6814	5832	0.855884943	9.75997E+01
6532	5579	0.854102878	9.89070E+01
6618	5663	0.855696585	9.77378E+01
6747	5779	0.856528828	9.71281E+01
6286	5397	0.858574610	9.56319E+01
6911	5906	0.854579656	9.85570E+01
Calculated CH <sub>3</sub> SH Gas Concentration =			9.74564E+01

Using Beer Lambert Law equation, the concentration value is 9.74564E+01 or close to 97.46 ppm. The experiment used CH<sub>3</sub>SH gas with the concentration of 100 ppm as stated by the manufacturer. Thus, the calculated gas concentration of CH<sub>3</sub>SH is around 2.54 ppm less. However, the result is acceptable. The main reason for the calculated gas concentration value is smaller due to noise that existed during the measurement. As stated in previous study (Manap, 2011; Tirpitz et al., 2019) that the noise can cause difficulty in determining the concentration measurement and can even cause incorrect concentration readings. Another reason is that, the true concentration of CH<sub>3</sub>SH gas in the tank provided by the manufacturer already decreased due to the shelf life of the gas itself.

#### 4.6 Summary

The absorption cross section spectra of CH<sub>3</sub>SH gas obtained from the experiment indicated that the system is able to detect CH<sub>3</sub>SH gas within UV spectral region of 200 to 270 nm. The analyses showed the experimental results were highly correlated and statistically significant with the theoretical datasets. Location of excellent peak of the spectra indicated that 200 to 210 nm as the potential band of the system. There is no interference issue for the proposed system when the absorption cross section spectra shown non-overlapping pattern of CH<sub>3</sub>SH with the breathing gases. Furthermore, CH<sub>3</sub>SH gas concentration can be measured with the proposed system.

## CHAPTER 5

### CONCLUSIONS

#### 5.1 Introduction

The history of halitosis and concern of the affected patients initiated undeniably reason for development of halitosis detection system. Most importantly, even though there are several detection systems and methods available in the dental field, the drawbacks made it possible for an alternative system to be constructed. This study was performed to develop the UV based methyl mercaptan system using OFS with the aim to detect halitosis and reliably use in the dental field. Details of the components used, the technique applied and the methodology of the experiment for the system have been highlighted and explained. The outcome and discussion of the experiment performed have been disclosed thoroughly. This final chapter is to conclude the successful efforts in developing the halitosis detection system as an alternative for the current detection methods available in the dental field.

#### 5.2 Conclusions

The UV based detection system which was constructed with combinations of available manufactured components is able to detect  $\text{CH}_3\text{SH}$  within the wavelength region of 200 to 270 nm. The system which coupled with absorption spectroscopy method using OFS was found to be suitable and reliable to use as the halitosis detection system for routine clinical usage in the dental field.

The analyses of the  $\text{CH}_3\text{SH}$  gas absorption cross section spectra which uniquely in good agreement with the theoretical datasets from the MPI-Mainz database, indicates that the system is able to specifically detect  $\text{CH}_3\text{SH}$  gas. It can also distinguish different VSCs due to the unique absorption cross section spectra for each of the compounds. The

CH<sub>3</sub>SH absorption cross section spectra exists within the UV-C region and indicates the suitability of UV as the light source. The wavelength region between 200 to 210 nm is where the excellent peak located and this range will be a good potential band selected for the development of any UV based detection system.

Cross sensitivity assessments of CH<sub>3</sub>SH gas with other breathing gases indicates that there was no interference issue because the absorption cross section spectra were not overlapping with each other. Thus, these breathing gases absorb very small amount of light within the same region as CH<sub>3</sub>SH, which is negligible. The calculated CH<sub>3</sub>SH gas concentration, 97.46 ppm that was obtained using the derivation of Beer Lambert Law equation almost reached the designated concentration of 100 ppm. Thus, the UV based detection system can be considered as reliable, objective and able to provide measurable result. For that reason, the proposed system is not just for plain detection of halitosis existence but also able to indicate the intensity of the halitosis.

### 5.3 Suggestions and Future Works

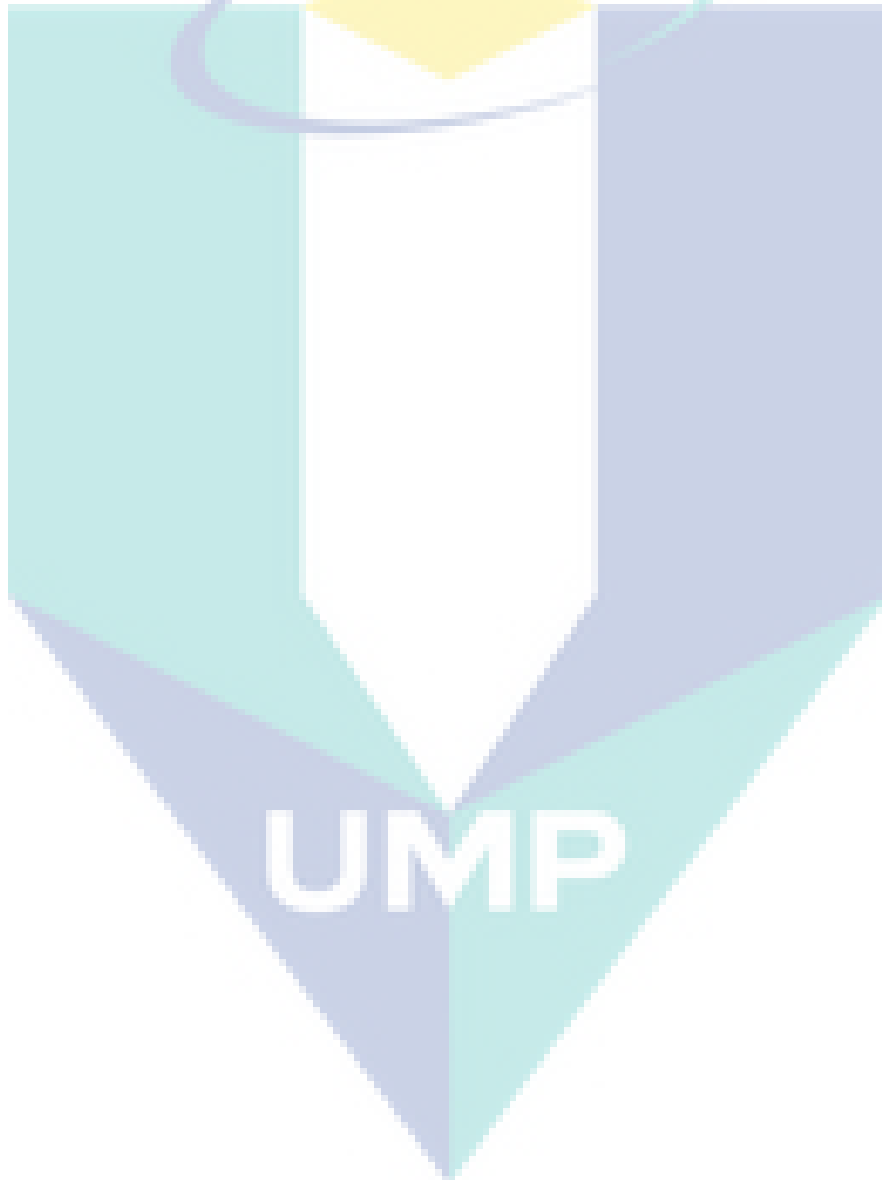
It was very clear that there is no potential interference for halitosis detection in the presence of the breathing gases if CH<sub>3</sub>SH is the halitosis contributor. Therefore, if the existence of VSCs is the main concern in halitosis detection, the developed UV based detection system should be able to detect other VSCs within the wavelength band. So, this work can be extended with the usage of other VSCs such as H<sub>2</sub>S and CH<sub>3</sub>CH<sub>3</sub>SH.

The best measurement take place around 200 to 210 nm wavelength region where the absorption of CH<sub>3</sub>SH is at maximum level. This range fell under the UV-C region of the light broadband. For commercialization purpose, to construct a device for halitosis detection according to the proposed system, more specific, cheap, small and has long lifetime UV light source such as UV-C LED can be utilised. Thus, the device is possible not just for routine clinical usage but also for home usage.

The cross sensitivity testing was carried out for breathing gases only but not with other compounds that may exist in the atmosphere. Therefore, when constructing the device to be used in the dental field, a small tube for exhale breath should be considered. The tube must be attached directly to the gas inlet of the gas cell to prevent from unwanted compounds that may affect the measurement. For clinical applications,

the miniature tube or probe can be utilised. Additionally, the gas cell with a diameter that is smaller than 1.20 mm can be considered (Katagiri *et al.*, 2018).

It is also recommend that in-situ halitosis detection and evaluation executed on real time basis at the dental clinics. Future work should take into account the development of a computer programming such as LabVIEW that is able to detect the existence of halitosis even at a very low concentration and to display the outcomes in real time for a better halitosis diagnosis.



## REFERENCES

- Agarwal, V., Kumar, P., Gupta, G., Khatri, M., & Kumar, A. (2013). Diagnosis Of Oral Malodor: A Review Of The Literature. *Indian Journal of Dental Sciences*, 5(3), 88–93.
- Agrawal, G. P. (2016). Optical Communication: Its History and Recent Progress. In *Optics in Our Time* (pp. 177–199). Cham: Springer International Publishing. [https://doi.org/10.1007/978-3-319-31903-2\\_8](https://doi.org/10.1007/978-3-319-31903-2_8)
- Alasqah, M., Khan, S., Elqomsan, M., Gufran, K., Kola, Z., & Hamza, M. Bin. (2016). Assessment of halitosis using the organoleptic method and volatile sulfur compounds monitoring. *Journal of Dental Research and Review*, 3(3), 94. <https://doi.org/10.4103/2348-2915.194833>
- Anbardan, S. J., Zahra, A., & Daryani, N. E. (2015). A review of the etiology, diagnosis and management of halitosis. *Govaresh*, 20(1), 49–56.
- Austin, E., van Brakel, A., Petrovich, M. N., & Richardson, D. J. (2009). Fibre optical sensor for C<sub>2</sub>H<sub>2</sub> gas using gas-filled photonic bandgap fibre reference cell. *Sensors and Actuators B: Chemical*, 139(1), 30–34. <https://doi.org/10.1016/j.snb.2008.07.028>
- Aydin, M., Bollen, C., & Özen, M. (2016). Diagnostic Value of Halitosis Examination Methods. *Compendium of Continuing Education in Dentistry*, 37(3), 174–178.
- Aydin, M., & Harvey-Woodworth, C. N. (2014). Halitosis: a new definition and classification. *British Dental Journal*, 217(1). <https://doi.org/10.1038/sj.bdj.2014.552>
- Aylikci, B., & Çolak, H. (2013). Halitosis: From diagnosis to management. *Journal of Natural Science, Biology and Medicine*, 4(1), 14. <https://doi.org/10.4103/0976-9668.107255>
- Barozzi, M., Manicardi, A., Vannucci, A., Candiani, A., Sozzi, M., Konstantaki, M., ... Cucinotta, A. (2017). Optical Fiber Sensors for Label-Free DNA Detection. *Journal of Lightwave Technology*, 35(16), 3461–3472. <https://doi.org/10.1109/JLT.2016.2607024>
- Bedos, C., Apelian, N., & Vergnes, J.-N. (2018). Social dentistry: an old heritage for a new professional approach. *British Dental Journal*, 225(4), 357–362. <https://doi.org/10.1038/sj.bdj.2018.648>
- Bhowmik, K., & Peng, G.-D. (2019). Polymer Optical Fibers. In *Handbook of Optical Fibers* (pp. 1–51). Singapore: Springer Singapore. [https://doi.org/10.1007/978-981-10-1477-2\\_38-1](https://doi.org/10.1007/978-981-10-1477-2_38-1)
- Bicak, D. A. (2018). A Current Approach to Halitosis and Oral Malodor- A Mini Review. *The Open Dentistry Journal*, 12(1), 322–330. <https://doi.org/10.2174/1874210601812010322>



- Bilro, L., Alberto, N., Pinto, J. L., & Nogueira, R. (2012). Optical Sensors Based on Plastic Fibers. *Sensors*, *12*(9), 12184–12207. <https://doi.org/10.3390/s120912184>
- Bingen, C., Robert, C., Hermans, C., Vanhellefont, F., Matshvili, N., Dekemper, E., & Fussen, D. (2019). A Revised Cross-Section Database for Gas Retrieval in the UV-Visible-Near IR Range, Applied to the GOMOS Retrieval Algorithm AerGOM. *Frontiers in Environmental Science*, *7*. <https://doi.org/10.3389/fenvs.2019.00118>
- Blair, W. P. (2018). The Basics of Light. Retrieved May 21, 2018, from <http://blair.pha.jhu.edu/spectroscopy/basics.html>
- Bollen, C. (2015). How to Handle Halitosis Examinations? *E-Cronicon Dental Science*, *2*(2), 254–259.
- Cavazzana, A., Röhrborn, A., Garthus-Niegel, S., Larsson, M., Hummel, T., & Croy, I. (2018). Sensory-specific impairment among older people. An investigation using both sensory thresholds and subjective measures across the five senses. *PLOS ONE*, *13*(8), e0202969. <https://doi.org/10.1371/journal.pone.0202969>
- Chawla, K., & Tariq Shaikh, S. (2015). Halitosis: An oversimplified complex issue. In *Archives of Dental and Medical Research* (Vol. 1). Retrieved from [http://www.aodmr.com/uploads/3/1/2/3/31236511/aodmr\\_chawla\\_and\\_shaikh.pdf](http://www.aodmr.com/uploads/3/1/2/3/31236511/aodmr_chawla_and_shaikh.pdf)
- Chen, S., Wang, Y., & Choi, S. (2013). Applications and Technology of Electronic Nose for Clinical Diagnosis. *Open Journal of Applied Biosensor*, *02*(02), 39–50. <https://doi.org/10.4236/ojab.2013.22005>
- Choi, K. Y., Lee, B. S., Kim, J. H., Kim, J. J., Jang, Y., Choi, J. W., & Lee, D. J. (2018). Assessment of Volatile Sulfur Compounds in Adult and Pediatric Chronic Tonsillitis Patients Receiving Tonsillectomy. *Clinical and Experimental Otorhinolaryngology*, *11*(3), 210–215. <https://doi.org/10.21053/ceo.2017.01109>
- Coelho Rezende, G., Le Calvé, S., Brandner, J. J., & Newport, D. (2019). Micro photoionization detectors. *Sensors and Actuators B: Chemical*, *287*, 86–94. <https://doi.org/10.1016/j.snb.2019.01.072>
- Correia, R., James, S., Lee, S.-W., Morgan, S. P., & Korposh, S. (2018). Biomedical application of optical fibre sensors. *Journal of Optics*, *20*(7), 073003. <https://doi.org/10.1088/2040-8986/aac68d>
- Dai, B., Jones, C., Pearl, M., Pelletier, M., & Myrick, M. (2018). Hydrogen Sulfide Gas Detection via Multivariate Optical Computing. *Sensors*, *18*(7), 2006. <https://doi.org/10.3390/s18072006>
- De Groen, P. C. (2017). History of the Endoscope [Scanning Our Past]. *Proceedings of the IEEE*, *105*(10), 1987–1995. <https://doi.org/10.1109/JPROC.2017.2742858>
- Demtröder, W. (2014). Absorption and Emission of Light. In *Laser Spectroscopy 1* (pp. 5–74). Berlin, Heidelberg: Springer Berlin Heidelberg. [https://doi.org/10.1007/978-3-642-53859-9\\_2](https://doi.org/10.1007/978-3-642-53859-9_2)



- Deng, Y., & Chu, D. (2017). Coherence properties of different light sources and their effect on the image sharpness and speckle of holographic displays. *Scientific Reports*, 7(1), 5893. <https://doi.org/10.1038/s41598-017-06215-x>
- Dhalla, N., Patil, S., Chaubey, K. K., & Narula, I. S. (2015). The detection of BANA micro-organisms in adult periodontitis before and after scaling and root planing by BANA-Enzymatic™ test kit: An in vivo study. *Journal of Indian Society of Periodontology*, 19(4), 401–405. <https://doi.org/10.4103/0972-124X.154167>
- Du, Z., Wan, J., Li, J., Luo, G., Gao, H., & Ma, Y. (2017). Detection of atmospheric methyl mercaptan using wavelength modulation spectroscopy with multicomponent spectral fitting. *Sensors (Switzerland)*, 17(2). <https://doi.org/10.3390/s17020379>
- Dudzik, A., Chomyszyn-Gajewska, M., & Łazarz-Bartyzel, K. (2015). An Evaluation of Halitosis using Oral Chroma™ Data Manager, Organoleptic Scores and Patients' Subjective Opinions. *Journal of International Oral Health: JIOH*, 7(3), 6–11. Retrieved from <http://www.ncbi.nlm.nih.gov/pubmed/25878470>
- Dung, T. T., Oh, Y., Choi, S.-J., Kim, I.-D., Oh, M.-K., & Kim, M. (2018). Applications and Advances in Bioelectronic Noses for Odour Sensing. *Sensors (Basel, Switzerland)*, 18(1). <https://doi.org/10.3390/s18010103>
- Elliott, D. A., Nabavizadeh, N., Seung, S. K., Hansen, E. K., & Holland, J. M. (2018). Radiation Therapy. In *Oral, Head and Neck Oncology and Reconstructive Surgery* (pp. 268–290). Elsevier. <https://doi.org/10.1016/B978-0-323-26568-3.00013-0>
- Fahr, A., & Nayak, A. (1996). Temperature dependant ultraviolet absorption cross sections of propylene, methylacetylene and vinylacetylene. *Chem. Phys.*, 203, 351–358.
- Falcão, D. P., Miranda, P. C., Almeida, T. F. G., Scalco, M. G. da S., Fregni, F., & Amorim, R. F. B. de. (2017). Assessment of the accuracy of portable monitors for halitosis evaluation in subjects without malodor complaint. Are they reliable for clinical practice? *Journal of Applied Oral Science: Revista FOB*, 25(5), 559–565. <https://doi.org/10.1590/1678-7757-2016-0305>
- Fanchenko, S., Baranov, A., Savkin, A., & Sleptsov, V. (2016). LED-based NDIR natural gas analyzer. *IOP Conference Series: Materials Science and Engineering*, 108, 012036. <https://doi.org/10.1088/1757-899X/108/1/012036>
- Fujita, H., Ueno, K., Morohara, O., Camargo, E., Geka, H., Shibata, Y., & Kuze, N. (2018). AlInSb Mid-Infrared LEDs of High Luminous Efficiency for Gas Sensors. *Physica Status Solidi (A)*, 215(8), 1700449. <https://doi.org/10.1002/pssa.201700449>
- Gancarz, M., Wawrzyniak, J., Gawrysiak-Witulska, M., Wiącek, D., Nawrocka, A., & Rusinek, R. (2017). Electronic nose with polymer-composite sensors for monitoring fungal deterioration of stored rapeseed. *International Agrophysics*, 31(3), 317–325. <https://doi.org/10.1515/intag-2016-0064>

- Glenn, S. (2020). Light. In *Britannica*. Encyclopædia Britannica, inc. Retrieved from <https://www.britannica.com/science/light>
- Gong, H., Kizil, M. S., Chen, Z., Amanzadeh, M., Yang, B., & Aminossadati, S. M. (2019). Advances in fibre optic based geotechnical monitoring systems for underground excavations. *International Journal of Mining Science and Technology*, 29(2), 229–238. <https://doi.org/10.1016/j.ijmst.2018.06.007>
- Greenman, J., Lenton, P., Seemann, R., & Nachnani, S. (2014). Organoleptic assessment of halitosis for dental professionals—general recommendations. *Journal of Breath Research*, 8(1), 017102. <https://doi.org/10.1088/1752-7155/8/1/017102>
- Hakim, M., Broza, Y. Y., Barash, O., Peled, N., Phillips, M., Amann, A., & Haick, H. (2012). Volatile Organic Compounds of Lung Cancer and Possible Biochemical Pathways. *Chemical Reviews*, 112(11), 5949–5966. <https://doi.org/10.1021/cr300174a>
- Han, T.-L., Yang, Y., Zhang, H., & Law, K. P. (2017). Analytical challenges of untargeted GC-MS-based metabolomics and the critical issues in selecting the data processing strategy. *F1000Research*, 6, 967. <https://doi.org/10.12688/f1000research.11823.1>
- Hartl, A., Kuhlmann, G., Wenig, M., Chan, K.-L., Ling, L.-Y., Zheng, N.-N., ... Liu, W.-Q. (2012). Comparing different light-emitting diodes as light sources for long path differential optical absorption spectroscopy NO<sub>2</sub> and SO<sub>2</sub> measurements. *Chinese Physics B*, 21(11), 119301. <https://doi.org/10.1088/1674-1056/21/11/119301>
- Henderson, B., Khodabakhsh, A., Metsälä, M., Ventrillard, I., Schmidt, F. M., Romanini, D., ... Cristescu, S. M. (2018). Laser spectroscopy for breath analysis: towards clinical implementation. *Applied Physics B*, 124(8), 161. <https://doi.org/10.1007/s00340-018-7030-x>
- Hidayat, W., Shakaff, A. Y. M., Ahmad, M. N., & Adom, A. H. (2010). Classification of Agarwood Oil Using an Electronic Nose. *Sensors*, 10(5), 4675–4685. <https://doi.org/10.3390/s100504675>
- Hodgkinson, J., & Tatam, R. P. (2013). Optical gas sensing: a review. *Measurement Science and Technology*, 24(1), 012004. <https://doi.org/10.1088/0957-0233/24/1/012004>
- House, J. E. (2018). Molecular Rotation and Spectroscopy. In *Fundamentals of Quantum Mechanics* (pp. 137–158). Elsevier. <https://doi.org/10.1016/B978-0-12-809242-2.00007-3>
- Hu, W., Wan, L., Jian, Y., Ren, C., Jin, K., Su, X., ... Wu, W. (2018). Electronic Noses: From Advanced Materials to Sensors Aided with Data Processing. *Advanced Materials Technologies*, 1800488. <https://doi.org/10.1002/admt.201800488>

- Iitani, K., Chien, P.-J., Suzuki, T., Toma, K., Arakawa, T., Iwasaki, Y., & Mitsubayashi, K. (2018). Fiber-Optic Bio-sniffer (Biochemical Gas Sensor) Using Reverse Reaction of Alcohol Dehydrogenase for Exhaled Acetaldehyde. *ACS Sensors*, 3(2), 425–431. <https://doi.org/10.1021/acssensors.7b00865>
- Ikporo, S. C., & Ogbu, N. H. (2016). Review of the Security Challenges of Fiber Optics Technologies in Network Connection in Nigeria and the Countermeasures. *International Journal of Engineering Science Invention*, 5(7), 36–41.
- Inoue, A., & Koike, Y. (2018). Low-Noise Graded-Index Plastic Optical Fiber for Significantly Stable and Robust Data Transmission. *J. Lightwave Technol.*, 36(24), 5887–5892. Retrieved from <http://jlt.osa.org/abstract.cfm?URI=jlt-36-24-5887>
- Ityaksov, D., Linnartz, H., & Ubachs, W. (2008). Deep-UV absorption and Rayleigh scattering of carbon dioxide. *Chemical Physics Letters*, 462(1–3), 31–34. <https://doi.org/10.1016/j.cplett.2008.07.049>
- Jin, W., Ho, H. L., Cao, Y. C., Ju, J., & Qi, L. F. (2013). Gas detection with micro- and nano-engineered optical fibers. *Optical Fiber Technology*, 19(6), 741–759. <https://doi.org/10.1016/j.yofte.2013.08.004>
- Kapoor, A., Grover, V., Malhotra, R., & Kaur, S. (2011). Halitosis - Revisited. *Indian Journal of Dental Sciences*, 3(5), 102–111.
- Kapoor, U., Sharma, G., Juneja, M., & Nagpal, A. (2016). Halitosis: Current concepts on etiology, diagnosis and management. *European Journal of Dentistry*, 10(2), 292. <https://doi.org/10.4103/1305-7456.178294>
- Katagiri, T., Shibayama, K., Iida, T., & Matsuura, Y. (2018). Infrared Hollow Optical Fiber Probe for Localized Carbon Dioxide Measurement in Respiratory Tracts. *Sensors (Basel, Switzerland)*, 18(4). <https://doi.org/10.3390/s18040995>
- Kayombo, C. M., & Mumghamba, E. G. (2017). Self-Reported Halitosis in relation to Oral Hygiene Practices, Oral Health Status, General Health Problems, and Multifactorial Characteristics among Workers in Ilala and Temeke Municipals, Tanzania. *International Journal of Dentistry*, 2017. <https://doi.org/10.1155/2017/8682010>
- Keller-Rudek, H., Moortgat, G. K., Sander, R., & Sörensen, R. (2013). The MPI-Mainz UV/VIS Spectral Atlas of Gaseous Molecules of Atmospheric Interest. *Earth System Science Data*, 5(2), 365–373. <https://doi.org/10.5194/essd-5-365-2013>
- Khan, S., Newport, D., & Le Calvé, S. (2019). Gas Detection Using Portable Deep-UV Absorption Spectrophotometry: A Review. *Sensors*, 19(23), 5210. <https://doi.org/10.3390/s19235210>
- Kher, S., & Kumar Saxena, M. (2019). Distributed, Advanced Fiber Optic Sensors. In *Applications of Optical Fibers for Sensing*. IntechOpen. <https://doi.org/10.5772/intechopen.83622>

- Kim, I. Y., Suh, S.-H., Lee, I.-K., & Wolfe, R. R. (2016). Applications of stable, nonradioactive isotope tracers in in vivo human metabolic research. *Experimental & Molecular Medicine*, 48(1), e203–e203. <https://doi.org/10.1038/emm.2015.97>
- Kinane, D. F., & Lowe, G. D. O. (2000). Perio 2000\_Periodontal Disease and Cardiovascular 2000. In *Periodontology 2000* (Vol. 23, pp. 121–126). Munksgaard. Retrieved from <https://www.scribd.com/document/41246670/Perio-2000-Periodontal-Disease-and-Cardiovascular-2000>
- Korposh, S., James, S. W., Lee, S.-W., & Tatam, R. P. (2019). Tapered Optical Fibre Sensors: Current Trends and Future Perspectives. *Sensors*, 19(10), 2294. <https://doi.org/10.3390/s19102294>
- Laleman, I., Dadamio, J., De Geest, S., Dekeyser, C., & Quirynen, M. (2014). Instrumental assessment of halitosis for the general dental practitioner. *Journal of Breath Research*, 8(1), 017103. <https://doi.org/10.1088/1752-7155/8/1/017103>
- Lampel, J., Pöhler, D., Tschritter, J., Frieß, U., & Platt, U. (2015). On the relative absorption strengths of water vapour in the blue wavelength range. *Atmospheric Measurement Techniques*, 8(10), 4329–4346. <https://doi.org/10.5194/amt-8-4329-2015>
- Leal-Junior, A. G., Diaz, C. A. R., Avellar, L. M., Pontes, M. J., Marques, C., & Frizzera, A. (2019). Polymer Optical Fiber Sensors in Healthcare Applications: A Comprehensive Review. *Sensors*, 19(14), 3156. <https://doi.org/10.3390/s19143156>
- Li, Y., Dvořák, M., Nesterenko, P. N., Nuchtavorn, N., & Macka, M. (2018). High power deep UV-LEDs for analytical optical instrumentation. *Sensors and Actuators B: Chemical*, 255, 1238–1243. <https://doi.org/10.1016/j.snb.2017.08.085>
- Lin, S. (2018). *The Dental Diet: The Surprising Link between Your Teeth, Real Food, and Life-Changing Natural Health*. Hay House, Inc.
- Lochbaum, A., Fedoryshyn, Y., Dorodnyy, A., Koch, U., Hafner, C., & Leuthold, J. (2017). On-Chip Narrowband Thermal Emitter for Mid-IR Optical Gas Sensing. *ACS Photonics*, 4(6), 1371–1380. <https://doi.org/10.1021/acsp Photonics.6b01025>
- Lopes, R. G., de Godoy, C. H. L., Deana, A. M., de Santi, M. E. S. O., Prates, R. A., França, C. M., ... Bussadori, S. K. (2014). Photodynamic therapy as a novel treatment for halitosis in adolescents: Study protocol for a randomized controlled trial. *Trials*, 15(1), 443. <https://doi.org/10.1186/1745-6215-15-443>
- Lu, X., Thomas, P. J., & Hellevang, J. O. (2019). A Review of Methods for Fibre-Optic Distributed Chemical Sensing. *Sensors*, 19(13), 2876. <https://doi.org/10.3390/s19132876>
- Lucas, J. (2017). What is Ultraviolet Light. Retrieved from <https://www.livescience.com/50326-what-is-ultraviolet-light.html>
- Magoun, A. B. (2019). The Electrical Engineer Who Clarified Glass [Scanning our Past]. *Proceedings of the IEEE*, 107(5), 928–932. <https://doi.org/10.1109/JPROC.2019.2908803>



- Manap, H. (2011). *An Ultra Violet Optical Fibre Based Sensor For Ammonia Detection in the Agricultural Sector*. University of Limerick.
- Manap, H., & Lewis, E. (2014). The Interference Study of Green-House Gases for an Ammonia Sensor. *Applied Mechanics and Materials*, 704, 244–247. <https://doi.org/10.4028/www.scientific.net/AMM.704.244>
- Masuo, Y., Suzuki, N., Yoneda, M., Naito, T., & Hirofuji, T. (2012). Salivary  $\beta$ -galactosidase activity affects physiological oral malodour. *Archives of Oral Biology*, 57(1), 87–93. <https://doi.org/10.1016/j.archoralbio.2011.07.015>
- McKelvie, K. H., & Thurbide, K. B. (2017). Analysis of sulfur compounds using a water stationary phase in gas chromatography with flame photometric detection. *Analytical Methods*, 9(7), 1097–1104. <https://doi.org/10.1039/C6AY03017C>
- McMillan, V. (1966). Personal communication to J.G. Calvert, J.N. Pitts, Jr., Photochemistry,. *John Wiley & Sons, New York*, 489.
- Méndez, A. (2016). Optics in Medicine. In *Optics in Our Time* (pp. 299–333). Cham: Springer International Publishing. [https://doi.org/10.1007/978-3-319-31903-2\\_13](https://doi.org/10.1007/978-3-319-31903-2_13)
- Morisawa, M., & Muto, S. (2004). A novel breathing condition sensor using plastic optical fiber. In *Proceedings of IEEE Sensors, 2004*. (Vol. vol.3, pp. 1277–1280). IEEE. <https://doi.org/10.1109/ICSENS.2004.1426414>
- Morris, A. S., & Langari, R. (2016). Sensor Technologies. In *Measurement and Instrumentation* (pp. 375–405). Elsevier. <https://doi.org/10.1016/B978-0-12-800884-3.00013-7>
- Murata, T., Rahardjo, A., Fujiyama, Y., Yamaga, T., Hanada, M., Yaegaki, K., & Miyazaki, H. (2006). Development of a Compact and Simple Gas Chromatography for Oral Malodor Measurement. *Journal of Periodontology*, 77(7), 1142–1147. <https://doi.org/10.1902/jop.2006.050388>
- Nakhleh, M., Quatredeniens, M., & Haick, H. (2017). Detection of halitosis in breath: Between the past, present, and future. *Oral Diseases*. <https://doi.org/10.1111/odi.12699>
- Nakhleh, M., Quatredeniens, M., & Haick, H. (2018). Detection of halitosis in breath: Between the past, present, and future. *Oral Diseases*, 24(5), 685–695. <https://doi.org/10.1111/odi.12699>
- Nani, B. D., Lima, P. O. de, Marcondes, F. K., Groppo, F. C., Rolim, G. S., Moraes, A. B. A. de, ... Franz-Montan, M. (2017). Changes in salivary microbiota increase volatile sulfur compounds production in healthy male subjects with academic-related chronic stress. *PLOS ONE*, 12(3), e0173686. <https://doi.org/10.1371/journal.pone.0173686>
- Naranjo, E., & Baliga, S. (2012). Early detection of combustible gas leaks using open path infrared (IR) gas detectors (p. 83660V). <https://doi.org/10.1117/12.919201>

- Nayak, S. P., & Das, S. (2018). Advanced Diagnostic Aids for Oral Malodour Detection - A Review. *International Journal of Scientific Research*, 7(5), 72–75. Retrieved from <https://wwjournals.com/index.php/ijsr/article/view/4439/4389>
- Nehir, M., Frank, C., Aßmann, S., & Achterberg, E. P. (2019). Improving Optical Measurements: Non-Linearity Compensation of Compact Charge-Coupled Device (CCD) Spectrometers. *Sensors*, 19(12), 2833. <https://doi.org/10.3390/s19122833>
- Oeding, M., & Wright, M. (2017). *Halitosis: A Clinical Review*.
- Okamoto, K. (2006). Optical fibers. In *Fundamentals of Optical Waveguides* (pp. 57–158). Elsevier. <https://doi.org/10.1016/B978-012525096-2/50004-0>
- Oliveira-Neto, J. M., Teixeira, W., Pereira, R., Nascimento, C., & Pedrazzi, V. (2018). Effect of Mouth Rinses with and without Alcohol on Halitosis: Randomized Crossover Controlled Trial Employing Gas Chromatography OPEN ACCESS. *Clinics in Surgery*, 3(2082).
- Oliveira, R., Sequeira, F., Bilro, L., & Nogueira, R. (2018). Polymer Optical Fiber Sensors and Devices. In *Handbook of Optical Fibers* (pp. 1–41). Singapore: Springer Singapore. [https://doi.org/10.1007/978-981-10-1477-2\\_1-2](https://doi.org/10.1007/978-981-10-1477-2_1-2)
- Orphal, J., Fellows, C. E., & Flaud, P.-M. (2003). The visible absorption spectrum of NO<sub>3</sub> measured by high-resolution Fourier transform spectroscopy. *Journal of Geophysical Research: Atmospheres*, 108(D3), n/a-n/a. <https://doi.org/10.1029/2002JD002489>
- Pacheco-Londoño, L. C., Ruiz-Caballero, J. L., Ramírez-Cedeño, M. L., Infante-Castillo, R., Gálan-Freyte, N. J., & Hernández-Rivera, S. P. (2019). Surface Persistence of Trace Level Deposits of Highly Energetic Materials. *Molecules*, 24(19), 3494. <https://doi.org/10.3390/molecules24193494>
- Panicker, K., Devi, R., Honibald, E., & Prasad, A. (2015). Oral malodor: A review. *Journal of Indian Academy of Dental Specialist Researchers*, 2(2), 49. <https://doi.org/10.4103/2229-3019.177916>
- Parkinson, W. H., & Yoshino, K. (2003). Absorption cross-section measurements of water vapor in the wavelength region 181–199 nm. *Chemical Physics*, 294(1), 31–35. [https://doi.org/10.1016/S0301-0104\(03\)00361-6](https://doi.org/10.1016/S0301-0104(03)00361-6)
- Pelosi, P., Zhu, J., & Knoll, W. (2018). From Gas Sensors to Biomimetic Artificial Noses. *Chemosensors*, 6(3), 32. <https://doi.org/10.3390/chemosensors6030032>
- Phe. (2018). *UK Standards for Microbiology Investigations - Indole Test*. UK. Retrieved from [https://assets.publishing.service.gov.uk/government/uploads/system/uploads/attachment\\_data/file/762018/TP\\_19i4.pdf](https://assets.publishing.service.gov.uk/government/uploads/system/uploads/attachment_data/file/762018/TP_19i4.pdf)
- Plümpe, M., Beckers, M., Mecnika, V., Seide, G., Gries, T., & Bunge, C.-A. (2017). Applications of polymer-optical fibres in sensor technology, lighting and further applications. In *Polymer Optical Fibres* (pp. 311–335). Elsevier. <https://doi.org/10.1016/B978-0-08-100039-7.00009-9>

- Pospišilová, M., Kuncová, G., & Trögl, J. (2015). Fiber-Optic Chemical Sensors and Fiber-Optic Bio-Sensors. *Sensors*, 15(10), 25208–25259. <https://doi.org/10.3390/s151025208>
- Potyrailo, R. A. (2016). Multivariable Sensors for Ubiquitous Monitoring of Gases in the Era of Internet of Things and Industrial Internet. *Chemical Reviews*, 116(19), 11877–11923. <https://doi.org/10.1021/acs.chemrev.6b00187>
- Ramdurg, P., & Mendigeri, V. (2014). Halitosis: A Review of Etiology and Management. *IOSR Journal of Dental and Medical Sciences*, 13(4), 50–55.
- Rao, A. S., & Kumar, V. (2013). *Halitosis: A mirror of systemic and oral health*. *IOSR Journal of Dental and Medical Sciences (IOSR-JDMS) e-ISSN* (Vol. 4). Retrieved from [www.iosrjournals.org](http://www.iosrjournals.org)
- Rao, M. U. S., Utharkar, S. M., & Sundaram, C. S. (2015). Halitosis: Classification, Causes, and diagnostic as well as Treatment Approach-A Review. *Research Journal of Pharmacy and Technology*, 8(12), 1707. <https://doi.org/10.5958/0974-360X.2015.00307.8>
- Razeghi, M., Lu, Q. Y., Bandyopadhyay, N., Zhou, W., Heydari, D., Bai, Y., & Slivken, S. (2015). Quantum cascade lasers: from tool to product. *Optics Express*, 23(7), 8462. <https://doi.org/10.1364/OE.23.008462>
- Reber, E. A. (2018). Gas Chromatography-Mass Spectrometry (GC-MS): Applications in Archaeology. In *Encyclopedia of Global Archaeology* (pp. 1–17). Cham: Springer International Publishing. [https://doi.org/10.1007/978-3-319-51726-1\\_340-2](https://doi.org/10.1007/978-3-319-51726-1_340-2)
- Saito, H., Hashimoto, Y., Minamide, T., Kon, T., Toma, K., Arakawa, T., & Mitsubayashi, K. (2016). Fiber Optic Biosniffer (Biochemical Gas Sensor) for Gaseous Dimethyl Sulfide. *Sensors and Materials*, 1. <https://doi.org/10.18494/SAM.2016.1291>
- Sakagami, H., Sheng, H., Ono, K., Komine, Y., Miyadai, T., Terada, Y., ... Oizumi, T. (2016). Anti-Halitosis Effect of Toothpaste Supplemented with Alkaline Extract of the Leaves of *Sasa senanensis* Rehder. *In Vivo (Athens, Greece)*, 30(2), 107–111. Retrieved from <http://www.ncbi.nlm.nih.gov/pubmed/26912820>
- Schmidt, J., Krause, F., & Haak, R. (2015). Halitosis: Measurement in daily practice. *Quintessence International*, 46, 633–641.
- Scully, C., & Greenman, J. (2012). Halitology (breath odour: aetiopathogenesis and management). *Oral Diseases*, 18(4), 333–345. <https://doi.org/10.1111/j.1601-0825.2011.01890.x>
- Severn, G. (2018). Physics 272 Laboratory Experiments. Retrieved May 16, 2018, from [https://home.sandiego.edu/~severn/p272/atomic\\_p272\\_s16\\_v1.html](https://home.sandiego.edu/~severn/p272/atomic_p272_s16_v1.html)



- Silva, J. C. da, Queiroz, A., Oliveira, A., & Kartnaller, V. (2017). Advances in the Application of Spectroscopic Techniques in the Biofuel Area over the Last Few Decades. In *Frontiers in Bioenergy and Biofuels*. InTech. <https://doi.org/10.5772/65552>
- Slot, D. E., De Geest, S., van der Weijden, F. A., & Quirynen, M. (2015). Treatment of oral malodour. Medium-term efficacy of mechanical and/or chemical agents: a systematic review. *Journal of Clinical Periodontology*, *42*, S303–S316. <https://doi.org/10.1111/jcpe.12378>
- Song, K., Mohseni, M., & Taghipour, F. (2016). Application of ultraviolet light-emitting diodes (UV-LEDs) for water disinfection: A review. *Water Research*, *94*, 341–349. <https://doi.org/10.1016/j.watres.2016.03.003>
- Tamaki, N., Kasuyama, K., Esaki, M., Toshikawa, T., Honda, S., & Ekuni, D. (2011). A new portable monitor for measuring odorous compounds in oral, exhaled and nasal air. *BMC Oral Health*, *11*(1), 15. <https://doi.org/10.1186/1472-6831-11-15>
- Thakur, P. (2019). Measurement and Monitoring of Mine Gases. In *Advanced Mine Ventilation* (pp. 313–323). Elsevier. <https://doi.org/10.1016/B978-0-08-100457-9.00019-5>
- Thomson, M. A. (2015). Mid-IR Spectroscopy as a Tool for Cleanliness Validation. In *Developments in Surface Contamination and Cleaning* (pp. 51–67). Elsevier. <https://doi.org/10.1016/B978-0-323-31303-2.00002-9>
- Thoppay, J. R., Filippi, A., Ciarrocca, K., Greenman, J., & De Rossi, S. S. (2019). Halitosis. In *Contemporary Oral Medicine* (pp. 1719–1747). Cham: Springer International Publishing. [https://doi.org/10.1007/978-3-319-72303-7\\_27](https://doi.org/10.1007/978-3-319-72303-7_27)
- Tian, F., Zhang, J., Yang, S., Zhao, Z., Liang, Z., Liu, Y., & Wang, D. (2016). Suppression of Strong Background Interference on E-Nose Sensors in an Open Country Environment. *Sensors*, *16*(2), 233. <https://doi.org/10.3390/s16020233>
- Tirpitz, J.-L., Pöhler, D., Bobrowski, N., Christenson, B., Rüdiger, J., Schmitt, S., & Platt, U. (2019). Non-dispersive UV Absorption Spectroscopy: A Promising New Approach for in-situ Detection of Sulfur Dioxide. *Frontiers in Earth Science*, *7*. <https://doi.org/10.3389/feart.2019.00026>
- Tomberg, T., Vainio, M., Hieta, T., & Halonen, L. (2018). Sub-parts-per-trillion level sensitivity in trace gas detection by cantilever-enhanced photo-acoustic spectroscopy. *Scientific Reports*, *8*(1), 1848. <https://doi.org/10.1038/s41598-018-20087-9>
- Tsuruta, M., Takahashi, T., Tokunaga, M., Iwasaki, M., Kataoka, S., Kakuta, S., ... Ansai, T. (2017). Relationships between pathologic subjective halitosis, olfactory reference syndrome, and social anxiety in young Japanese women. *BMC Psychology*, *5*(1), 7. <https://doi.org/10.1186/s40359-017-0176-1>
- Tungare, S., & Paranjpe, A. G. (2019). *Halitosis*. StatPearls. StatPearls Publishing. Retrieved from <http://www.ncbi.nlm.nih.gov/pubmed/30521280>

- U.S. National Library of Medicine. (2018). HSDB. Retrieved February 1, 2018, from <https://toxnet.nlm.nih.gov/help/newtoxnet/toxnetfs.html>
- Vaghjiani, G. L. (1993). CH<sub>3</sub>SH ultraviolet absorption cross sections in the region 192.5–309.5 nm and photodecomposition at 222 and 193 nm and 296 K. *The Journal of Chemical Physics*, *99*(8), 5936–5943.
- Vincent, T. A., & Gardner, J. W. (2016). A low cost MEMS based NDIR system for the monitoring of carbon dioxide in breath analysis at ppm levels. *Sensors and Actuators B: Chemical*, *236*, 954–964. <https://doi.org/10.1016/j.snb.2016.04.016>
- Vitiello, M. S., Scalari, G., Williams, B., & De Natale, P. (2015). Quantum cascade lasers: 20 years of challenges. *Optics Express*, *23*(4), 5167. <https://doi.org/10.1364/OE.23.005167>
- Wei, Y., Jiao, Y., An, D., Li, D., Li, W., & Wei, Q. (2019). Review of Dissolved Oxygen Detection Technology: From Laboratory Analysis to Online Intelligent Detection. *Sensors*, *19*(18), 3995. <https://doi.org/10.3390/s19183995>
- Weiss, T., Soroka, T., Gorodisky, L., Shushan, S., Snitz, K., Weissgross, R., ... Sobel, N. (2019). Human Olfaction without Apparent Olfactory Bulbs. *Neuron*, *105*(1), 35–45.e5. <https://doi.org/10.1016/j.neuron.2019.10.006>
- Wilson, A. D. (2018). Applications of Electronic-Nose Technologies for Noninvasive Early Detection of Plant, Animal and Human Diseases. *Chemosensors*, *6*(4), 45. <https://doi.org/10.3390/chemosensors6040045>
- Wu, Y.-J., Lu, H.-C., Chen, H.-K., Cheng, B.-M., Lee, Y.-P., & Lee, L. C. (2007). Photoabsorption cross sections of NH<sub>3</sub>, NH<sub>2</sub>D, NHD<sub>2</sub>, and ND<sub>3</sub> in the spectral range 110–144nm. *The Journal of Chemical Physics*, *127*(15), 154311. <https://doi.org/10.1063/1.2790440>
- Yaegaki, K., Brunette, D. M., Tangerman, A., Choe, Y. S., Winkel, E. G., Ito, S., ... Imai, T. (2012). Standardization of clinical protocols in oral malodor research. *Journal of Breath Research*, *6*(1). <https://doi.org/10.1088/1752-7155/6/1/017101>
- Yamunadevi, A., Selvamani, M., Mohan Kumar, K., Basandi, P., & Madhushankari, G. (2015). Halitosis - An overview: Part-I - Classification, etiology, and pathophysiology of halitosis. *Journal of Pharmacy and Bioallied Sciences*, *7*(6), 339. <https://doi.org/10.4103/0975-7406.163441>
- Yoneda, M., Suzuki, N., & Hirofujii, T. (2015). Current Status of the Techniques Used for Halitosis Analysis. *Austin Chromatography*, *2*(1), 6–8.
- Yoshino, K., Cheung, A. S.-C., Esmond, J. R., Parkinson, W. H., Freeman, D. E., Guberman, S. L., ... Merienne, M. F. (1988). Improved absorption cross-sections of oxygen in the wavelength region 205–240 nm of the Herzberg continuum. *Planetary and Space Science*, *36*(12), 1469–1475. [https://doi.org/10.1016/0032-0633\(88\)90012-8](https://doi.org/10.1016/0032-0633(88)90012-8)

- Zaera, F. (2014). New advances in the use of infrared absorption spectroscopy for the characterization of heterogeneous catalytic reactions. *Chem. Soc. Rev.*, 43(22), 7624–7663. <https://doi.org/10.1039/C3CS60374A>
- Zhang, Y.-J., Hsu, J.-C., Tsao, J.-H., & Sun, Y.-S. (2019). Fabrication of a Bare Optical Fiber-Based Biosensor. *Micromachines*, 10(8), 522. <https://doi.org/10.3390/mi10080522>
- Zhu, D., & Humphreys, C. J. (2016). Solid-State Lighting Based on Light Emitting Diode Technology. In *Optics in Our Time* (pp. 87–118). Cham: Springer International Publishing. [https://doi.org/10.1007/978-3-319-31903-2\\_5](https://doi.org/10.1007/978-3-319-31903-2_5)
- Zhu, X., & Gao, T. (2019). Spectrometry. In *Nano-Inspired Biosensors for Protein Assay with Clinical Applications* (pp. 237–264). Elsevier. <https://doi.org/10.1016/B978-0-12-815053-5.00010-6>
- Zou, Y., Zhang, Y., Hu, Y., & Gu, H. (2018). Ultraviolet Detectors Based on Wide Bandgap Semiconductor Nanowire: A Review. *Sensors*, 18(7), 2072. <https://doi.org/10.3390/s18072072>



UMP

**APPENDIX A**  
**MANUAL FOR CALIBRATING THE WAVELENGTH OF THE**  
**MAYA2000PRO SERIES SPECTROMETERS**

# Calibrating the Wavelength of the Maya2000Pro Series Spectrometers

## Overview

This appendix describes how to calibrate the wavelength of your spectrometer. Though each spectrometer is calibrated before it leaves Ocean Optics, the wavelength for all spectrometers will drift slightly as a function of time and environmental conditions. Ocean Optics recommends periodically recalibrating the Maya2000Pro Series.

## About Wavelength Calibration

You are going to be solving the following equation, which shows that the relationship between pixel number and wavelength is a third-order polynomial:

$$\lambda_p = I + C_1 p + C_2 p^2 + C_3 p^3$$

Where:

$\lambda$  = the wavelength of pixel  $p$

$I$  = the wavelength of pixel 0

$C_1$  = the first coefficient (nm/pixel)

$C_2$  = the second coefficient (nm/pixel<sup>2</sup>)

$C_3$  = the third coefficient (nm/pixel<sup>3</sup>)

You will be calculating the value for  $I$  and the three  $C$ s.

# Calibrating the Spectrometer

## Preparing for Calibration

To recalibrate the wavelength of your spectrometer, you need the following components:

- A light source capable of producing spectral lines

**Note**

Ocean Optics' HG-1 Mercury-Argon lamp is ideal for recalibration. If you do not have an HG-1, you need a light source that produces several (at least 4-6) spectral lines in the wavelength region of your spectrometer.

- A Maya2000Pro Series spectrometer
- An optical fiber (for spectrometers without a built-in slit, a 50- $\mu\text{m}$  fiber works best)
- A spreadsheet program (Excel or Quattro Pro, for example) or a calculator that performs third-order linear regressions

**Note**

If you are using Microsoft Excel, choose **Tools | Add-Ins** and check **AnalysisToolPak** and **AnalysisToolPak-VBA**.

## Calibrating the Wavelength of the Spectrometer

► **Procedure**

Perform the steps below to calibrate the wavelength of the spectrometer:

1. Place the spectrometer operating software into Scope mode and take a spectrum of your light source. Adjust the integration time (or the A/D conversion frequency) until there are several peaks on the screen that are not off-scale.
2. Move the cursor to one of the peaks and position the cursor so that it is at the point of maximum intensity.
3. Record the pixel number that is displayed in the status bar or legend (located beneath the graph). Repeat this step for all of the peaks in your spectrum.
4. Use the spreadsheet program or calculator to create a table like the one shown in the following figure. In the first column, place the exact or true wavelength of the spectral lines that you used. In the second column of this worksheet, place the observed pixel number. In the third column, calculate the pixel number squared, and in the fourth column, calculate the pixel number cubed.



**A: Calibrating the Wavelength of the Maya2000 Series**

Independent Variable	Dependent Variables			Values Computed from the Regression Output	
True Wavelength (nm)	Pixel #	Pixel # <sup>2</sup>	Pixel # <sup>3</sup>	Predicted Wavelength	Difference
253.65	175	30625	5359375	253.56	0.09
296.73	296	87616	25934336	296.72	0.01
302.15	312	97344	30371328	302.40	-0.25
313.16	342	116964	40001688	313.02	0.13
334.15	402	161604	64964808	334.19	-0.05
365.02	490	240100	117649000	365.05	-0.04
404.66	604	364816	220348864	404.67	-0.01
407.78	613	375769	230346397	407.78	0.00
435.84	694	481636	334255384	435.65	0.19
546.07	1022	1044484	1067462648	546.13	-0.06
576.96	1116	1245456	1389928896	577.05	-0.09
579.07	1122	1258884	1412467848	579.01	0.06
696.54	1491	2223081	3314613771	696.70	-0.15
706.72	1523	2319529	3532642667	706.62	0.10
727.29	1590	2528100	4019679000	727.24	0.06
738.40	1627	2647129	4306878883	738.53	-0.13
751.47	1669	2785561	4649101309	751.27	0.19

- Use the spreadsheet or calculator to calculate the wavelength calibration coefficients. In the spreadsheet program, find the functions to perform linear regressions.
  - If using Quattro Pro, look under **Tools | Advanced Math**
  - If using Excel, look under **Analysis ToolPak**
- Select the true wavelength as the dependent variable (Y). Select the pixel number, pixel number squared, and the pixel number cubed as the independent variables (X). After executing the regression, you will obtain an output similar to the one shown below. Numbers of importance are noted.

**Regression Statistics**

Multiple R 0.999999831  
 R Square 0.999999663 ← R Squared  
 Adjusted R Square 0.999999607  
 Standard Error 0.125540214  
 Observations 22

**Coefficients**      **Standard Error**

Intercept 190.473993      0.369047536 ← First coefficient

X Variable 1 0.36263983 ← 0.001684745

X Variable 2 -1.174416E-05 ← 8.35279E-07

X Variable 3 -2.523787E-09 ← 2.656608E-10 ← Second coefficient

Third coefficient

7. Record the Intercept, as well as the First, Second, and Third Coefficients. Additionally, look at the value for R squared. It should be very close to 1. If not, you have most likely assigned one of your wavelengths incorrectly.

Keep these values at hand.

## Saving the New Calibration Coefficients: USB Mode

Ocean Optics programs wavelength calibration coefficients unique to each Maya2000Pro Series Spectrometer onto an EEPROM memory chip in the spectrometer.

You can overwrite old calibration coefficients on the EEPROM using the Maya2000Pro Series Spectrometer via the USB port.

### ► Procedure

To save wavelength calibration coefficients using the USB mode, perform the following steps:

1. Ensure that the Maya2000Pro Series is connected to the PC and that you have closed all other applications.
2. Point your browser to <http://www.oceanoptics.com/technical/softwaredownloads.asp> and scroll down to **Microcode**. Select **USB EEPROM Programmer**.
3. Save the setup file to your computer.
4. Run the **Setup.exe** file to install the software. The **Welcome** screen appears.
5. Click the **Next** button. The **Destination Location** screen appears.
6. Accept the default installation location, or click the **Browse** button to specify a directory. Then, click the **Next** button. The **Program Manager Group** screen appears.
7. Click the **Next** button. The **Start Installation** screen appears.
8. Click the **Next** button to begin the installation. Once the installation finishes, the **Installation Complete** screen appears.
9. Click the **Finish** button and reboot the computer when prompted.
10. Navigate to the **USB EEPROM Programmer** from the Start menu and run the software.
11. Click on the desired spectrometer displayed in the left pane of the **USB Programmer** screen.
12. Double-click on each of the calibration coefficients displayed in the right pane of the **USB Programmer** screen and enter the new values acquired in Steps 5 and 6 of the [Calibrating the Wavelength of the Spectrometer](#) section in this appendix.
13. Repeat Step 12 for all of the new values.
14. Click on the **Save All Values** button to save the information, and then **Exit** the **USB Programmer** software.

The new wavelength calibration coefficients are now loaded onto the EEPROM memory chip on the Maya2000Pro Series Spectrometer.



**APPENDIX B**  
**EXPERIMENTAL DATA OF CH<sub>3</sub>SH ABSORPTION CROSS SECTION**  
**SPECTRA**

$\lambda$	$\sigma$	$\lambda$	$\sigma$
201.0	5.394E-18	236.0	6.030E-19
202.0	5.733E-18	237.0	5.972E-19
203.0	6.145E-18	238.0	5.830E-19
204.0	6.357E-18	239.0	5.722E-19
205.0	6.294E-18	240.0	5.550E-19
206.0	6.020E-18	241.0	5.365E-19
207.0	5.621E-18	242.0	5.136E-19
208.0	4.985E-18	243.0	4.968E-19
209.0	4.378E-18	244.0	4.875E-19
210.0	3.829E-18	245.0	4.532E-19
211.0	3.236E-18	246.0	4.215E-19
212.0	2.440E-18	247.0	3.980E-19
213.0	1.972E-18	248.0	3.210E-19
214.0	1.430E-18	249.0	2.982E-19
215.0	1.150E-18	250.0	2.776E-19
216.0	1.043E-18	251.0	2.513E-19
217.0	9.237E-19	252.0	2.254E-19
218.0	8.564E-19	253.0	2.122E-19
219.0	8.029E-19	254.0	1.865E-19
220.0	7.292E-19	255.0	1.807E-19
221.0	7.181E-19	256.0	1.680E-19
222.0	6.815E-19	257.0	1.562E-19
223.0	6.550E-19	258.0	1.399E-19
224.0	6.414E-19	259.0	1.321E-19
225.0	6.332E-19	260.0	1.214E-19
226.0	6.298E-19	261.0	9.116E-20
227.0	6.274E-19	262.0	8.490E-20
228.0	6.253E-19	263.0	8.170E-20
229.0	6.211E-19	264.0	7.948E-20
230.0	6.208E-19	265.0	7.173E-20
231.0	6.196E-19	266.0	6.781E-20
232.0	6.187E-19	267.0	5.986E-20
233.0	6.053E-19	268.0	5.243E-20
234.0	6.205E-19	269.0	4.625E-20
235.0	6.203E-19	270.0	4.374E-20

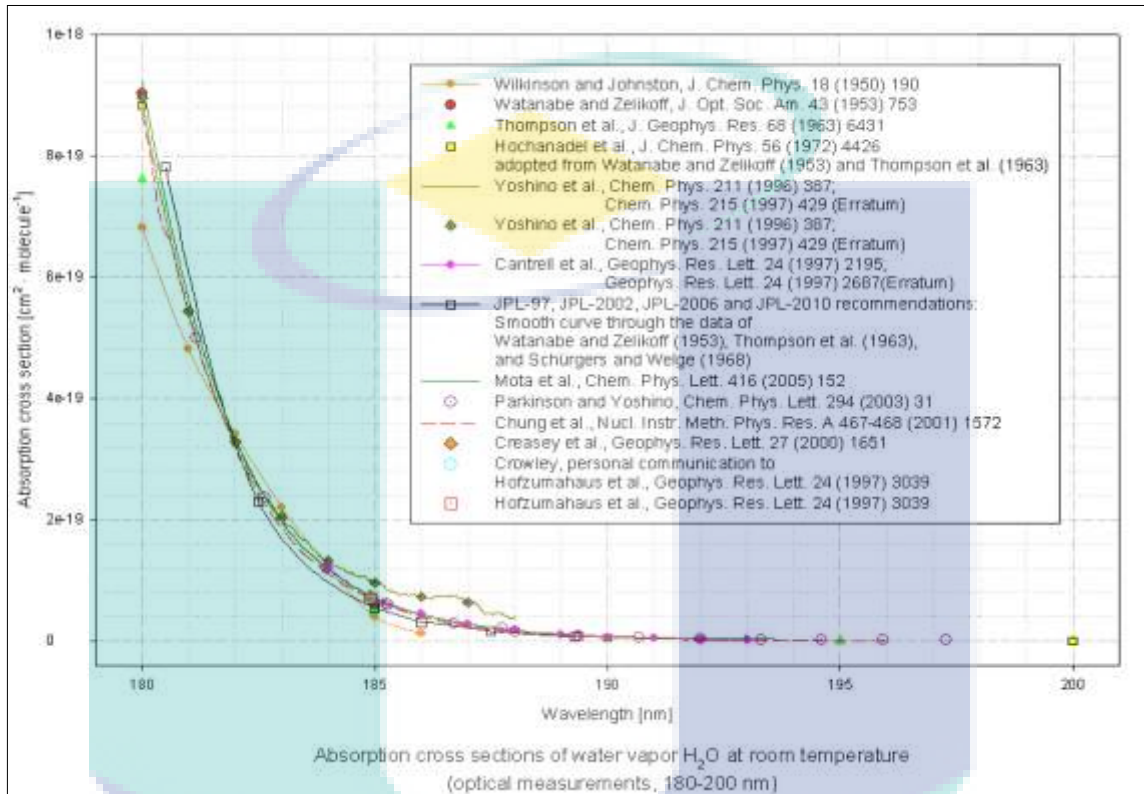
**APPENDIX C**  
**CH<sub>3</sub>SH ABSORPTION CROSS SECTION SPECTRA FROM MPI-MAINZ**  
**DATABASE**

Vaghjiani (1993)

McMillan (1966)

$\lambda$	$\sigma$	$\lambda$	$\sigma$	$\lambda$	$\sigma$	$\lambda$	$\sigma$
201	7.24E-18	236	6.41E-19	201	5.74E-18	236	5.96E-19
202	7.89E-18	237	6.25E-19	202	6.31E-18	237	5.81E-19
203	8.33E-18	238	6.09E-19	203	6.69E-18	238	5.62E-19
204	8.49E-18	239	5.85E-19	204	6.86E-18	239	5.43E-19
205	8.33E-18	240	5.62E-19	205	6.88E-18	240	5.16E-19
206	7.83E-18	241	5.41E-19	206	6.60E-18	241	4.93E-19
207	7.08E-18	242	5.15E-19	207	5.74E-18	242	4.59E-19
208	6.12E-18	243	4.89E-19	208	4.78E-18	243	4.32E-19
209	5.06E-18	244	4.62E-19	209	3.82E-18	244	4.01E-19
210	4.04E-18	245	4.34E-19	210	3.06E-18	245	3.75E-19
211	3.10E-18	246	4.05E-19	211	2.49E-18	246	3.48E-19
212	2.36E-18	247	3.75E-19	212	2.03E-18	247	3.25E-19
213	1.79E-18	248	3.51E-19	213	1.62E-18	248	3.06E-19
214	1.38E-18	249	3.23E-19	214	1.34E-18	249	2.87E-19
215	1.10E-18	250	2.98E-19	215	1.15E-18	250	2.68E-19
216	9.23E-19	251	2.74E-19	216	9.56E-19	251	2.49E-19
217	8.12E-19	252	2.49E-19	217	8.41E-19	252	2.33E-19
218	7.43E-19	253	2.25E-19	218	7.65E-19	253	2.18E-19
219	7.00E-19	254	2.04E-19	219	7.26E-19	254	2.03E-19
220	6.75E-19	255	1.83E-19	220	6.88E-19	255	1.91E-19
221	6.62E-19	256	1.63E-19	221	6.61E-19	256	1.78E-19
222	6.56E-19	257	1.45E-19	222	6.48E-19	257	1.64E-19
223	6.56E-19	258	1.28E-19	223	6.39E-19	258	1.53E-19
224	6.57E-19	259	1.13E-19	224	6.32E-19	259	1.43E-19
225	6.62E-19	260	9.82E-20	225	6.31E-19	260	1.34E-19
226	6.65E-19	261	8.55E-20	226	6.31E-19	261	1.24E-19
227	6.71E-19	262	7.39E-20	227	6.31E-19	262	1.15E-19
228	6.74E-19	263	6.36E-20	228	6.31E-19	263	1.07E-19
229	6.75E-19	264	5.41E-20	229	6.31E-19	264	9.94E-20
230	6.78E-19	265	4.65E-20	230	6.31E-19	265	9.18E-20
231	6.78E-19	266	3.95E-20	231	6.31E-19	266	8.60E-20
232	6.75E-19	267	3.31E-20	232	6.30E-19	267	8.03E-20
233	6.71E-19	268	2.78E-20	233	6.27E-19	268	7.46E-20
234	6.64E-19	269	2.30E-20	234	6.21E-19	269	6.96E-20
235	6.53E-19	270	1.92E-20	235	6.12E-19	270	6.50E-20

**APPENDIX D**  
**ABSORPTION CROSS SECTION OF WATER VAPOUR, H<sub>2</sub>O FROM**  
**VARIOUS STUDIES**



## LIST OF PUBLICATIONS

- Suzalina, K., & Manap, H. 2018. An Ultraviolet Halitosis Detection Using An Open-Path Optical Fibre Based Sensor. *International Journal of Engineering Inventions*, 7(5), 25-30.
- Nurulain, S. & Radin, M. R., Suzalina, K. & Manap, H. 2017. Spectra Comparison for an Optical Breathing Gas Sensor Development. *AIP Conference Proceedings: Engineering Technology International Conference 2016*, pp. 1-6.
- Manap, H. & Suzalina, K., & Najib, M. S. 2016. A Potential Development of Breathing Gas Sensor Using An Open Path Fibre Technique. *Microelectronic Engineering*, 164: 59-62.
- Manap, H., Nor Mazlee, Norazmi, Suzalina, K., & Najib, M.S. 2016. An Open-Path Optical Fibre Sensor For Ammonia Measurement In The Ultra Violet Region. *ARPN Journal of Engineering and Applied Sciences*, 11(18): 10940-10943.



UMP